Microbiology of phase-separated reactor systems for biomethanation at high temperatures (55 - 75 °C)

Vorgelegt von Dipl.-Biol. Antje Rademacher

Von der Fakultät III - Prozesswissenschaften
der Technischen Universität Berlin
zur Erlangung des akademischen Grades

Doktor der Naturwissenschaften
- Dr. rer. nat. -
genehmigte Dissertation

Promotionsausschuss:

Vorsitzender: Prof. Dr.-Ing. Sven-Uwe Geißen
Berichter: Prof. Dr. Ulrich Szewzyk
Berichterin: Prof. Dr. Elisabeth Grohmann
Berichter: Dr. Michael Klocke

Tag der wissenschaftlichen Aussprache: 13.06.2013

Berlin 2013
D 83

Die vorliegende Arbeit wurde am Leibniz-Institut für Agrartechnik Potsdam-Bornim e.V. (Abteilung Bioverfahrenstechnik) unter der Anleitung von Herrn Dr. M. Klocke in der Zeit von 2009 bis 2012 erstellt.

Gefördert wurde diese Arbeit vom Bundesministerium für Bildung und Forschung (BMBF) durch den Projektträger Jülich (Förderkennzeichen 03SF0349C).

DANKSAGUNG

Im Folgenden möchte ich mich herzlich bei den Menschen bedanken, die mich während meines Promotionsvorhabens begleitet und unterstützt haben.

Allen voran möchte ich mich bei Herrn Dr. Michael Klocke für seine wissenschaftliche Betreuung und Unterstützung bedanken. Er war mir stets Ansprechpartner und bereicherte meine Arbeit mit Ideen, Anregungen und konstruktiver Kritik.

Dank gilt auch Herrn Prof. Dr. Ulrich Szewzyk für die Begleitung meines Promotionsvorhabens, die Anregungen zu meiner Arbeit sowie für deren Begutachtung.

Ebenso gilt mein Dank Frau Prof. Dr. Elisabeth Grohmann für ihre Anregungen und die konstruktive Kritik zu meiner Arbeit sowie für die Übernahme des Gutachtens.

Mein herzlicher Dank gilt Dipl.-Ing. Mandy Schönberg und Dipl.-Ing. Carsten Joost für die gute Zusammenarbeit im BMBF-Projekt, für den Aufbau und Betrieb der Versuchsanlage und die Bereitstellung von Versuchsdaten für die weitere Auswertung.

Des Weiteren möchte ich den Mitarbeiterinnen und Mitarbeitern der AG Analytik des ATBs für die Analyse der Reaktorproben danken, sowie Kerstin Mundt für ihre kompetente Unterstützung im Labor. Zusätzlich möchte ich den vielen weiteren Kolleginnen und Kollegen des ATBs, insbesondere der Abteilung 1, für die angenehme Arbeitsatmosphäre danken. An dieser Stelle seien Angelika H., Antje F., Beate K., Edith N., Ingo Ba., Ingo Be., Johanna K., Kay B., Kathrin H., Katrin G., Lena H., Matthias B., Sarah H., Susanne K. und Susanne T. namentlich genannt. Vielen Dank für eure Unterstützung, die fruchtvollen Gespräche und die netten Stunden.

Mein weiterer Dank gilt Herrn Dr. Andreas Ulrich für seine Hilfe und Unterstützung bei der Einführung der TRFLP-Methodik am ATB.

Nicht zuletzt gilt mein besonderer Dank meinen Eltern sowie meinem Freund für die andauernde Unterstützung, Geduld und den notwendigen Rückhalt während der letzten Jahre.

EIDESSTATTLICHE ERKLÄRUNG

Ich erkläre an Eides Statt, dass die vorliegende Dissertation in allen Teilen von mir selbständig angefertigt wurde und die benutzten Hilfsmittel vollständig angegeben worden sind. Veröffentlichungen von irgendwelchen Teilen der vorliegenden Dissertation sind von mir, wie umseitig dargelegt, vorgenommen worden.

Weiter erkläre ich, dass ich nicht schon anderweitig einmal die Promotionsabsicht angemeldet oder ein Promotionseröffnungsverfahren beantragt habe.

_____ _____

Ort, Datum Unterschrift

Teile dieser Arbeit wurden bereits wie folgt veröffentlicht:

Rademacher A, Zakrzewski M, Schlüter A, Schönberg M, Szczepanowski R, Goesmann A, Pühler A & Klocke M (2012) Characterization of microbial biofilms in a thermophilic biogas system by high-throughput metagenome sequencing. *FEMS Microbiology Ecology* **79**, 785-799, DOI: 10.1111/j.1574-6941.2011.01265.x

Rademacher A, Nolte C, Schönberg M & Klocke M (2012) Temperature increases from 55 to 75 °C in a two-phase biogas reactor result in fundamental alterations within the bacterial and archaeal community structure. *Applied Microbiology and Biotechnology* **96**, 565-576, DOI: 10.1007/s00253-012-4348-x

Eikmeyer F, **Rademacher A**, Hanreich A, Hennig M, Jaenicke S, Maus I, Wibberg D, Zakrzewski M, Pühler A, Klocke M & Schlüter A (2013) Detailed analysis of metagenome datasets obtained from biogas-producing microbial communities residing in biogas reactors does not indicate the presence of putative pathogenic microorganisms. *Biotechnology for Biofuels* **6**, 49, DOI:10.1186/1754-6834-6-49

Rademacher A, Hanreich A, Bergmann I & Klocke M (2012) Black-Box-Biogasreaktor - Mikrobielle Gemeinschaften zur Biogaserzeugung. *Biospektrum* **18**, 727-729, DOI:10.1007/s12268-012-0253-1

Hanreich A, **Rademacher A** & Klocke M (2012) Mikrobielles Leben im Biogasreaktor – Einblicke in einen komplexen und dynamischen Mikrokosmos. In *Biogas Potenziale - Erkennen, Erforschen, Erwirtschaften*, p. 114-123. Potsdam, Leibniz-Institut für Agrartechnik Potsdam-Bornim e.V.

BMBF-Schlussbericht (2013) Bioprozesstechnik der Hydrolyse: Verfahrenstechnische Optimierung des Bioleaching-Verfahrens unter thermophilen bis hyperthermophilen Bedingungen und Analyse der hydrolytischen Mikroflora (Förderkennzeichen 03SF0349C). eds. Schönberg M, **Rademacher A**, Klocke M & Linke B, Hannover, TIB/UB.

ZUSAMMENFASSUNG

In den letzten Jahren nahm die Zahl an landwirtschaftlichen Biogasanlagen in Deutschland stetig zu. Im Jahr 2011 wurden 7.215 Biogasanlagen mit einer installierten elektrischen Leistung von 2.904 MW betrieben. Thermophile Temperaturen sowie eine räumliche Trennung der Prozessphasen Hydrolyse und Acidogenese von der Methanogenese können gegenüber den häufig verwendeten, mesophilen, einphasigen Rührkesselreaktoren den Biogasprozess verbessern und stabilisieren. Für eine weitere Optimierung solcher Anlagen ist ein detailliertes Wissen über die bakterielle und archaeelle Gemeinschaft, die am Abbau der Biomasse und der nachfolgenden Methanproduktion beteiligt sind, unabdingbar.

In dieser Studie wurden deshalb drei identische *Leach-bed* Biogasreaktorsysteme mit räumlich getrennten Prozessphasen untersucht, die jeweils mit Roggen-Ganzpflanzensilage und Stroh mit einer Verweilzeit von 21 Tagen betrieben wurden. Jedes Reaktorsystem bestand aus einem *Leach-bed* Reaktor (LBR), dessen Temperatur schrittweise von 55 auf 75 °C erhöht wurde, einem Prozessflüssigkeitsspeicher und einem nachgeschalteten Anaerobfilter (AF), der konstant während des gesamten Versuchs bei 55 °C betrieben wurde. Verschiedene kultivierungsunabhängige Methoden wurden genutzt um die mikrobielle Gemeinschaft im Reaktorsystem zu charakterisieren und zu quantifizieren sowie deren Dynamik zu verfolgen. Neben der Analyse von Genbibliotheken, TRFLP Fingerprintanalysen, Metagenomanalysen und qPCR Analysen wurden die Proben auch mittels Fluoreszenz *in situ* Hybridisierung sowie DAPI- und Propidiumiodid-Färbung untersucht.

Die Ergebnisse der Studie zeigten, dass die beabsichtigte Phasentrennung zwischen der Hydrolyse und Acidogenese im LBR und der Methanogenese im AF durch die Etablierung von spezialisierten Gemeinschaften zumindest teilweise erreicht wurde. Im Vergleich zum AF wurden im LBR verstärkt hydrolytische Bakterien und somit ein erhöhtes genetisches Potential zum Abbau von Kohlenhydraten festgestellt. Während einer 21-tägigen Fermentation bei konstanter Temperatur zeigte diese bakterielle Gemeinschaft dynamische Veränderungen, die mit Konzentrationsänderungen der Fermentationsprodukte und somit dem Grad des Biomasseabaus einhergingen.

Auch bei einer schrittweisen Erhöhung der Temperatur im LBR kam es zu Veränderungen in der bakteriellen Gemeinschaft. Bis zu einer Reaktortemperatur von

65 °C dominierten Vertreter der Clostridia. Ab 70 °C kam es zu einer verstärkten Ansiedlung von Vertretern der Klassen Bacteroidia, Thermotogae und Bacilli. Diese scheinen somit vor allem bei hyperthermophilen Temperaturen wichtig für den anaeroben Abbau von Biomasse zu sein. Entsprechende Veränderungen zeigten sich auch bei der Analyse des genetischen Potentials für den anaeroben Abbau von Biomasse. Ab einer Reaktortemperatur von 70 °C veränderte sich das genetische Potential bestimmte polysaccharidabbauende Glycosidhydrolasen zu exprimieren. Parallel dazu reduzierte sich die Abbaurate der eingebrachten Biomasse deutlich. Mittels einer Anreicherung mit Kompost konnten leichte Verbesserungen in der Reaktorleistung bei 70 °C erzielt werden, die jedoch nicht von Dauer waren. Um eine langanhaltende positive Veränderung erzielen zu können, scheint somit eine kontinuierliche Anreicherung notwendig zu sein.

Die methanogene Gemeinschaft im AF zeigte nur leichte Variationen in ihrer Zusammensetzung während der Temperaturerhöhung im LBR. Sowohl Vertreter der Methanobacteriales als auch der Methanosarcinales wurden identifiziert. Es ist somit wahrscheinlich, dass verschiedene methanogene Stoffwechselwege, wie die acetoklastische und hydrogenotrophe Methanogenese, im AF parallel ablaufen.

Des Weiteren wurde das Reaktorsystem hinsichtlich seines potentiellen Risikos, Wachstum und Verbreitung von Pathogenen zu gewährleisten, untersucht. Die hierfür untersuchten Metagenome zeigten jedoch, dass das Risiko für die Verbreitung von potentiellen Pathogenen durch die Ausbringung von Gärresten auf landwirtschaftlich genutzte Ackerflächen als sehr gering angesehen werden kann.

Die Studie gibt Aufschluss über Struktur und Dynamik der bakteriellen und archaeellen Gemeinschaft sowie über das genetische Potential zum anaeroben Abbau von pflanzlichen Polysacchariden bei hohen Temperaturen in zweiphasigen *Leach-bed* Biogassystemen. Insgesamt wurde die beste Reaktorleistung bei Temperaturen von 55 bis 60 °C festgestellt, ein Temperaturbereich, der sich vorteilhaft auf die mikrobielle Gemeinschaft im Reaktorsystem auswirkt. Des Weiteren zeigen die Ergebnisse potentielle prozessrelevante Bakterien sowie Glycosidhydrolasen auf, die als Biomarker für eine Überwachung von weiteren thermophilen Biogassystemen genutzt werden können. Die Ergebnisse dieser Studie dienen somit als Grundlage für eine Prozessüberwachung und eine zukünftige Optimierung von thermophilen Biogasprozessen mit Prozessphasentrennung.

ABSTRACT

In recent years, the number of agricultural biogas plants, as a means of generation of renewable energy, has risen constantly in Germany. In 2011, 7,215 agricultural biogas plants were operated with a total installed electric capacity of 2,904 MW.

Thermophilic temperatures and a spatial separation of the process phases hydrolysis and acetogenesis from methanogenesis are known strategies for improving and stabilizing biogas production. A deep understanding of the underlying bacterial and archaeal community involved in the breakdown of plant-derived biomass and the subsequent production of methane in phase-separated, thermophilic systems is of major importance for further improvement.

Pursuant to this aim, phase-separated leach-bed biogas systems, which were supplied with rye silage and straw lasting for 21 days, were analyzed. Each system consisted of a leach-bed reactor (LBR), whose temperature was increased stepwise from 55 to 75 °C, a leachate storage reactor and a downstream anaerobic filter reactor (AF), whose temperature remained at 55 °C throughout the experiment. Various culture-independent methods were used for the characterization, quantification and monitoring of the microbial community within these biogas systems. The culture-independent methods were based on the genetic information of cells, applying gene library construction, TRFLP fingerprinting, metagenomic and qPCR analyses and on the microscopical quantification of intact, but not cultivated cells.

The results indicated that the intended spatial separation of process phases, such as hydrolysis and acidogenesis, performed by different hydrolytic and fermentative bacteria, from the methanogenesis phase, performed by methanogenic archaea, was achieved at least in part within these biogas systems. For instance, hydrolytic bacteria and hence the genetic potential to degrade carbohydrates were strongly increased in the LBR in comparison to the AF.

In addition, changes in the bacterial community were detected in the LBR during the 21 days of fermentation as a consequence of changes in the VFA concentration due to the anaerobic digestion process.

Further, the stepwise increase in the fermentation temperature of the LBR also led to alterations within the bacterial community. Above 65 °C, the community changed from

being Clostridia-dominated toward being dominated by members of the Bacteroidia, Clostridia, Thermotogae and Bacilli. These groups seemed to be important for the anaerobic degradation of plant-derived biomass at hyperthermophilic temperatures. In addition to these results, the genetic potential for the expression of glycoside hydrolases, enzymes catalyzing the hydrolysis of glycosidic linkages of carbohydrates, was also affected by the temperature and changed strongly at an LBR temperature of 70°C.

Simultaneously with the changes in the bacterial community at 70 °C, the reactor performance also decreased strongly. A bioaugmentation with compost at this temperature led to slight improvements in the reactor performance, which did not persist at 75 °C. This indicated that a permanent positive effect of bioaugmentation can possibly only be realized by a continuous application.

The methanogenic community in the AF showed slight alterations during temperature increase in the LBR, which was most likely affected by the changes in the intermediate production of the bacterial community. The monitored archaeal community was mainly composed of members of the Methanobacteriales and Methanosarcinales. This indicated that different pathways for methane production, such as the acetoclastic and hydrogenotrophic pathway, occurred simultaneously in the AF.

Furthermore, samples of both the LBR and the AF were analyzed to assess the potential risk for the growth of pathogens in such biogas systems. It was shown that the operation of phase-separated thermophilic biogas systems presents only a very low risk for an unintended proliferation of putative pathogens and hence for a potential infection of humans, animals or plants through the application of digestate on farmland.

The present study revealed the composition and dynamics of the microbial community and their genetic potential for carbohydrate degradation in two-phase leach-bed biogas systems at thermophilic to hyperthermophilic temperatures. Temperatures of 55 to 60 °C in the LBR had a positive effect on the microbial community responsible for the production of biogas, leading to the best reactor performance. Furthermore, the results indicated potentially process-relevant bacteria and glycoside hydrolases, which may serve as target for the monitoring of thermophilic biogas reactors in future. Hence, the results gained in this study provide a promising basis for the monitoring and the prospective improvement of thermophilic biogas systems with phase-separation.

TABLE OF CONTENTS

LIST OF FIGURES

LIST OF TABLES

ABBREVIATIONS

16S rRNA	16S ribosomal RNA of the prokaryotic 30S small subunit
ADP	Adenosine diphosphate
AF	Anaerobic filter reactor
ARDRA	Amplified ribosomal DNA restriction analysis
ATB	Leibniz Institut für Agrartechnik Potsdam-Bornim e.V. (Leibniz Institute for Agricultural Engineering Potsdam-Bornim)
ATP	Adenosine triphosphate
BFR	Bundesanstalt für Risikobewertung (Federal Institute for Risk Assessment)
BLAST	Basic Local Alignment Search Tool
bp	Base pair
BSA	Bovine serum albumin
C	Compost sample
Camp.	Genus *Campylobacter*
Cl.	Genus *Clostridium*
C/N	Carbon/nitrogen ratio
$CaCl_2$	Calcium chloride
CARD-FISH	Catalyzed reporter deposition fluorescence *in situ* hybridization
CARMA	Software pipeline for the characterization of metagenomic sequences
CAZY	Carbohydrate-active enzymes database
CeBiTec	Center for Biotechnology, Bielefeld University, Germany
CO_2	Carbon dioxide
CoA	Coenzyme A
COD	Chemical oxygen demand
CoM	Coenzyme M
$CrK(SO_4)_2$	Chromium potassium sulfate
CSTR	Continuously stirred tank reactor
C_t	Threshold cycle number
CTAB	Hexadecyltrimethylammonium bromide
Cy5	Cyanine 5
D	Digestate sample
DAPI	4′,6-diamidino-2-phenylindole
DGGE	Denaturing gradient gel electrophoresis
DNA	Deoxyribonucleic acid
dNTP	Deoxyribonucleotide triphosphates
DOPE-FISH	Double labeling of oligonucleotide probes for fluorescence *in situ* hybridization
dsDNA	Double strand DNA
DSMZ	Deutsche Sammlung von Mikroorganismen und Zellkulturen GmbH (German Collection of Microorganisms and Cell Cultures)
E.	Genus *Escherichia*
EDTA	Ethylenediaminetetraacetic acid
EEG	Erneuerbare-Energien-Gesetz (Renewable energy law)

EGT	Environmental gene tag
EHEC	Enterohemorrhagic *E. coli* strain
FAM	6-carboxyfluorescein
FISH	Fluorescence *in situ* hybridization
FNR	Fachagentur nachwachsende Rohstoffe (Agency for Renewable Resources)
FP	FastDNA® Spin Kit for Soil
(x) g	Acceleration of gravity
Gb	Gigabase
GC	Guanine and cytosine
GH	Glycoside hydrolase
GOLD	Genome OnLine Database
GS	Genome Sequencer
H_2	Hydrogen
H_2O	Water
H_2O_2	Hydrogen peroxide
HAc eq.	Acetic acid equivalents
HCl	Hydrogen chloride
hPa	Hectopascal
HPLC-H_2O	High-performance liquid chromatography water
IPTG	Isopropyl β-D-1-thiogalacto-pyranoside
KCl	Potassium chloride
KEGG	Kyoto Encyclopedia of Genes and Genomes
KH_2PO_4	Monopotassium phosphate
L 0 - 21	Leachate sample at different time points of fermentation
L.	Genus *Listeria*
LB	Lysogeny broth
LBR	Leach-bed reactor
LOD	Limit of detection
LOQ	Limit of quantification
LR	Leachate reservoirNa
M	molar (mol L^{-1})
Mcu.	Genus *Methanoculleus*
Msr.	Genus *Methanosarcina*
Mtb.	Genus *Methanothermobacter*
Mb	Megabase
$MgCl_2$	Magnesium chloride
NA	Not analyzed
Na_2HPO_4	Sodium hydrogen phosphate
NaCl	Sodium chloride
NaOH	Sodium hydroxide
NCBI	National Center for Biotechnology Information
NH_3	Free ammonia
NH_4- N	Total ammonia nitrogen
NMDS	Non-metric multidimensional scaling
ODM	Organic dry matter
oS	Organic substance
OTU	Operational taxonomic unit
P	Packing sample of the AF
PBS	Phosphate-buffered saline
PCR	Polymerase chain reaction
pEGT	Prokaryotic environmental gene tag

pH	Pondus hydrogenii
PI	Propidium iodide
PS	PowerSoil® DNA Isolation Kit
Ps.	Genus *Pseudomonas*
PVPP	Polyvinylpolypyrrolidone
qPCR	Quantitative real-time PCR
RDP	Ribosomal Database Project
rfu	Channel intensity
RNA	Ribonucleic acid
rRNA	Ribosomal ribonucleic acid
rrs	16S rRNA gene
S	Rye silage sample
Salm.	Genus *Salmonella*
SDS	Sodium dodecyl sulfate
Sh.	Genus *Shigella*
SOC	Super optimal broth with catabolite repression
sp.	Species
R^2	Squared correlation coefficient
SSCP	Single strand conformation polymorphism
ssDNA	Single strand DNA
ST	Step by step DNA extraction
St	Straw sample
STB	Step by step DNA extraction with beating step
str.	Strain
TAMRA	6-carboxytetramethyl-rhodamine
TRF	Terminal restriction fragment
TRFLP	Terminal restriction fragment length polymorphism
U	Enzyme unit
UASSR	Upflow anaerobic solid-state reactor
VFA	Volatile fatty acids
WHO	World health organization
X-Gal	5-bromo-4-chloro-indolyl-β-D-galactopyranoside

The terms mesophilic, thermophilic and hyperthermophilic temperatures (or biogas systems, biogas reactors, conditions etc.) were used to indicate temperature ranges between 35-45°C, 55-65°C and 70-75°C, although these terms are logically incorrect due to the fact that e.g. thermophilic (= ”heat-loving”) temperatures do not exist.

1 INTRODUCTION

1.1 Renewable energy sources

The enduring use of fossil fuels, such as coal, petroleum and natural gas, as a source of energy is unsustainable due to supply limitations and greenhouse gas emissions. The global energy reserves of non-renewable raw material make up approximately 39,375 exajoule (= 10^{18} joule) focusing on the currently technically and economically recoverable quantities (DERA, 2011). With an average annual production of 479 exajoule for global consumption, non-renewable energy reserves will last for the next 82 years (DERA, 2011). However, the total amount of resources is much higher focusing on the geologically identified quantities of non-renewable raw material, which are currently not economically or technically recoverable (DERA, 2011).

Nevertheless, the supply of some non-renewable energy sources will run out in the coming decades. For instance, petroleum will be the first fossil fuel whose rising demand cannot be met (DERA, 2011). In contrast, the non-renewable raw material uranium, which is used for nuclear power production, will last for the next decades (DERA, 2011), but nuclear power bears a substantial risk for the environment during operation and also afterwards due to the need for nuclear waste storage.

The limitations on fossil fuels, the problems of greenhouse gas emission and the potential risk of nuclear events, as occurred in the nuclear power plant Daichii (Fukushima, Japan) in 2011, combined with the demographic and industrial increase have intensified the urgent need to strengthen the usage and the efficiency of renewable energy sources in recent years. Since 2000, the German renewable energy

law (EEG) favors renewable energy sources, such as wind and water power or biogas, and hence the reduction of the greenhouse gas emission by prescribing incentives for renewable energy supply. Furthermore, it schedules the nuclear phase-out for 2022, supports the expansion and modernization of the electric supply network and supports the further expansion of all renewable energies in Germany (BMU, 2012).

In 2011, renewable energy sources accounted for 12.5% of final energy consumption in Germany, which includes the consumption of electricity, heat and motor fuel. This is an increase by 36% within the last 5 years (BMU, 2012). In detail in 2011, 20.3% of electricity generation, 11% of heat supply and 5.5% of motor fuel consumption based on total energy consumption were provided by renewable energy sources (Figure 1.1). For instance, biogas represents the fourth most prevalent renewable energy source for the generation of electricity with 14.2% (Figure 1.1). Furthermore, it also contributes to heating supply with 11.8% (biogas, sewer and landfill gas were combined as biogenic gaseous fuel; Figure 1.1).

The production of biogas prevents an emission of 549 g CO_2 equivalent per kWh in electricity generation and 171 g CO_2 equivalent per kWh in heating supply (BMU, 2012). In comparison, the generation of electricity by water or wind power prevents an emission of 779 g and 721 g CO_2 equivalent per kWh, respectively (BMU, 2012). Although the production of biogas is not as effective as water or wind power in preventing CO_2 emission, it still contributes to the reduction of greenhouse gas and air pollutant emission.

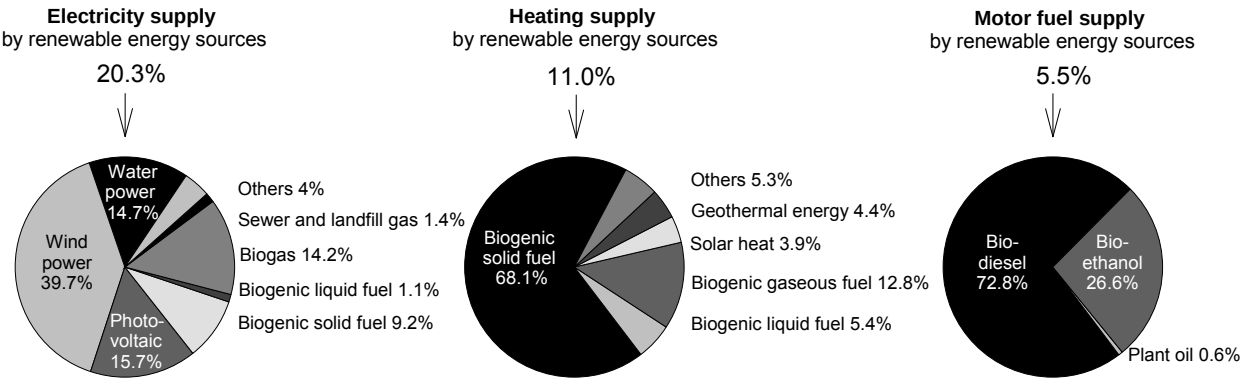

Figure 1.1 Proportion of renewable energy based on the total energy consumption in Germany 2011 (BMU, 2012)

Beside the direct generation of electricity and heat supply via a communal heating power station, biogas can also be used as biomethane after the reduction of impurities, such as carbon dioxide (CO_2), below 5% (Weiland et al., 2010). This can be achieved by different purification and concentration steps in order to reach the quality requirements for biomethane injection into the natural gas grid. In 2011, 83 biogas plants were purifying their biogas to biomethane for the injection into the natural gas grid (FNR, 2012b) and the tendency is to increase. This biomethane can also be used as motor fuel and also for electricity and heat generation in many places due to the distribution via the natural gas grid.

1.2 Agricultural biogas production

In Germany in 2011, 7,215 biogas plants were in operation with a total installed electric capacity of 2,904 MW, which is enough to replace four coal-burning power plants or two large nuclear power plants (FNR, 2012a).

In the most cases agricultural biogas plants were fed with renewable primary products and animal manure. A survey of operators of German biogas plants in 2010 (n = 622) indicated that 46% of the total substrates fed (based on weight) were renewable primary products (energy crops), 45% livestock excrement, 7% biowaste and 2% industrial and agricultural residues (DBFZ, 2011). Hence, energy crops, mainly maize silage, play an important role in the production of biogas.

In 2010, approximately 5% of the 11.8 million hectares of German cropland was used for the cultivation of biogas energy crops, whereas the percentage increased to approximately 7% in 2011 (FNR, 2012c; Statistisches Bundesamt, 2012). To prevent an excessive utilization of cropland and the monocropping of maize, several attempts have been made to analyze and improve the utilization of other substrates, such as industrial food waste (Kastner et al., 2012; Merlino et al., 2012) or grass silage (Nizami et al., 2010, 2011; Nizami & Murphy, 2011; Lehtomäki et al., 2008).

The majority of agricultural biogas plants use substrates in continuously stirred tank reactors (CSTRs) with a dry matter content of below 15% (so-called wet fermentation;

FNR, 2012a). Such systems are thoroughly stirred by a stirring device and usually consist of more than one biogas-producing fermenter, while applying no phase-separation between microbial conversion steps, such as hydrolysis or acidogenesis and methanogenesis. These biogas systems are called two (or more) stage biogas plants. In contrast to that, agricultural biogas plants with phase-separation converting substrates with a dry matter content of up to 40% (so-called dry fermentation; FNR, 2012a) have been rare up to now. Dry fermentation combined with a separation of process phases can lead to improvements due to the fact that optimal parameters for each microbial conversion step can be set. This was supported by the findings of Demirer and Chen (2005), who have achieved higher biogas yields in experimental two-phase systems compared to one-phase reactors.

Beside the configuration of biogas plants, the temperature for the fermentation in those systems also plays an important role. Although the majority of agricultural biogas plants are operated at mesophilic temperatures (FNR, 2012a), it has been assumed that thermophilic systems are more productive. Hence, a biogas system operated under thermophilic conditions can achieve higher methane rates than a comparable mesophilic system (Dugba & Zhang, 1999).

The biogas produced by agricultural biogas plants is versatile. The majority of agricultural biogas plants convert the biogas to electricity and heat via communal heating power stations (FNR, 2010). Prior to that, the biogas consisting of methane, CO_2, water vapor and hydrogen sulfide has to be purified. First of all, the biogas is desulfurized and dried due to the fact that hydrogen sulfide and water vapor react to produce sulfuric acid, which can corrode parts of the communal heating power station (FNR, 2010). Afterwards, the biogas can be converted to electricity and heat.

To inject biomethane into the natural gas grid, further purification steps are needed (FNR, 2010). Impurities, such as CO_2 and traces of oxygen are separated from the residual biomethane. After the addition of an odor-producing compound to the odorless biomethane and the adjustment to the gross calorific value of natural gas, the biomethane can be injected into the natural gas grid.

Beside the energy carrier methane, the digestates produced in agricultural biogas plants are also utilized and applied on agricultural lands as fertilizers. A survey of operators of German biogas plants in 2010 (n = 334) indicated that 78% of the digestates were applied mainly without any treatment to their own fields (DBFZ, 2011).

In contrast to a direct application of undigested manure as fertilizer, the digestate has an altered nutrient composition. The main differences consist in an increase in phosphor, potassium and total nitrogen, which are mainly fixed as inorganic compounds. Further, the dry matter content and the C/N ratio in the digestate are reduced due to the anaerobic digestion of organic compounds (FNR, 2010). Whether this leads, combined with an increased production of energy crops (need of carbon-rich soils), to a lack of carbon in soils is still in dispute (Willms et al., 2008). However, any such effects can be improved by other parameters, such as crop rotation (Willms et al., 2008).

1.3 The biogas production process

1.3.1 Anaerobic digestion of plant-derived biomass

The first step in the anaerobic digestion process is the hydrolysis of plant-derived carbohydrates, lipids and peptides (Figure 1.2). Energy crops, a widely used substrate for biogas plants, are rich in carbohydrates, such as the energy store starch or the plant cell wall polymers pectin, cellulose, hemicellulose and lignin. The degradation of these polymers is of major importance for the whole biogas-producing process.

Starch consists of a large number of D-glucose molecules forming the linear, helical amylose and the branched amylopectin. These polymers are easily degradable by bacteria with the help of amylases. For instance, α-amylase cleaves the α-glycosidic bonds within the starch polymer.

In contrast to easily degradable carbohydrates, the cell wall polysaccharides are more recalcitrant to bacterial hydrolysis due to the complex network of different types of polysaccharides.

Lignin, a complex aromatic heteropolymer, is the most recalcitrant component of plant cell walls. It can be slowly degraded under aerobic conditions by white-rot and partly brown-rot fungi (Dashtban et al., 2010). Only a few bacteria were identified with lignin

degrading activity, such as species of the *Streptomycetes*, *Sphingomonas*, *Pseudomonas* and *Acinetobacter* genera (Ahmad et al., 2010; Bugg et al., 2011). Different enzymes, such as laccases and peroxidases were essential ligninolytic enzymes. Laccases are multicopper oxidoreductases, which catalyze the oxidation of aromatic and non-aromatic compounds by radical-catalyzed reactions (Claus, 2004). Peroxidases, heme-containing enzymes, catalyze H_2O_2-dependent oxidations of lignin-associated aromatic compounds (Reddy & D`Souza, 1994). Furthermore, the enzyme glyoxal oxidase is also essential for the extracellular lignin degradation (Whittaker et al., 1999).

The cell wall polysaccharide, hemicellulose, consists of branched heteropolymers, such as xylan, xyloglucan, arabinoxylan and (gluco-) mannan, which were formed by different pentoses, such as xylose and arabinose and by hexoses, such as mannose and glucose. However, the structure of hemicellulose can vary strongly in different plants (Gaillard, 1965). Several hemicellulolytic enzymes are responsible for the modification and degradation of hemicellulose. Enzymes, such as xylanase and β-xylosidase are involved in the breakdown of xylan. The former enzyme cleaves the β-1,4-xylosidic bond within xylan, whereas the latter enzyme cleaves xylose residues from the non-reducing end of xylan. Furthermore, enzymes, such as β-mannase or arabinase, act on the hemicellulolytic polymers mannan and arabinan. Hemicellulolytic enzymes were summarized in different glycoside hydrolase (GH) families, such as GH 10, 11 and 43 (Henrissat, 1991; Cantarel et al., 2009). In particular, the GH families 10 and 11 compromise a high number of the enzymes acting on xylan (Collins et al., 2005).

Pectin, another component of the plant cell wall, is mostly composed of galacturonic acids, such as the α-1,4-linked homogalacturonan and rhamnogalacturonan (O'Neill et al., 1990). These polymers are linked to other cell wall polysaccharides and hence form part of the cellulosic, hemicellulosic network. Some of the pectinolytic enzymes, such as the (exo-) polygalacturonase, exo-polygalacturonosidase and rhamno-galacturonase are summarized in the GH family 28 (Henrissat, 1991; Cantarel et al., 2009). For instance, the polygalacturonase catalyzes the hydrolysis of the α-1,4-bond within the homogalacturonan polymer. This enzyme is mainly studied in the context of the fruit-ripening process of plants (Giovannoni et al., 1989; Downs et al., 1992), but also in the context of pectin modification or degradation performed by different microorganisms (Barnby et al., 1990; McKay, 1990; Karam & Belarbi, 1995). However,

further enzymes such as pectin lyase and pectin esterase are also involved in the degradation and modification of pectin (Jayani et al., 2005).

Furthermore, the homopolymer cellulose consists of D-glucose residues, which are linked to each other by β-1,4-glycosidic bonds and form long linear chains. Multiple layers of these linear polymers are linked to each other by hydrogen bonds forming crystalline microfibrils. For degradation to occur, the β-1,4-glycosidic bonds as well as the hydrogen bonds between the linear polymers must be cleaved by cellulases, i.e., endo- and exoglucanases and β-glucosidases (Lynd et al., 2002). The endoglucanases act within the homopolymer cellulose in an amorphous region and cleave the β-1,4-glycosidic bonds. The exoglucanases, such as cellobiohydrolases and glucanohydrolases, release cellobiose and glucose residues, respectively, from the end of the (crystalline) cellulosic chains. Finally, glucose residues are released from short glucose chains, such as cellobiose or cellodextrin by the β-glucosidases (Lynd et al., 2002). These cellulolytic enzymes are grouped in different GH families, such as GH 5, 6, 7, 9, 12 and 48 (Cantarel et al., 2009). However, the highest number of cellulase genes was grouped in the GH families 5 and 9 (Schülein, 2000).

A high number of anaerobic bacteria, belonging to the Clostridiaceae, Syntrophomonadaceae, Lachnospiraceae and Eubacteriaceae families, were identified to hydrolyze crystalline cellulose (Schwarz, 2001). Particularly, members of the Clostridiaceae family have a specialized extracellular cellulose-degrading enzyme complex, the so-called cellulosome. Several studies have been published, which analyzed the cellulosomal structure of *Clostridium* species and particularly *Cl. thermocellum* (Bayer et al., 1985; Bayer & Lamed, 1986; Lamed et al., 1987). Furthermore, cellulosomal structures were also detected within other anaerobic bacteria, such as *Acetivibrio* or *Bacteroides* (Lamed et al., 1987; Ponpium et al., 2000; Xu et al., 2003) and also within anaerobic fungal species, such as *Neocallimastix patriciarum* (Wang et al., 2011). Cellulosomal complexes consist of many polysaccharide degrading enzymes, such as cellulases and hemicellulases. These enzymes are linked to the non-catalytic subunit, scaffoldin, which performs different functions, such as the binding to the substrate cellulose and to the surface of the host cell (Bayer et al., 1994; Shoham et al., 1999).

1.3.2 Production of precursors to methanogenesis

The hydrolysis of polymers, such as carbohydrates, produces precursors to acidogenesis (Figure 1.2). The di- and monomers produced are transported into the cells and metabolized by various fermentative bacteria into volatile fatty acids (VFA), alcohols, CO_2 and H_2. Both, the hydrolysis of polymers and the production of VFA are performed by hydrolytic and fermentative bacteria. Members of the Clostridia class, such as *Clostridium*, *Ruminococcus*, *Caldicellulosiruptor* or *Anaerobacter*, degrade various carbohydrates and produce VFA and alcohols as fermentation end products (De Vos et al., 2009). Different studies on biogas-producing communities have already indicated an important role for these microorganisms (e.g., Klocke et al., 2007; Krause et al., 2008a; Schlüter et al., 2008; Liu et al., 2009; Krakat et al., 2010a; Wirth et al., 2012).

In contrast to acetate, the other VFAs have to be converted to acetate by acetogenic bacteria (Figure 1.2) to make them useable for methanogenesis. The oxidation of VFAs, such as propionate, is only thermodynamically favorable under reduced H_2 partial pressure, which can be achieved by a syntrophic interaction with H_2-scavenging microorganisms, such as hydrogenotrophic methanogens (Scholten & Conrad, 2000; Ahring, 2003). Furthermore, Siriwongrungson and coworkers (2007) have indicated that homoacetogenic bacteria could also act as H_2 sinks. They showed that the H_2 produced after butyrate oxidation was directly used together with CO_2 for the production of acetate via homoacetogenesis (Figure 1.2) at least under thermophilic, methanogenesis-repressed conditions. However, they supposed that homoacetogenic microorganisms also occur in normally operated biogas processes.

Different syntrophic VFA-oxidizing bacteria, such as *Syntrophomonas wolfei* (McInerney et al., 1981) or *Syntrophothermus lipocalidus* (Sekiguchi et al., 2000) and also syntrophic propionate-oxidizing bacteria, such as *Syntrophobacter fumaroxidans* (Harmsen et al., 1998) or *Pelotomaculum thermopropionicum* (Imachi et al., 2002), were identified. The transfer of H_2 between the VFA-oxidizing bacterium and its syntrophic H_2-scavenging methanogenic partner is enabled via direct interspecies transfer as shown for *Pelotomaculum thermopropionicum* and *Methanothermobacter thermautotrophicus* (Ishii et al., 2005).

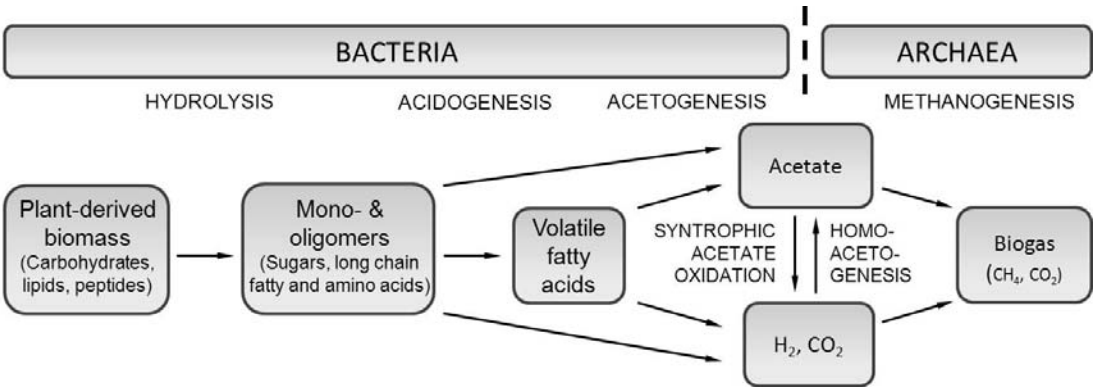

Figure 1.2 Scheme of the anaerobic digestion process leading to the production of biogas (modified after Weiland, 2010)

The acetate produced by syntrophic VFA oxidation can be directly converted by acetoclastic methanogens or can be oxidized to CO_2 and H_2 by syntrophic acetate-oxidizing bacteria (Figure 1.2). Hence, syntrophic acetate oxidizers compete with acetoclastic methanogens for acetate uptake, having an advantage at reduced acetic acid concentration and thermophilic temperatures (Ahring, 1995). Furthermore, this syntrophic reaction is also thermodynamically more favorable the lower the H_2 partial pressure (Ahring, 2003). Up to now, only few syntrophic acetate-oxidizing bacteria are known, which are capable to oxidize acetate in cooperation with H_2-scavenging partners: the rod-shaped strain AOR (Lee & Zinder, 1988), *Cl. ultunense* (Schnürer et al., 1996), *Thermacetogenium phaeum* (Hattori et al., 2000), *Thermotoga lettingae* (Balk et al., 2002), *Syntrophaceticus schinkii* (Westerholm et al., 2010) and *Tepidanaerobacter acetatoxydans* (Westerholm et al., 2011).

The breakdown of plant-derived biomass and the subsequent production of VFA, acetate and CO_2 and H_2 is a complex interaction of various microorganisms leading to the production of precursors to methanogenesis (Figure 1.2).

1.3.3 The production of methane

The main precursors to methanogenesis are acetate and CO_2 and H_2 (Figure 1.2), but also other precursors, such as formate, mono-, di- and trimethylamine or methanol can

be used for the production of methane by methanogenic archaea (Boone & Castenholz, 2001). The conversion of these precursors to methane has been well studied by different authors (Thauer et al., 1993; Blaut, 1994; Deppenmeier et al., 1996). Various enzymes play an important role in hydrogenotrophic, methylotrophic and acetoclastic methanogenesis and some of these enzymes are exclusively found in methanogens (Blaut, 1994).

The hydrogenotrophic pathway, using CO_2, H_2 or formate, starts with the initial reduction of CO_2 to formyl methanofuran for which H_2 or formate serves as electron donor (Deppenmeier et al., 1996). Then, several enzymes catalyze the subsequent stepwise reduction to methane. The H_2 supply can be achieved via direct interspecies transfer between the hydrogenotrophic methanogen and a syntrophic, H_2-producing bacterium (Ishii et al., 2005).

The methylotrophic pathway converts methanol or methylamines to methane and CO_2. One main difference to the hydrogenotrophic pathway is the way of electron donor supply for the reduction to methane. The reducing equivalents are obtained by an oxidation of a methyl group to CO_2, which is subsequently used to reduce other methyl groups to methane (Blaut, 1994).

Finally, the acetoclastic pathway converts acetate to methane and CO_2. The first step is the activation of acetate to acetyl-CoA, which is subsequently cleaved. The resulting methyl residue is then reduced to methane (Blaut, 1994).

Despite these changes, the last step of the methanogenesis, the reductive demethylation of methyl-CoM to methane, is found in the hydrogenotrophic, methylotrophic and acetoclastic pathways. This reduction is catalyzed by the methyl coenzyme-M reductase enzyme, whose gene has been often used as target for the characterization of methanogenic archaea (e.g., Nettmann et al., 2008; Steinberg & Regan, 2009; Tale et al., 2011; Zhu et al., 2011; Ellis et al., 2012).

Archaea with the capacity for methane production (so-called methanogenic archaea or methanogens) are found in six orders: Methanobacteriales, Methanococcales, Methanocellales, Methanomicrobiales, Methanosarcinales and Methanopyrales. Members of the Methanopyrales do not grow below 80 °C (Boone & Castenholz, 2001) and therefore play no role in the production of methane in biogas plants. Further, the Methanocellales and its mesophilic, hydrogenotrophic type strain *Methanocella*

paludicoda, which has been proposed recently by Sakai and coworkers (2008), have not yet been identified to play a role in biogas-producing plants.

The Methanobacteriales, Methanococcales and Methanomicrobiales orders encompass hydrogenotrophic methanogens using CO_2 and H_2 or formate for the production of methane. Some strains of these orders may also be capable of using methanol (Boone & Castenholz, 2001). Particularly members of the Methanobacteriales and Methanomicrobiales are well known as part of the methanogenic community in mesophilic and thermophilic biogas systems as they were identified in different studies (e.g., Bauer et al., 2008; Klocke et al., 2008; Schlüter et al., 2008; Krakat et al., 2010b; Kongjan et al., 2011). Their apparent abundance in biogas plants might be favored by the fact that they seem to be robust against environmental factors, such as increased nitrogen concentrations (Koster & Lettinga, 1984).

However, members of the Methanosarcinales were also identified as prevalent within mesophilic and thermophilic biogas-producing communities (e.g., Godon et al., 1997; Karakashev et al., 2005; Ziganshin et al., 2011; Ellis et al., 2012; Lerm et al., 2012). The two families of the Methanosarcinales order differ strongly from each other. Members of the Methanosarcinaceae are able to use the broadest spectrum of precursors (e.g., acetate, CO_2/H_2, methanol) for methane production, whereas members of the Methanosaetaceae are strict acetoclastic methanogens, exclusively using acetate for the production of methane (Boone & Castenholz, 2001). In particular, members of the latter group were identified as reacting more sensitively to high nitrogen or VFA concentrations (Karakashev et al., 2005; Nettmann et al., 2010), which can be accumulated during the biogas fermentation process.

1.4 Purported proliferation of pathogens in biogas systems

Agricultural biogas plants are still the focus of the public interest due to a potential risk for unintended proliferation and distribution of pathogens infecting animals, humans and plants. Pathogens derived from substrates, such as manure or energy crops, are

assumed to proliferate during the anaerobic digestion process bearing the risk of distribution through the application of the digestate as fertilizers on fields. The outbreak of the enterohemorrhagic *E*. *coli* str. O104:H4 (EHEC) in Germany 2011 increased the attention towards biogas production plants as a potential distributor of pathogens. During this outbreak, about 3,900 humans were infected by the *E*. *coli* str. O104:H4, suffering from (bloody) diarrhea and also from hemolytic-uremic syndrome (WHO, 2011). After extensive investigations, fenugreek sprouts and not biogas plants were identified to be the most likely cause of this foodborne infection (BfR, 2011).

Beside the *E*. *coli* strain, pathogenic members of the genus *Clostridium*, such as *Cl*. *botulinum*, *Cl*. *perfringens*, *Cl*. *difficile* or *Cl*. *tetani*, were also alleged to proliferate in biogas plants leading to an endangering of humans and also animals health. For instance, *Cl*. *botulinum*, which was recently detected in cattle feces (Dahlenborg et al., 2003), can cause botulism in cattle. This pathogen in addition to other clostridial pathogens were assumed to find perfect growth conditions in biogas plants due to the fact that numerous, non-pathogenic *Clostridium* species, such as *Cl*. *thermocellum* or *Cl*. *stercorarium*, play an important role in biomass degradation and the subsequent acidogenic pathway. However, some studies already indicate that the risk for an unintended proliferation of pathogenic *Clostridium* species is rather low (e.g., Dohrmann et al., 2011).

Additionally, other pathogens, such as *L*. *monocytogenes*, *Campylobacter jejuni* or *Salmonella enterica*, which are also in focus of the public interest as causing foodborne infections in humans and were also considered in this study.

An unintended proliferation of pathogens may also affect plants due to the application of digestates as fertilizer. Particularly plant pathogens infecting agricultural crops with economic importance may raise the concerns not only of farmers. One important plant pathogen is *Clavibacter michiganensis* (Actinobacteria), which infects tomatoes and potatoes (Gartemann et al., 2003). Various attempts have been made to find a control method of this plant-pathogenic species. Wittmann and coworkers (2010) isolated proteins from a *Clavibacter michiganensis* infecting bacteriophage, which showed *Clavibacter*-specific bacteriolytic activity leading to a potential biocontrol of this plant pathogen. However, other plant-pathogenic species are also responsible for infections in potatoes or tomatoes, such as *Synchytrium endobioticum, Rhizoctonia solani*, *Helminthosporium solani* or *Ralstonia solanacearum*. Further plant pathogens, such as *Fusarium oxysporum* and *Sclerotinia sclerotiorum* can also lead to infections of grain.

1.5 Characterization and monitoring of the microbial community

A deep understanding of the microbial community within biogas reactor systems is of major importance for the improvement of such systems. Culture-dependent methods, although indispensable for the detection of new isolates, can only reflect a marginal amount of the broad microbial diversity due to limitations in cultivation conditions. Different authors have indicated that the number of cultivable bacteria varies between 0.1 and 1% in seawater and meso- and oligotrophic lake habitats using viable plate count analysis (Ferguson et al., 1984; Staley & Konopka, 1985). Further, Wagner and coworkers (1993) have reported higher recoveries of 14% for activated sludge samples using specialized media. However, culture-independent methods are important to gain deeper insights into the microbial structure.

Therefore, a polyphasic approach composed of different culture-independent methods was performed for the characterization, quantification and monitoring of the microbial community residing in the two-phase biogas reactor systems. On the one hand, the culture-independent methods were based on the genetic information of cells, applying 16S rRNA (*rrs*) gene sequence analysis, terminal restriction fragment length polymorphism (TRFLP) fingerprinting, microbial metagenome and quantitative polymerase chain reaction (qPCR) analyses. On the other hand intact, but not cultivated cells were analyzed by fluorescence *in situ* hybridization (FISH) as well as 4′,6-diamidino-2-phenylindole (DAPI) and propidium iodide (PI) staining. Both approaches were extensively used to analyze microbial communities in different environmental habitats as indicated below.

1.5.1 Analysis of bacterial and archaeal *rrs* gene sequences

The construction and analysis of gene libraries is a widely applied method for the determination of the composition of microbial communities in different habitats (e.g., Großkopf et al., 1998; Vetriani et al., 1999; Danon et al., 2008; Soo et al., 2009) as well as in biogas reactor systems (e.g., Chouari et al., 2005; Klocke et al., 2007, 2008; Cardinali-Rezende et al., 2009; Liu et al., 2009; Biswas & Turner, 2012). The *rrs*

gene is an often used and well-studied target gene encoding the 16S rRNA, which forms together with different proteins the 30S small subunit of bacterial and archaeal ribosomes. The *rrs* gene is 1.541 kb long, as identified after the analysis of *E*. *coli* in 1978 (Brosius et al.) and consists of nine hypervariable regions (van de Peer et al., 1996). This allows the application of different phylogenetic approaches, such as the differentiation between bacterial or archaeal groups on a higher or lower taxonomic level depending on the *rrs* region used for primer design. In this study, primer sets were used for the characterization of the bacterial and archaeal community, which spans the first five hypervariable regions.

However, independent of the target gene, this method is based on a DNA amplification step using target specific primer sets. Afterwards, the PCR product is cloned into plasmids, which were subsequently transformed into competent *E*. *coli* cells. Cells transformed were cultivated and the plasmids carrying the gene of interest were isolated and sequenced. The sequence data obtained yields information about the composition of the target community.

Furthermore, with the help of different statistical parameters, deeper insights into the diversity and evenness of the underlying microbial community can be obtained. The Simpson and Shannon diversity indices (Simpson, 1949; Shannon & Weaver, 1963) reflect the quantity of operational taxonomic units (OTUs) and the distribution within these OTUs, assessing the diversity of the target community. The parameter Evenness (Lloyd & Ghelardi, 1964; Hill, 1973) gives information about the distribution of OTUs obtained. So a value of 1 means an equal distribution of OTUs and a reduced value indicates a strong prevalence of a specific OTU. Additionally, to check the quality of the coverage of the gene libraries, Good's coverage (Good, 1953) and the Chao-I estimator (Chao, 1987) can also be calculated. Good's coverage indicates the percentage coverage of the underlying microbial community, whereas the Chao-I estimator values indicate the extrapolated number of species or in this case OTUs. Both parameters take those species (or OTUs) into account, which have only a rare abundance.

1.5.2 Terminal restriction fragment length polymorphism

The TRFLP method is a powerful, fingerprinting tool for the analysis and comparison of microbial communities within different habitats. Spatial and temporal changes in the composition of microbial communities can also be monitored (Lukow et al., 2000; Marsh, 2005). This method has been introduced by Liu and coworkers in 1997. Up to now, this valuable method has also been widely applied by different authors in the field of biogas production (e.g., Feng et al., 2010; Wang et al., 2010; Carballa et al., 2011; Pycke et al., 2011; Ziganshin et al., 2011).

In comparison to other fingerprinting methods, such as denaturing gradient gel electrophoresis (DGGE), amplified ribosomal DNA restriction analysis (ARDRA) and single strand conformation polymorphism (SSCP), the TRFLP method bears two main advantages. First, this method allows the analysis of a large number of samples at once and can be seen as high-throughput method (Enwall & Hallin, 2009). Second, the separation of DNA fragments in a gel-filled capillary as performed by the TRFLP analysis leads to a higher resolution and a more detailed estimation of the fragment size. Hence, the immediate digital output is another advantage leading to a better comparison of multiple profiles (Marsh, 1999).

TRFLP analysis is based, as with many culture-independent methods, on a PCR step (Figure 1.3) amplifying the ribosomal, but also functional genes. One of the primers used for the PCR is labeled with a fluorescent dye, such as 6-carboxyfluorescein (FAM) or cyanine 5 (Cy5). After DNA amplification, the fluorescently labeled PCR product is digested by a restriction endonuclease (Figure 1.3), which reveals the evolutionary based differences within the target gene (Marsh, 2005). For a high resolution of a complex community, a digest with two or even more restriction endonucleases can reduce the possibility that more than one microbial group results in the same fragment size (Kitts, 2001). Afterwards, the fluorescently labeled fragments were separated together with an internal size standard by an automated capillary gel electrophoresis system after electrokinetic injection (Figure 1.3). The use of an internal size standard allows a size calculation of the terminal restriction fragments (TRFs) with an accuracy of one base up to a fragment size of 700 bp (Kitts, 2001; Schütte et al., 2008).

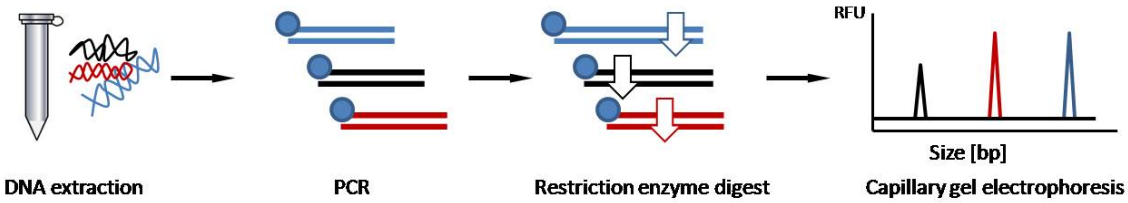

Figure 1.3 Short workflow of the sample preparation for the TRFLP analysis. RFU – channel intensity

The raw data obtained have to be processed before data analysis and interpretation can be performed. One point is to separate true fragments from the background noise. Several methods have been applied by different authors, such as using a manually set baseline threshold (Osborn et al., 2000; Lueders & Friedrich, 2003), applying a constant percentage (Lukow et al., 2000; Sait et al., 2003) or a variable percentage threshold (Osborne et al., 2006).

Furthermore, an analysis of at least duplicate samples, taking only TRFs represented in both samples into account, could reduce potential "background" fragments as reported by Dunbar and coworkers (2001). Additionally, these authors have developed recommendations for the normalization of TRFLP data to solve the issue of different loads of DNA to the capillary gel electrophoresis. For normalization, the total fluorescence (based on TRF height) of each sample has to be summed, reflecting the total DNA injected. Afterwards, the sample with the smallest amount of total fluorescence is successively divided by the total fluorescence of the other samples in the dataset resulting in a correction factor for each sample. This factor is then multiplied by the height of each TRF of the respective sample resulting in the same total fluorescence as the sample with the smallest total fluorescence. This normalization method for TRFLP data was used as basis for further data analysis in this study.

However, another approach also addressing the issues of fragment identification from background noise as well as the variations in DNA loads has been introduced by Abdo and coworkers (2006). Their statistical method also produced standardized data ready for further data analysis. First, each fragment area was divided by the total area of all fragments of one sample, resulting in relative fragment areas. Then, to distinguish between true and background fragments, the standard deviation of the sample was calculated and fragments with a relative area, showing a larger value than three

standard deviations, were identified to be true. This iterative procedure was performed until no true fragment could be identified anymore.

Afterwards, these processed data must be aligned due to slight variations in separation accuracy in order to compare TRFLP profiles derived from various samples. In earlier studies, this has been achieved by a manual binning, which is a time-consuming and error-prone process. An automated and hence more sophisticated approach is the use of alignment tools, such as the web-based T-Align (Smith et al., 2005) and T-Rex tool (Culman et al., 2009). Both tools use an algorithm, which clusters all TRFs within a specific clustering threshold (in this study 0.8 bp), starting with the smallest TRF within the samples. The clustering threshold can be adjusted by the user in both applications. However, the T-Rex software is more versatile, allowing the analysis of more than duplicate samples and the use of different output options.

This multi-level processing of data can be performed on the basis of the TRF height or area. Different authors have favored the TRF height (Dunbar et al., 2001; Caffaro-Filho et al., 2007) or the TRF area (Kitts, 2001; Sait et al., 2003), but other show no preference between the both approaches (Schütte et al., 2008). Hence, both methods can be used for data processing and the subsequent graphic visualization of the results, but also for further statistical approaches, such as the calculation of similarity indices. The calculation of these indices allows an estimation of the similarity of two different samples. In this study, the Jaccard index improved by Chao (Chao et al., 2005) and the Bray-Curtis similarity index (Magurran, 1988) were used. Whereas the Jaccard index is a qualitative index based on the presence and absence of values (in this case TRFs), the Chao-Jaccard index also takes the potential presence of unseen shared species of two samples into account (Chao et al., 2005). In contrast, the Bray-Curtis index (Magurran, 1988) also gives information about the numerical quantity of values (TRFs) from two samples.

For further interpretation of potential differences of TRFLP results, statistical ordination methods, such as non-metric multidimensional scaling (NMDS), can be applied. The NMDS approach tries to reduce the complex correlation between objects (samples) on the basis of the order of similarity (or dissimilarity) values to resolve ideally in a two-dimensional space by applying an iterative algorithm (Leyer & Wesche, 2008). In contrast to other ordination methods, NMDS only requires a monotonous relationship between the similarity values of the objects in the data matrix. To confirm the quality of such ordination methods, Kruskal and coworkers (1964) have introduced a factor of

goodness, the so-called stress value, which has been reinterpreted by Clarke (1993). He suggested that a stress value of up to 0.1 shows a good ordination and stress values up to 0.2 still can lead to usable ordination plots.

In this study, the Bray-Curtis similarity index was used as basis for non-metric multidimensional scaling. The stress values obtained, which described the quality of the NMDS analysis, were indicated for each NMDS plot. Furthermore, a scree plot analysis was constructed for ensuring that the reduction to two dimensions is appropriate. This test has been proposed by Cattell (1966) and has been used in the context of the multidimensional scaling by Kruskal and Wish (1978).

1.5.3 Analysis of microbial metagenomes by high-throughput DNA sequencing

High-throughput DNA sequencing approaches, so-called next generation sequencing methods, were applied for whole genome sequencing, metagenome or transcriptome sequencing and also further applications. In contrast to the Sanger dideoxy sequencing method, which was introduced in 1977 (Sanger et al., 1977), these methods allow an extremely increased sequence throughput at less cost and in less time (Margulies et al., 2005).

In 2005, 454 Life Science (now a Roche Company, Branford, USA) introduced the Genome Sequencer (GS) 20 system applying the 454-pyrosequencing method (Margulies et al., 2005), which since then has been widely employed (e.g., Leininger et al., 2006; Turnbaugh et al., 2006; Warnecke et al., 2007; Krause et al., 2008a; Schlüter et al., 2008). The recent available GS FLX^{TM} Titanium system is a further development, which when combined with the latest chemistry, allows the analysis of one million sequences per run with a mean sequence length of 800 bp, accounting for 700 Mb of total sequence information (454 Life Science, 2012).

Recently other high-throughput sequencing technologies have been introduced, such as the HiSeq and MiSeq systems by Illumina (San Diego, USA) and the SOLiD^{TM} system by Applied Biosystems (a Life Technologies brand, Carlsbad, USA). These methods result in shorter sequence length than achieved by 454-pyrosequencing, but

are able to sequence more bases per run (up to 600 Gb) (Applied Biosystems, 2011; Illumina Inc., 2012). In 2011, Pacific Biosciences (Menlo Park, USA) commercialized their SMRT™ sequencing technology, which enables mean sequence length of up to 3,000 bp (Pacific Biosciences, 2012). These technical developments in the field of the next generation sequencing have raised the number of (meta-) genomic studies immensely.

At the end of 2012, the Genome OnLine Database (GOLD; Pagani et al., 2012) encompassed a total number of 18,896 genomes for worldwide access and comprehensive analysis of genomic data. Furthermore, a number of 345 metagenomic studies analyzing 2,145 environmental samples were also deposited in the GOLD database. A total of 10 studies each focused on waste water and solid waste samples. However, the greatest effort has been applied to analyze aquatic habitats with 149 metagenomic studies.

For the analysis of metagenomes, the 454-pyrosequencing technology is favorable due to the fact that a relatively high sequence length can be achieved. Hence, it was also used in this study. First of all, highly pure and unshared genomic DNA, extracted from an environmental sample, is needed for the downstream 454-pyrosequencing (Figure 1.4), which has been described in detail by Margulies and coworkers (2005) and Droege and Hill (2008). After DNA extraction and purification, adaptors (A and B) are ligated to the DNA (Figure 1.4), which is nebulized into 300 to 800 bp long fragments. These fragments are then bound to sepharose beads by their adaptors. Afterwards, a “water in oil” amplification of these DNA fragments is performed (Figure 1.4), which results in millions of the same DNA fragments per bead. Each of these beads is loaded into a well of a 454 PicoTiterPlate™ together with the reaction chemistry for sequencing. When the plate is loaded onto the GS FLX™ system, nucleotides are flowed successively across this plate in a fixed order. If a nucleotide is complementary to the sequence, it will be incorporated in the DNA strand by the DNA polymerase and a light signal will be generated. The intensity of the light signal is to a certain extent proportional to the number of nucleotides incorporated (Figure 1.4). This enzymatic reaction is initialized by the incorporation of the nucleotide into the DNA strand. The pyrophosphate released can be converted into ATP in the presence of adenosine 5'-phosphosulfate, which is catalyzed by the ATP sulfurylase enzyme. Afterwards, the ATP-required conversion of luciferin to oxyluciferin, which is catalyzed by the luciferase enzyme, produced the light signal detected by a charge-coupled

device camera. Due to the fact that the type of nucleotide which is flowed across the plate is known, the sequence of the DNA strand can be amended. After the light signal detection, the residual nucleotides per well are degraded, a reaction, which is catalyzed by the enzyme apyrase. Then, a second type of nucleotide is flowed across the PicoTiterPlate™ and will be incorporated, if complementary. These steps are repeated until the decoding of the DNA sequence is completed.

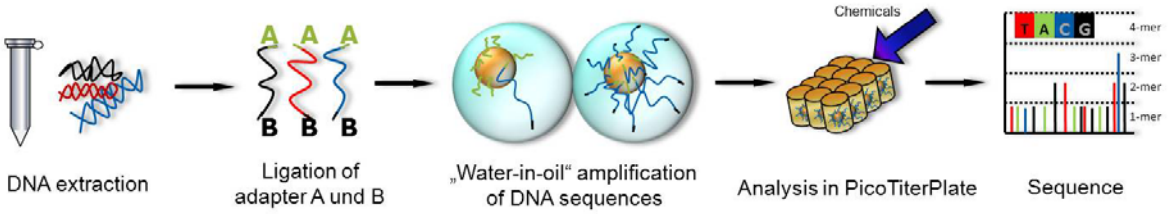

Figure 1.4 Short workflow of the 454-pyrosequencing analysis using the GS FLX™ Titanium System (454 Life Science, a Roche Company, Branford, USA)

The analysis of such huge datasets is a sophisticated effort for bioinformatics. In the case of whole genome studies, the assembly of many overlapping metagenomic sequences is performed, which can also compensate the sequencing error rate (Margulies et al., 2005). In contrast to that, an assembly of metagenomic sequences is limited particularly when analyzing very complex microbial communities (Mende et al., 2012). Further, a taxonomic assignment of metagenomic sequences assembled to large contigs is only reliable on higher taxonomic levels (Schlüter et al., 2008). To achieve more detailed phylogenetic information about the metagenomic sequences, no assembly was performed in this study.

Phylogenetic information can be drawn on the basis of metagenomic sequences encoding the 16S rRNA. Furthermore, the metagenomic sequences representing functional genes can improve the phylogenetic insights. Beside these phylogenetic assignments, such a metagenomic approach also provides information of the genetic potential and hence the enzymatic capacity of a specific microbial community, which is in contrast to an exclusive analysis of the *rrs* gene. These different applications of sequence interpretation have been applied by various authors analyzing the metagenome in different habitats (e.g., Bench et al., 2007; Krause et al., 2008a; Kröber et al., 2009). In this study, these analyses were performed with the MetaSams platform 0.99, which has been recently introduced by Zakrzewski and coworkers (2013). This platform, accessible via a web interface provided by the Center for

Biotechnology (Bielefeld University, Bielefeld, Germany), has integrated different approaches for metagenomic data analyses.

1.5.4 Quantification of bacterial *rrs* genes by quantitative PCR

The qPCR technique is an often applied method for the detection and quantification of microorganisms. Several authors have quantified methanogenic or biogas communities on the basis of the *rrs* gene applying qPCR (e.g., Yu et al., 2005, 2006; Bergmann et al., 2010; Blume et al., 2010). This method follows the principle of a PCR, but allows a simultaneous quantification of DNA after each qPCR cycle due to double-strand (ds) DNA-intercalating fluorescent dyes or group-specific fluorescently labeled probes. Thereby, the fluorescence signal detected reflects the concentration of the target gene in real-time (Zhang & Fang, 2006). The dsDNA-intercalating fluorescent dye (e.g., SYBR Green) can be easily used with each standard PCR protocol, but it also presents some problems. The fact that these dyes bind unspecifically not only to the target dsDNA, but also to primer dimers or non-target DNA could distort the qPCR results (Sharkey et al., 2004; Zhang & Fang, 2006).

More specific is the use of group-specific, fluorescently labeled probes (e.g., TaqMan probes) and its corresponding primer pairs. The TaqMan probe is labeled by a reporter (e.g., FAM) and a quencher dye (e.g., TAMRA) and binds to the target gene within the binding site of the primer pair. Due to the close proximity of the reporter and the quencher dye, the fluorescent signal is repressed. During DNA amplification the TaqMan probe is degraded by the exonuclease activity of the DNA polymerase, which leads to an enlarged distance between both dyes. Now, the detection of the fluorescence of the reporter dye is possible. These and further general aspects of the qPCR analyses have been reviewed in detail by different authors, such as Bergmann (2012) and Zhang and Fang (2006).

In this study, a TaqMan approach, targeting the *rrs* gene, was used for the absolute quantification of both Bacteria as a whole and a specific putatively process-relevant bacterium.

1.5.5 Microscopical analyses

The use of microscopical analyses, such as FISH or DAPI staining, allows a visualization of microbial cells and has been widely applied by different authors to gain information about the number of microbial cells in various biogas reactors (e.g., Burrell et al., 2004; Chouari et al., 2005; Krakat et al., 2010b; Nettmann et al., 2010; Biswas & Turner, 2012). DAPI staining allows the detection of all microbial cells due to the fact that DAPI can pass through intact membranes and intercalates in the minor groove of the DNA. In contrast to that the fluorescent dye PI intercalates in DNA and RNA, but only within cells having reduced membrane integrity. Hence, this dye has been often used for estimations of potential cell damage, for instance, in flow cytometry analyses (e.g., Belloc et al., 1994; Fröhling, 2010; Khan et al., 2010). However, potential cell damage, indicated by the PI staining, could also be a reversible process as indicated by Davey and Hexley (2011). They showed that a certain number of stressed yeast cells did not incorporate PI after some time of recovery. Therefore, a reduced membrane integrity detected by PI staining may at least indicate changes in the cell status.

For a specific differentiation of microbial groups, FISH has been developed by Amann and coworkers (1995). The functional principle of this method lies in the binding of fluorescently labeled oligonucleotide probes to the complementary region within the ribosomal RNA of the target cells. Cells hybridized with a fluorescently labeled probe could then be visualized by fluorescence microscopy.

Depending on the samples analyzed, the background fluorescence, caused by plant material, could infer the detection of the probe-labeled cells. Therefore, further developments of the FISH method, such as the Catalyzed Reporter Deposition FISH (CARD-FISH; Speel et al., 1999; Pernthaler et al., 2002) and the Double Labeling of Oligonucleotide Probes for FISH (DOPE-FISH; Stoecker et al., 2010) have been proposed for improving the signal intensity and compensating the background fluorescence. The DOPE-FISH method is based on the fluorescent labeling of the 5’ and 3’ end of oligonucleotide probes. In contrast, the CARD-FISH method is based on the binding of oligonucleotide probes labeled with horseradish peroxidase and a separated signal amplification using a fluorescently labeled tyramide.

Several recent studies use a variety of oligonucleotide probes for targeting different groups of microorganisms. The online resource probeBase (Loy et al., 2007) gives an overview and detailed information of probes designed for different microbial groups.

1.6 The Aims of this study

The main aim of this study was the characterization, quantification and monitoring of the microbial community in three identically constructed phase-separated leach-bed biogas systems under thermophilic to hyperthermophilic conditions. A deep understanding of the microbial community involved in the breakdown of plant-derived biomass and the subsequent production of methane is of major importance for a further improvement of biogas reactors.

The biogas systems analyzed in this study consisted of a leach-bed reactor (LBR) for hydrolysis and acidogenesis, a leachate storage reactor and a downstream anaerobic filter reactor (AF) for methanogenesis. The LBR was supplied with rye silage and straw over a period of 21 days and was operated at temperatures from 55 to 75 °C. The temperature of the AF remained at 55 °C throughout the experiment.

In detail, the various aspects listed below were analyzed to achieve the main aim.

- To derive an overview about the microbial community in the two-phase biogas system, the bacterial and archaeal community in the LBR and in the downstream AF was characterized.
- To check the intended separation of process phases within this phase-separated biogas system, the spatial distribution of the microbial community was analyzed.
- To assess changes in the microbial community as a consequence of biomass degradation, the bacterial and archaeal community was analyzed at different time points within the 21-day fermentations of one load of substrate.
- To assess temperature-dependent changes, the bacterial and archaeal community was analyzed during the stepwise temperature increases in the LBR.

- To gain deeper insights into the anaerobic digestion of plant-derived biomass, the genetic potential for the expression of glycoside hydrolases, enzymes involved in the breakdown of glycosidic linkages of carbohydrates, was determined.
- To evaluate the putative risk of an unintended proliferation of pathogens, selected pathogens and enzymes relevant for pathogenicity were analyzed.
- To evaluate the effect of a bioaugmentation with compost at hyperthermophilic temperatures, the microbial community and the biogas reactor performance were analyzed after bioaugmentation.
- To determine the total number of microorganisms, Bacteria, Archaea and a putatively process-relevant bacterium residing in the two-phase biogas system were quantified.

These community analyses were performed applying different culture-independent methods. The polyphasic approach comprised the construction of *rrs* gene libraries and the application of the TRFLP fingerprinting method to characterize and monitor the community. Furthermore, the analysis of microbial metagenomes also revealed insights into the genetic potential of the microbial community in the biogas system. The quantification of Bacteria, Archaea and the putatively process-relevant bacterium was performed by qPCR analyses based on the *rrs* gene and by microscopical studies of intact, but not cultivated cells.

2 MATERIAL AND METHODS

2.1 The two-phase leach-bed biogas systems

2.1.1 Reactor setup and operation

Three identically constructed two-phase biogas systems, which have been operated at the ATB (Potsdam, Germany) since 2006 by M. Schönberg (Schönberg & Linke, 2012), were analyzed in this study. The majority of the results refer to the first reactor system. The second and third reactor system was analyzed at specific time points to confirm the reproducibility of the results.

These two-phase biogas systems consisted each of three stainless steel reactors (Figure 2.1) with gastight top covers of acryl glass: a leach-bed reactor (LBR; net volume 100 L), a leachate reservoir (LR; net volume 60 L) and a downstream anaerobic filter reactor (AF; net volume 30 L) with 390 packings (Bioflow 40; Rauschert GmbH, Judenbach-Heinersdorf, Germany) each with a surface area of 305 m^2 m^{-3}. Two internal circulations of leachate were applied using membrane pumps (W100, Wilden Pump & Engineering LLC, Grand Terrace, CA, USA) to distribute nutrients, microorganisms and to keep the moisture and temperature level consistent. Each LBR was supplied discontinuously with 10 kg of rye silage (agricultural farm Damsdorf GbR H. & T. Wessels, Damsdorf, Germany) with a chaff length of 2 cm (silage period 100 days without an ensiling agent). In addition to the silage, 0.5 to 1.0 kg of winter barley straw (Lehr- und Versuchsanstalt für Tierzucht und Tierhaltung e.V., Groß Kreutz, Germany) or wheat straw (agricultural farm Bornim, Potsdam, Germany) were

used as bulking material. The rye silage was stored at 4 °C and the straw material at room temperature until usage. The retention time of the substrates was 21 days. After that fermentation period, the digestate was removed and each LBR reactor was refilled with fresh substrate.

All reactors were heated by a water jacket. Each AF reactor was operated throughout the experiment at a temperature of 55 °C, whereas the temperature of the LBR reactor was increased stepwise from 55 to 75 °C by 5 °C increments. Three fermentation periods of 21 days were conducted at each of the mentioned temperature regimes (LBR 55 - 75 °C) before further temperature increase was applied (Figure 2.2). After the temperature regime of 70 °C, a bioaugmentation by addition of 4-week-old compost (5 kg, OTS content 14.55%, pH 8.17; Biowork GmbH, Schmergow, Germany) to the substrate was conducted while maintaining the LBR temperature at 70 °C. After two fermentations with compost lasting 21 days, 10 kg of rye silage and 1 kg of straw material were digested again in the LBR for 21 days at 70 °C as a control. Afterwards, the temperature regime in each LBR was increased to 75 °C following the previous scheme. To ensure that the micronutrients were not a limiting factor for microbial growth, approximately 50 g of a DSMZ 144 micronutrient medium (2.5x concentrated; DSMZ GmbH, Braunschweig, Germany) was added to each AF before reactor restart with new substrate.

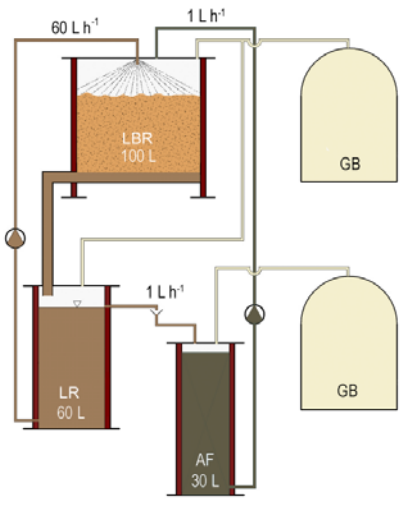

Figure 2.1 Scheme of the thermophilic two-phase leach-bed biogas reactor system. Circulation rates of the two internal leachate circulations were indicated. LBR, leach-bed reactor (net volume 100 L); LR, leachate reservoir (net volume 60 L); AF, anaerobic filter reactor (net volume 30 L); GB, gas bag (modified after Schönberg & Linke, 2012)

2.1.2 Analysis of process parameters

To monitor the biogas process, various process parameters were determined by the analytical chemistry work group at the ATB. Prior to each 21-day anaerobic digestion, the pH value (cf. pH measurement below), dry matter and the organic dry matter (ODM) content of the substrates were measured. The dry matter was determined through evaporation of the water content in substrates by heating to 105 °C until no further weight loss occurred. The ODM was determined by ashing the samples at 550 °C. After 21 days of fermentation, the degradation of organic material was calculated based on the ODM before and after the fermentation. This value was corrected by the nondegradable lignin fraction of the substrate supplied.

During the first five days of fermentation, pH, chemical oxygen demand (COD) and concentrations of acetic acid, n-butyric acid, propionic acid, valeric acid, total VFA, ethanol and propanol in the leachate derived from the LBR and the AF were measured once a day. Afterwards, the intervals were enlarged to two or three days.

The pH was measured using a calibrated pH meter 340i (WTW GmbH, Weilheim, Germany).

The COD was determined using potassium dichromate solution for solid samples and the COD-cuvette-test for liquid samples (Hach Lange GmbH, Düsseldorf, Germany).

The concentrations of acetic acid, n-butyric acid, propionic acid, valeric acid, ethanol and propanol were analyzed after filtration of a cold water extract with toluol by the Varian CP-3800 gas chromatograph (Varian Inc., Palo Alto, CA, USA) and a Permabond®-FFAP capillary column (Macherey-Nagel GmbH & Co. KG, Düren, Germany). The VFA were calculated as acetic acid equivalents (HAc eq.).

The total ammonia nitrogen (NH_4-N) was determined once a week. For this purpose, the samples were analyzed by a Vapodest 20 distillations system (C. Gerhardt GmbH & Co. KG, Königswinter, Germany). The concentration of free ammonia (NH_3) was calculated according to Anthonisen and coworkers (1976) using the following formula:

$$NH_3 = (\text{total ammonia nitrogen} * 10^{pH}) (K_b/K_w + 10^{pH})^{-1};$$

where the total ammonia nitrogen concentration is measured in g L^{-1}, K_b/K_w is $e^{(6344/(273+t))}$ with t equal to the temperature in °C.

The biogas generated was collected in TECOBAG gas bags (100 L, Tesseraux Spezialverpackungen GmbH, Bürstadt, Germany). Every day, an automatic gas analysis was conducted by a TG05/5 drum-type gas meter (Ritter Apparatebau GmbH & Co. KG, Bochum, Germany) and a SSM 600 biogas analyzer (Pronova Analysentechnik GmbH & Co. KG, Berlin, Germany). The biogas obtained was standardized to the norm temperature 0 °C (273.15 K) and to the norm pressure of 1,013 hPa with the following formula:

$$Biogas_{normed} = biogas_{measured} * ((p_{measured} - p_{H20})\ T_o\ (T_{measured} * p_o)^{-1}),$$

where $p_{measured}$ is the air pressure at the point of measurement, p_{H2O} is vapor pressure of water at the point of measurement, T_o is the norm temperature (273.15 K), $T_{measured}$ is the temperature in Kelvin at the point of measurement and p_o is the norm air pressure (1,013 hPa).

Then, the $biogas_{normed}$ was calculated on the basis of the total organic substances used for biogas production (including ODM, VFA and alcohol). The biogas data were provided by M. Schönberg (ATB, Potsdam, Germany) for subsequent data analysis.

2.1.3 Reactor sampling

Depending on the method applied, different samples were taken from the biogas reactor system. Samples were taken at the earliest after one fermentation period of 21 days at each temperature regime (LBR 55 - 75 °C; Figure 2.2) to ensure adaption of the microbial community to the increased temperature. The one exception was the experimental run 12 (Figure 2.2) which was analyzed directly after temperature increase to 70 °C in order to monitor the immediate bacterial response to temperature increase.

About 50 g of the substrate samples (i.e., rye silage (S), straw (St) and compost (C)) were taken before filling the LBR. The leachate samples (L) of the LBR (approximately 50 mL each) were obtained from the leachate reservoir, whereas the leachate samples of the AF were derived from the plug of the AF reactor (Figure 2.1). These samples were taken after draining the plug by 500 mL to prevent sampling of stale leachate

within the tube. The digestate samples (D, approximately 50 g each) were obtained after a fermentation period of 21 days from the LBR at each temperature regime. Before aliquotation, the digestate was mixed manually.

The packing (P) samples of the AF were taken from the upper half of the AF at each temperature regime of the LBR. The gastight reactor was opened at the end of the fermentation period to prevent a disturbance of the biogas production process. The biofilms of these packings were rinsed with 1x phosphate-buffered saline (1x PBS; pH 7.4, 80 g L^{-1} NaCl, 2 g L^{-1} KCl, 26.8 g L^{-1} Na_2HPO_4 x 7 H_20, 2.4 g L^{-1} KH_2PO_4) in order to remove the planktonic cells and were afterwards detached using a sterile scalpel. All samples were stored at -20 °C until further processing.

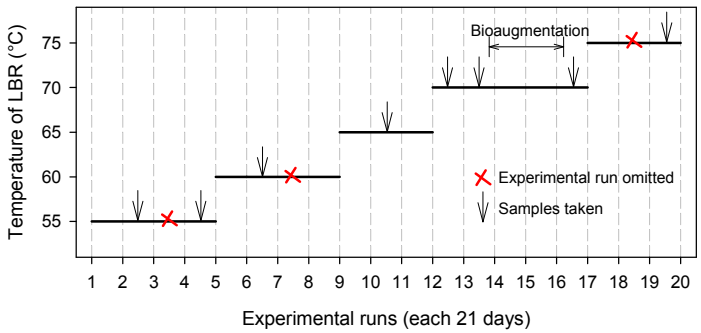

Figure 2.2 Experimental runs of the three two-phase biogas systems and sampling of the first biogas system. Arrows, samples taken for molecular biological analyses; x, data of these experimental runs were omitted from results due to technical problems

2.2 Extraction and quantification of genomic DNA

2.2.1 DNA extraction protocols

To evaluate the bias caused by DNA extraction and to define the standard DNA extraction protocol for the following analyses, four DNA extraction methods were compared. Digestate (0.25 g) derived from the LBR was used for extraction and the efficiency and reproducibility subsequently analyzed using the TRFLP method. The

different DNA extraction methods were performed applying the PowerSoil® DNA Isolation Kit (MO Bio Laboratories, Inc., supplied by Dianova GmbH, Hamburg, Germany), the FastDNA® Spin Kit for Soil (MP Biomedicals GmbH, Heidelberg, Germany) as well as a step by step DNA extraction protocol with and without a beating step. Both DNA extraction kits are based on a mechanical cell lysis and were used according to the manufacturer's instructions. The step by step protocol without a beating step used chemicals (SDS) and enzymes (lysozyme) for cell lysis. The fourth protocol, the step by step DNA extraction with beating step (cf. protocol below) combined the chemical and enzymatic lysis with a beating step on a test tube shaker for 10 min at maximum power, using sterile glass beads. Depending on the applied molecular analysis, two different DNA extraction protocols were applied as standard protocols.

The FastDNA® Spin Kit for Soil (MP Biomedicals GmbH, Heidelberg, Germany) was applied as standard DNA extraction protocol for TRFLP analyses, *rrs* gene library construction and qPCR analyses. Cell pellets were collected from 2 to 4 mL of leachate by centrifugation at 14,000 x g for 10 min (C5417R centrifuge; Eppendorf GmbH, Hamburg, Germany) and were added directly to the supplied Lysing Matrix E tubes. To isolate DNA from solid materials, 0.2 g of digestate from the LBR, 0.2 g of biofilm material from the packing of the AF and 0.05 g of straw material were added directly to the tubes mentioned above. The subsequent DNA extraction was performed as described in the manufacturer's instructions.

For archaeal positive controls of the *rrs* gene amplification, the DNA of the methanogenic pure cultures *Mtb*. *thermautotrophicus* DSM 1053, *Methanosarcina thermophila* DSM 1825 and *Mcu*. *marisnigri* DSM 1498 (DSMZ GmbH, Braunschweig, Germany) were also extracted using the FastDNA® Spin Kit for Soil.

The step by step DNA extraction protocol was performed for metagenomic analyses according to Rheims and Stackebrandt (1999) and Klocke and coworkers (2008). In order to yield highly pure and high-molecular-weight DNA for the 454-pyrosequencing, three digestate samples of the LBR at 55 °C (D 55), 65 °C (D 65) and 70 °C (D 70) as well as one biofilm sample of the packing derived from the AF (P 55) at an LBR temperature of 55 °C were analyzed. For each of these four samples, the DNA of ten subsamples was extracted to reduce a potential DNA extraction bias. The subsamples of the digestate (0.3 g each) were resuspended in 1 mL saline-EDTA (0.1 M EDTA, 0.15 M NaCl), whereas the packing's subsamples (0.2 g each) were washed twice with

1 mL sodium-phosphate buffer (0.1 M, pH 7.0) to reduce contamination of humins. These samples were then centrifuged at 3,500 x g for 15 min (C5417R centrifuge; Eppendorf GmbH, Hamburg, Germany). The cell pellets obtained were also resuspended in 1 mL saline-EDTA.

In addition to the chemical and enzymatic cell lysis, a mechanical lysis step with a lower intensity than the FastPrep® Instrument was applied to keep the genomic DNA unshared. In detail, sterile glass beads (1 x 4 mm and 20 x 1.5 mm in diameter) were added to the samples, which were homogenized at maximum speed on a test tube shaker (Heidolph Instruments GmbH & Co. KG, Schwabach, Germany) for 5 min. Afterwards, 15 to 20 mg of polyvinylpolypyrrolidone (PVPP) and 30 µL of lysozyme solution (10 mg mL^{-1} lysozyme, 10 mM Tris/HCl) were added and the samples were incubated at 37 °C for 60 min. Briefly, 30 µL of proteinase K (10 mg mL^{-1} proteinase K, 50 mM Tris/HCl, 1.5 mM calcium acetate), 120 µL of SDS (10% w/v) and 120 µL of $CaCl_2$ (10 mM) were added for lysing the cells. After incubation at 65 °C for 45 min, the samples were centrifuged at 6,000 x g for 10 min (C5417R centrifuge, Eppendorf GmbH, Hamburg, Germany) and the supernatants were adjusted to 0.7 M NaCl and 5% (w/v) CTAB (hexadecyltrimethylammonium bromide). The samples were incubated on a heating block (Eppendorf GmbH, Hamburg, Germany) at 65 °C for 30 min. Subsequently, the DNA was extracted twice with an equal volume of chloroform-isoamylalcohol (24:1 v/v) and precipitated from the obtained water phase by adding 0.1 volumes of 3 M sodium acetate (pH 5.2) and an equal volume of isopropanol. The precipitated DNA was collected by centrifugation at 4 °C with 20,817 x g for 20 min (C5417R centrifuge, Eppendorf GmbH, Hamburg, Germany). The DNA pellets were washed twice with ethanol (70% v/v), dried and resuspended in 50 µL of HPLC-H_2O. All chemicals were provided by AppliChem GmbH (Darmstadt, Germany).

The genomic DNAs derived from the subsamples of the respective metagenomic samples was pooled and then purified with the NucleoBond CB 20 Kit (Macherey-Nagel, Düren, Germany) according to the manufacturer`s instructions. The DNAs, extracted from the digestates of the LBR and the biofilm of the AF had concentrations of 1.04 µg $µL^{-1}$ (D 55), 0.62 µg $µL^{-1}$ (D 65), 0.53 µg $µL^{-1}$ (D 70) and 0.43 µg $µL^{-1}$ (P 55), respectively, and were highly pure with an absorption ratio of A_{260}/A_{280} = 1.82 ± 0.03 and A_{260}/A_{230} = 2.08 ± 0.29.

This protocol was also used for the DNA extraction from the rye silage as the DNA extraction using the FastDNA® Spin Kit for Soil was not applicable for this substrate.

Chemical lysis was applied for extracting DNA of the pure cultures *Cl*. *tyrobutyricum* DSM 2637, *Escherichia coli* DSM 1116 and *Ps*. *fluorescens* DSM 50090 (DSMZ GmbH, Braunschweig, Germany), which were used as bacterial positive controls for the *rrs* gene amplification. In detail, 2 mL of a liquid culture were centrifuged at 14,000 x g for 5 min (C5417R centrifuge, Eppendorf GmbH, Hamburg, Germany). The supernatant was removed and the pellet obtained was resuspended in 200 µL of the residual supernatant. Then, 200 µL of cell lysis solution (2.5% SDS, 25 mM NaOH) was added and the sample was incubated in a heating block at 95 °C for 15 min. The obtained lysate was centrifuged at 6,000 x g for 10 min (C5417R centrifuge, Eppendorf GmbH, Hamburg, Germany) and the supernatant containing the extracted DNA was collected.

The successful DNA isolation was validated by a 1.2% agarose gel electrophoresis (Biozyme Scientific GmbH, Hessisch Oldendorf, Germany) stained with ethidium bromide (0.3 µg mL^{-1}), VWR International GmbH, Darmstadt, Germany). A total of 2 µL of DNA together with 18 µl loading buffer (0.1 M EDTA, 40% glycerol, 0.1% SDS, 0.025% bromphenol blue) were applied to the gel. Additionally, 6 µl of DNA size standard (Lambda DNA/*Eco*RI+*Hin*dIII; Fermentas GmbH, part of Thermo Fisher Scientific, St. Leon-Rot, Germany) was used for size evaluation. The DNA was stored at 4 °C until further use.

2.2.2 DNA purity and quantification

The purity of genomic DNA was measured using the NanoPhotometer (Implen, München, Germany) according to the manufacturer's instructions. The ratios of the absorbance at 260 nm and 280 nm as well as at 260 nm and 230 nm were used as quality index for DNA purity.

The DNA quantification for the metagenomic and qPCR analyses was performed using the NanoDrop 3300 (Thermo Fisher Scientific, Wilmington, USA). The DNA concentration was determined after applying the DNA intercalating fluorescent dye PicoGreen (Quant-iT™ PicoGreen® dsDNA; Life Technologies GmbH, Darmstadt, Germany). In equal parts, the PicoGreen dye (1:200) was incubated together with the

DNA of the sample for 5 min before measuring the emission at 525 nm (excitation at 470 nm). The standard curve was designed using calf thymus DNA (Sigma-Aldrich Chemie Gmbh, München, Germany) with concentrations between 20 and 2,000 ng per mL following the scheme described above.

2.3 Construction of *rrs* gene libraries

Two bacterial and one archaeal *rrs* gene libraries were constructed to gain insights into the composition of the microbial community, to verify the TRFLP data and to identify the TRFs obtained.

For an optimal amplification of the bacterial and archaeal *rrs* gene, the 27f forward primer (bacterial assay, Table 2.1) and the 109f forward primer (archael assay, Table 2.1) were tested with several reverse primers: 926r (5' CCGTCAATTCCTTTGAG TTT 3') (Moeseneder et al., 1999), 926Rr (5' CCGTCAATTCCTTTRAGTTT 3') (Muyzer et al., 1995), 926MRr (Table 2.1), 1492r (5' GGYTACCTTGTTACGACTT 3') (Sait et al., 2003) and 16Srev (5' TACGGYTACCTTGTTACGACTT 3') (Klocke et al., 2007) for the bacterial assay and Ar912r (Table 2.1), Ar915r (5' GTGCTCCCCCGCCAATT CCT 3') (Großkopf et al., 1998) and Ar958r (5' YCCGGCGTTGAMTCCAATT 3') (DeLong, 1992) for the archaeal assay. The reaction mix was as follows in a total volume of 25 µL: 1x PCR buffer, 1.75 mM $MgCl_2$ (bacterial assay) or 2 mM $MgCl_2$ (archaeal assay), 0.2 mM dNTPs, 0.4 µM of each primer and 1.2 U (bacterial assay) or 1 U (archaeal assay) of the recombinant *Taq* DNA polymerase (all: Fermentas GmbH, part of Thermo Fisher Scientific, St. Leon-Rot, Germany). The thermal profiles of the PCR reactions were performed as follows: (1) 95 °C for 3 min, (2) 94 °C for 30 s, (3) 50 °C for 40 s (primer 926r, 926Rr, 926MRr) or (3) 51 °C for 30 s (primer 1492r, 16Srev) or (3) 47 to 52 °C (gradient) for 30 s (primer Ar912r, Ar915r, Ar958r), (4) elongation at 72 °C for 90 s, steps 2 to 4 were repeated 25 times followed by a final extension at 72 °C for 8 min.

After primer evaluation, the optimal concentration of chemicals and enzymes, such as the $MgCl_2$ and *Taq* DNA polymerase, and the optimal annealing temperature were

evaluated. Furthermore, to optimize the PCR reaction and to estimate the robustness of the TRFLP method, the cycle numbers of the PCR reactions were evaluated. The protocols described below were used as standard protocols for the characterization of Bacteria and Archaea by *rrs* gene sequence and TRFLP analyses.

For the construction of the *rrs* gene library, DNAs extracted from the leachate of the LBR at 55 and 75 °C on day 7 were used for the bacterial *rrs* gene libraries, whereas DNA from the packing's biofilm of the AF at an LBR temperature of 55 °C was used for the archaeal *rrs* gene library construction. For the amplification of the bacterial *rrs* gene, the 27f forward primer and the 926MRr reverse primer (Table 2.1) were used. For the amplification of the archaeal *rrs* gene, the Ar109f forward primer and the Ar912r reverse primer (Table 2.1) were applied (all: Biomers, Ulm, Germany). The following reaction mix was used as standard protocol for the DNA amplification in a total volume of 25 µL: 1x PCR buffer, 2 mM $MgCl_2$ (bacterial assay) or 2.5 mM $MgCl_2$ (archaeal assay), 0.2 mM dNTPs, 0.4 µM of each primer and 1 U of the recombinant *Taq* DNA polymerase (all: Fermentas GmbH, part of Thermo Fisher Scientific, St. Leon-Rot, Germany). The thermal profile for the DNA amplification was as follows: (1) initial denaturation at 95 °C for 3 min, (2) denaturation at 94 °C for 30 s, (3) annealing at 51 °C (bacterial assay) or (3) 52 °C (archaeal assay) for 30 s, (4) elongation at 72 °C for 90 s, steps 2 to 4 were repeated 25 times for the bacterial assay or 28 times for the archaeal assay followed by a final extension at 72 °C for 8 min (Thermal Cycler 2720, Applied Biosystems by Life Technologies, Darmstadt, Germany; $T_{Gradient}$ and $T_{Professional}$, Biometra GmbH, Göttingen, Germany).

The PCR amplification was validated by 1.2% agarose gel electrophoresis (AppliChem GmbH, Darmstadt, Germany). After purification using the QIAquick PCR Purification Kit (Qiagen, Hilden, Germany), the PCR products were ligated into a pGem®-T vector (Promega, Mannheim, Germany) at 4 °C over night. Then the ligation mixtures were transformed into competent *E. coli* JM 109 cells (Promega GmbH, Mannheim, Germany) at 42 °C for 45 s and incubated in SOC medium (20 g L^{-1} tryptone, 5 g L^{-1} yeast extract, 0.5 g L^{-1} NaCl, 2.5 mM KCl, pH 7; after sterilization 20 mM sterile glucose solution, 10 mM sterile $MgCl_2$ solution were added) for 1.5 h at 37 °C on a test tube shaker. After the incubation, 100 µL transformation mix was plated onto LB plates containing ampicillin (50 µg mL^{-1}), IPTG (60 µg mL^{-1}) and X-Gal (60 µg mL^{-1}, all provided by AppliChem GmbH, Darmstadt, Germany). The plates were incubated at 37 °C over night. White colonies were picked after blue-white screening and incubated

over night at 37 °C in LB broth (Carl Roth GmbH & Co. KG, Karlsruhe, Germany) containing ampicillin (50 µg mL^{-1}). Recombinant plasmids were extracted using the NucleoSpin® Plasmid kit (Macherey-Nagel, Düren, Germany) according to the manufacturer's protocol. The cloning was verified by means of DNA restriction in a total volume of 20 µL using 1 U *Nco*I and 1 U *Sal*I (Fermentas GmbH, part of Thermo Fisher Scientific, St. Leon-Rot, Germany) together with double-concentrated Tango buffer for 2 to 3 h. For each of the three *rrs* gene libraries, 96 plasmids with inserts of expected length were sequenced by GATC Biotech AG (Konstanz, Germany). The quality of sequences was checked using the Chromas software tool (version 1.43; Technelysium Pty Ltd, South Brisbane, QLD, Australia). Chimeric sequences were identified applying the Mallard 1.02 software (Ashelford et al., 2006). A total of 9% of all sequences were identified as chimera and were removed from the study. The remaining *rrs* sequences were clustered into OTUs with a p-distance of 0.03 to each other applying the Mega 5.05 software (Tamura et al., 2011). The sequences were blasted against the NCBI nr database applying the megablast algorithm. Sequences from environmental or uncultured species were excluded from the BLAST analysis.

The statistical analyses of the *rrs* gene clone libraries were conducted with the PAST software (Hammer et al., 2001), using the default settings, in the case of the Simpson and Shannon diversity indices (Simpson, 1949; Shannon & Weaver, 1963) and the Evenness value (Lloyd & Ghelardi, 1964; Hill, 1973). The Chao-I estimator (Chao, 1987) based on the bias-corrected formula was calculated with the EstimateS software version 8.0.0 (Colwell, 2009). Furthermore, Good's coverage was calculated according to Good (1953). The Bray-Curtis similarity indices (Magurran, 1988) were calculated using the default settings of the EstimateS software version 8.0.0 (Colwell, 2009).

2.4 Terminal restriction fragment length polymorphism analysis

Two TRFLP assays were established focusing on the *rrs* genes of Bacteria and Archaea, respectively. The first step for TRFLP analysis was the amplification of the *rrs* gene. For bacterial *rrs* gene amplification, the 27f forward primer labeled with Cy5

(5' end) and the 926MRr reverse primer (Table 2.1) were used. For the amplification of the archaeal *rrs* gene, the Ar109f forward primer also labeled with Cy5 (5' end) and the Ar912r reverse primer (Table 2.1) were applied (all: Biomers, Ulm, Germany). The amplification of the *rrs* gene was performed using the amplification protocol as described above (cf. 2.3). Positive controls were set up using genomic DNA purified from following cultures as template: *E. coli* (DSM 1116), *Ps. fluorescens* (DSM 50090) and *Cl. tyrobutyricum* (DSM 2637) for the bacterial TRFLP assay and *Mtb. thermautotrophicus* (DSM 1053), *Msr. thermophila* (DSM 1825) and *Mcu. marisnigri* (DSM 1498, DSMZ GmbH, Braunschweig, Germany) for the archaeal assay.

The PCR amplification was validated by 1.2% agarose gel electrophoresis (AppliChem GmbH, Darmstadt, Germany). The PCR products were purified using the QIAquick PCR Purification Kit (Qiagen, Hilden, Germany) according to manufacturer's instructions and again checked by gel electrophoresis. The concentrations of the PCR products were determined using the NanoPhotometer (Implen, München, Germany).

For the restriction enzyme digestion of the PCR products, seven different enzymes for the bacterial and archaeal assay (*Alu*I, *Bfa*I, *Hae*III, *Hin*6I, *Msp*I, *Taq*I, *Tas*I; Fermentas GmbH, part of Thermo Fisher Scientific, St. Leon-Rot, Germany) and three enzyme combinations for the bacterial assay (*Msp*I and *Hin*6I, *Hae*III and *Msp*I, *Hae*III and *Hin*6I) were tested with preference for enzymes resulting in the most heterogeneous fingerprint profile.

As standard protocol, a total of 200 to 250 ng DNA was digested enzymatically in a total volume of 20 µL at 37 °C for 4 h using 10 U of each enzyme, *Msp*I and *Hin*6I, in the case of the bacterial assay or *Alu*I for the archaeal assay according to the manufacturer's instructions. Complete digestion of the PCR products was checked using the capillary gel electrophoresis.

The digested PCR products were purified by ethanol precipitation using 0.1 volume of 3 M sodium acetate and 200 µL 75% ethanol (protocol based on A. Ulrich, ZALF, Müncheberg, Germany and amended by the sodium acetate step). The samples were incubated in the dark for 30 min and centrifuged at 20,817 x g at 4 °C. The supernatant was removed and again 200 µL ethanol was loaded into the samples, repeating the centrifugation step. Then the pellets were dried in a vacuum concentrator (concentrator 5301, Eppendorf GmbH, Hamburg, Germany) for 3 to 5 min and resuspended in 20 µL (archaeal assay) or 40 µL (bacterial assay) HPLC-H_2O.

Electrophoretic separation and detection of TRFs, which were labeled with the fluorescent dye Cy5, were conducted using a GenomeLab™ GeXP Genetic Analysis System (Beckman Coulter, Krefeld, Germany). Each sample was loaded together with 0.2 to 0.5 µL of DNA size standard labeled with D1 dye (S-600, Beckman Coulter, Krefeld, Germany) comprising DNA fragments from 60 to 640 nucleotides. The samples were filled up to a volume of 30 µL with sample loading solution (SLS, Beckman Coulter, Krefeld, Germany) and denatured at 90 °C for 120 s. The electrokinetic injection of samples and size standards lasted 10 to 20 s at 2 kV and the separation lasted 70 to 90 min applying 4.8 kV. A separation time of 90 min was used to confirm a complete restriction enzyme digestion. After validating the complete digestion, the separation time was reduced to 70 min.

Parts of the bacterial TRFLP analyses of the 21-day fermentation period at 60, 65 and 70 °C were conducted in the context of the Bachelor thesis of C. Nolte (2011) and provided the basis for further analysis and interpretation of the data in this study.

Recording and analysis of data were performed with the GeXP analysis software (version 10.2, Beckman Coulter, Krefeld, Germany). The size of the TRFs was calculated with the quartic model based on the migration time of the size standard. The calibration curve was generated arranging the fragment size of the size standard against the migration time. The size standard fragment with 140 bp was omitted from the analyses, which improved the squared correlation coefficient of the calibration curve. The squared correlation coefficient and the standard deviation of the size standard were above 0.99 and between 0.3 to 0.4 nucleotides, respectively, during all measurements, indicating a good DNA fragment separation. Due to the size standard, TRFs between 60 and 650 bp were analyzed in this study. Further, TRFs showing fluorescence intensities below 370 channel intensity (rfu) were not measurable within a linear range and were therefore removed from this study. The TRFLP data obtained were subsequently normalized focusing on the total fluorescence intensity of the peak height corresponding to Dunbar and coworkers (2001). A comparison between results based on the peak height and peak area was applied to evaluate potential differences in the TRFLP results due to the analysis of the peak area. Afterwards, the analysis based on the TRF heigh was used as standard.

Alignment of TRFs with a clustering threshold of 0.8 was conducted applying the T-Rex software (Culman et al., 2009). For further downstream analyses, the only TRFs used were those which were represented in at least two of the conducted triplicates per

sample. For the bar charts, TRFs with fluorescence intensities below 3% of the total detected fluorescence intensity were removed from the analysis. Then the relative abundance of each TRF was calculated based on the aligned and normalized data set according to Wang and coworkers (2010) and displayed using SigmaPlot 8.0 (Systat Software, Erkrath, Germany). The similarity indices, Bray-Curtis (Magurran, 1988) and Chao-Jaccard (Chao et al., 2005), were calculated for different TRFLP profiles using the default settings of the EstimateS software version 8.0.0 (Colwell, 2009). The non-metric multidimensional scaling (NMDS) was constructed on the basis of a Bray-Curtis similarity matrix. The NMDS was performed applying the Statistica software (StatSoft GmbH, Hamburg, Germany) using the Standard Guttman-Lingoes option as starting configuration. Up to 6 dimensions were analyzed for each TRFLP profile for scree plot construction in order to confirm that a reduction to two dimensions, as shown in the NMDS plots, was appropriate.

To identify TRFs, the plasmids of interest were amplified using the T7 and SP6 (Table 2.1) promoter primers (Eurofins MWG GmbH, Ebersberg, Germany). The reaction protocol was as follows using a total volume of 20 µL: 1x PCR buffer, 1.5 mM $MgCl_2$, 0.2 mM dNTPs, 0.2 µM of each primer and 0.8 U of the recombinant *Taq* DNA polymerase (all: Fermentas GmbH, part of Thermo Fisher Scientific, St. Leon-Rot, Germany). The thermal profile started with (1) an initial denaturation at 94 °C for 2 min, followed by (2) a denaturation step at 94 °C for 30 s, (3) an annealing step at 47 °C 1 min and (4) an elongation step at 70 °C for 2 min. Steps 2 to 4 were repeated 30 times and were finished by a final extension at 70 °C for 10 min. After the QIAquick PCR purification, a second PCR was applied focusing on the bacterial or archaeal *rrs* gene using the TRFLP primers and the thermal profile mentioned above (cf. 2.4). PCR products were purified, digested, precipitated by ethanol and finally analyzed on the GenomeLab™ GeXP Genetic Analysis System as described before (cf. 2.4). The identification and phylogenetic assignment of TRFs monitored for the reactor samples were conducted on the basis of the cloned *rrs* gene sequences resulting in a TRF of similar size.

2.5 Metagenomic analysis applying 454-pyrosequencing technology

To analyze the microbial metagenome, the genomic DNA, isolated from the digestate of the LBR at 55 (D 55), 65 (D 65) and 70 °C (D 70) and from the packing's biofilm of the AF at an LBR temperature of 55 °C (P 55), was used. The 454-pyrosequencing analysis was performed at the Center for Biotechnology (CeBiTec, Bielefeld University, Germany) using the Genome Sequencer (GS) FLX^{TM} platform (Roche Applied Science, Mannheim, Germany). Altogether, four libraries of the DNA samples were constructed applying the GS Rapid Library Prep Kit (Roche Applied Science, Mannheim, Germany) according to the manufacturer's protocol. These four libraries representing different microbial communities were sequenced on a PicoTiterPlate on the GS FLX^{TM} system using the Titanium sequencing chemistry (Roche Applied Science, Mannheim, Germany). The raw data were processed by CeBiTec using the analysis pipeline for whole genome shotgun sequence reads applying the GS FLX^{TM} System Software (version 2.3, Roche Applied Science, Mannheim, Germany).

The subsequent phylogenetic assignment and functional annotation were conducted on the basis of the unassembled metagenomic sequences, using the MetaSAMS platform 0.99 (Zakrzewski et al., 2013), a tool for metagenomic data analysis. This platform was also provided by CeBiTec via web interface. The integrated Ribosomal Database Project classifier (RDP classifier; Wang et al., 2007) was applied for the phylogenetic assignment based on *rrs* gene sequences. To identify *rrs* gene fragments, a search using the Basic Local Alignment Search Tool (BLAST) (Altschul et al., 1990) versus the RDP database (Release 10.19) was conducted. To allow the analysis of metagenomic sequences with low complexity, the sequence complexity filter was disabled (option '-F F'). Reads with an E-value threshold of 10^{-10} and a confidence value of at least 80% were extracted and classified using the RDP classifier. The accuracy of RDP classification ranges between 99.5% to 99.8% at phylum level and 83.2% to 88.7% at genus level for 200 to 400 nucleotides segments analyzing type strain sequences and further rRNA coding sequences (Wang et al., 2007).

A further classifier, CARMA version 2 (Krause et al., 2008b) was used for phylogenetic assignment and functional annotation of metagenomic sequences representing functional genes (so-called environmental gene tags, EGTs). Using the default settings

(Krause et al., 2008b), EGTs were identified by matching metagenomic sequences on protein family (Pfam) members (Pfam database 24.0), which were represented by multiple sequence alignments and hidden Markov models (Finn et al., 2008). In a further step, the functional information based on the Pfam accessions was combined with the results of the phylogenetic assignment obtained by CARMA. CARMA allows classification with specificity of 97% at superkingdom and 68% at genus level analyzing short EGTs of a synthetic dataset produced from 77 complete genomes (Krause et al., 2008b).

To get an impression of the genetic potential for carbohydrate degradation, methanogenesis and pathogenicity in the microbial community, the Pfam (Finn et al., 2008) profiles obtained from CARMA were used. For this purpose, enzymes relevant to the degradation of biomass and to the methanogenesis were identified with the help of KEGG (Ogata et al., 1999) and grouped according to Pfam protein families. Furthermore, enzymes relevant to pathogenicity of selected pathogens were determined with the help of the Pfam database (Punta et al., 2012).

2.6 Quantitative real-time PCR

The qPCR is a powerful tool for quantifying microorganisms within various habitats. The number of Bacteria as well as the number of a specific potentially process-relevant bacterium in the two-phase biogas reactor (TRF 304) was quantified. This bacterium was dominant in the TRFLP analysis and *rrs* gene library analysis after seven days of fermentation at LBR temperatures of 55 and 60 °C, which indicated a potentially important role in biomass degradation.

To quantify Bacteria, a Bacteria-specific primer set with Bac338f, Bac516TaqMan and Bac805r (Table 2.1) was used, which amplifies a 468 bp fragment. Furthermore, a TRF 304-specific primer set, composed of the 304f forward primer, the TaqMan304 probe and the 304r reverse primer (Table 2.1), was designed, applying the software tools Primer Express® version 3.0 (Applied Biosystems by Life Technologies, Darmstadt, Germany) and Primer 3 version 0.4.0 (Rozen & Skaletsky, 2000). This primer set

amplifies a 151 bp fragment. Afterwards, the target specificity was analyzed in order to identify false negative and positive assignments. Therefore, the *rrs* gene libraries were checked after a sequence alignment using the software Mega 5.05 (Tamura et al., 2011). Furthermore, the primer set 304 was checked for false positive and false negative matches applying the Primer BLAST tool of NCBI (Altschul et al., 1990; Wheeler et al., 2007) and the probe match tool of RDP (Cole et al., 2009).

For standard curve construction, the corresponding plasmid of TRF 304 (ATB-AR_23384; accession number HE804843) was used for the primer set 304 and the *Pectobacterium carotovorum* ssp. *carotovorum* DSM 30168 strain as a representative of the Bacteria was used for the primer set Bac. The cultivation, DNA extraction and amplification, cloning into the pGem vector and isolation of plasmids of this strain were performed as described in Bergmann (2012). The plasmid of TRF 304 (HE804843) was retransformed into *E. coli* JM 109 cells and extracted as described above for the *rrs* gene library construction (cf. 2.3). The plasmids were linearized in a total volume of 40 µL, using 2 U *Sca*I (Fermentas GmbH, part of Thermo Fisher Scientific, St. Leon-Rot, Germany) for 16 h at 37 °C and 80 °C for 20 min (inactivation of the enzyme). Linearization was validated by 1.2% agarose gel electrophoresis followed by a purification of the linearized plasmids using the QIAquick purification kit (Qiagen, Hilden, Germany). The concentrations of genomic DNAs and plasmid DNAs were determined using the NanoDrop 3300 (Thermo Fisher Scientific, Wilmington, USA), following the previously described scheme (cf. 2.2.2). For standard curve design, the number of plasmid copies was calculated as follows, according to Bergmann (2012):

$$N_{DNA} = (C_{DNA} * N_A) \, (l_{plasmid} * m_{mol,bp})^{-1},$$

where N_{DNA} is the number of DNA copies (μL^{-1}), C_{DNA} is the DNA concentration (g μL^{-1}), N_A is the Avogadro constant ($6.022 * 10^{23}$ mol^{-1}), $l_{plasmid}$ is the plasmid length in base pairs and $m_{mol,bp}$ is the average molar mass of a base pair (660 g mol^{-1}). Afterwards, serial dilutions with copy numbers between 10^1 and 10^9 were made.

The amplification of the target sequences was performed using the ABI 7300 System (Applied Biosystems by Life Technologies, Darmstadt, Germany). The qPCR for both assays was performed in a total volume of 25 µL using 12.5 µL TaqMan universal PCR master mix (Applied Biosystems by Life Technologies, Darmstadt, Germany), 0.9 µM of each primer, 0.2 µM TaqMan probe (FAM/TAMRA) and 1 ng template DNA. All DNA

samples were measured in triplicates. The thermal profile for the bacterial primer set (Bergmann, 2012) and the primer set 304 were as follows: 2 min at 50 °C, 10 min at 95 °C, followed by 45 cycles (primer set Bacteria) or 40 cycles (primer set 304) of 15 s at 95 °C, 30 s at 57 °C (only for primer set Bacteria) and 1 min at 60 °C. At the end of each cycle, the fluorescence emitted from the samples was detected.

The analysis of the results was conducted by applying the 7300 Real-Time PCR Sequence Detection Software (version 1.3; Applied Biosystems by Life Technologies, Darmstadt, Germany). The calibration curve was generated by plotting the plasmid concentration of the standard against the number of cycles. The squared correlation coefficient (R^2) and the slope of the calibration curve ranged between 0.992 and 0.995 and between -3.28 and -3.37, respectively, for all measurements. The slope of the standard curve was used to determine the efficiency of the PCR reaction by the following formula:

$$\text{efficiency} = (10^{(-1/\text{slope})}) - 1.$$

The calculated PCR efficiency was between 0.980 and 1.018, which indicated an efficient standard curve calibration (Zhang & Fang, 2006).

The limit of detection (LOD) and the limit of quantification (LOQ) were calculated according to Bergmann (2012). For the bacterial qPCR analysis, C_t values (threshold cycle number) of 40.7 and 40.0 were achieved for LOD and LOQ, respectively. For the analysis, using the TRF 304 primer set, the LOD and LOQ values ranged from 35.0 to 35.6 and from 34.4 to 35.2, respectively. All samples measured showed C_t values above these calculated limits.

For graph design, the number of *rrs* gene copies per mL leachate was calculated as follows:

> *rrs* gene copies (mL^{-1}) = (*rrs* gene copy number * DNA concentration (ng mL^{-1})) (used volume for DNA extraction)$^{-1}$.

2.7 Microscopical analyses

Three different methods for staining and counting microbial cells derived from the two-phase biogas system were applied. To determine the total cell counts in the leachate, the microbial cells were stained with DAPI. To quantify the bacterial and archaeal cells in the reactor samples, DOPE-FISH was performed. Further, the percentage of microbial cells with reduced membrane integrity was estimated by PI staining. This fluorescent dye intercalates in DNA and RNA, but only in cells having reduced membrane integrity.

Parts of the total cell count analysis as well as the DOPE-FISH and PI analyses were performed in the context of the Diploma thesis of C. Krumrei (2010).

For the total cell count and the DOPE-FISH analyses, the leachate of the LBR was sampled on day 7 of the 21-day fermentation at each temperature regime due to the fact that an active community should have been established after one week of fermentation. The samples were fixed immediately. To this end, 500 µL of the leachate were washed twice with 1x PBS (pH 7.4), centrifuged at 3.500 x g for 15 min and incubated in 2.8% formaldehyde (Carl Roth GmbH & Co.KG, Karlsruhe, Germany) at 4 °C over night. The samples were centrifuged as described above and the pellets were washed two times with 1x PBS (pH 7.4). The pellets were resuspended in equal parts of 1x PBS (pH 7.4) and 96% ethanol (AppliChem GmbH, Darmstadt, Germany). All samples were stored at -20 °C until further processing.

For both analyses, the fixed samples were washed again with 1x PBS (pH 7.4) and centrifuged at 15,000 x g for 5 min. Each sample, resuspended in 1x PBS (pH 7.4), was sonicated (Sonoplus GW2070; Bandelin, Berlin, Germany) two times with 50% power (about 35 W) at pulse level 1 for 30 s to destroy cell aggregates according to Nettmann and coworkers (2010). Triplicates of the samples (10 µL each) were transferred on a Teflon-coated slide (Gerhard Menzel GmbH, Braunschweig, Germany), which was covered with 0.1% gelatine and 0.01% $CrK(SO_4)_2$ (AppliChem GmbH, Darmstadt, Germany).

To analyze the total cell counts, the samples were stained using 5 µL Citifluor AF1 (Citifluor Ltd, London, UK) antifading reagent and 0.2 µL DAPI (33 µg mL^{-1}, Carl Roth GmbH & Co.KG, Karlsruhe, Germany). Stained microbial cells were detected on the Olympus BX51 fluorescent microscope (Olympus, Hamburg, Germany) at a

magnification of 600 using the filter set WU for DAPI detection. Images of the samples were taken with a digital Olympus DP72 camera applying the software cell F (Olympus, Hamburg, Germany). For each triplicate of the samples, about 1,000 stained cells were counted from randomly taken images. The calculation of the total cell count was performed according to Raizada (2004) with the following formula:

$$\text{total cell count } (mL^{-1}) = A_{well} / A_{count} * Xm * v,$$

where A_{well} is the area of each well, A_{count} is the area of each counted image, Xm is the average cell number per image and v is the dilution factor.

For DOPE-FISH analysis, the samples on Teflon-coated slides were permeabilized with 10 µL freshly prepared lysozyme solution (10 mg mL^{-1} lysozyme; 50 mM EDTA, pH 8; 0.3 M Tris/HCl, pH 8) for an improved uptake of hybridization probes. The samples were incubated at 37 °C for 30 min in a 50 mL reaction tube together with wet paper to create a humid atmosphere. The slide was rinsed briefly with distilled H_2O and dehydrated by a stepwise incubation (3 min each) in 50%, 80% and 96% ethanol (AppliChem GmbH, Darmstadt, Germany). Hybridization of the samples was performed on dried slides. The hybridization buffer was prepared with a stringency of 50% (0.9 M NaCl; 0.02 M Tris/HCl; 10x sterile Denhardt reagent - containing 1% FicoII, 1% PVPP, 1% BSA; 50% formamide and 0.01% SDS; from AppliChem GmbH, Darmstadt, Germany and Carl Roth GmbH & Co. KG, Karlsruhe, Germany). To each sample well, 9 µL of the hybridization buffer was applied together with 1 µL $Arch915_{FITC}$ (50 ng L^{-1}, Table 2.1) for the detection of archaea, 1 µL $EUB338_{Cy3}$ I (50 ng L^{-1}, Table 2.1) and 1 µL of a 1:1 solution of $EUB338_{Cy3}$ II and III (each 50 ng L^{-1}, Table 2.1) for the detection of bacteria. Furthermore, 1 µL of the nonsense probe $NON338_{Cy3\ or\ FITC}$ (each 50 ng L^{-1}, Table 2.1) having no binding site in the 16S rRNA of Bacteria and Archaea as well as µL of the probe $UNIV1390_{Cy3\ or\ FITC}$ (each 50 ng L^{-1}, Table 2.1) binding to both Bacteria and Archaea were analyzed in order to detect false positive hybridization and to determine the hybridization rate, respectively. Then, the slide was incubated in a 50 mL reaction tube at 46 °C for 2 h in a hybridization oven (HL 2000, UVP Ltd, Cambridge, UK) together with paper moistened with the residual hybridization buffer.

After hybridization, the slide was washed carefully in a 48 °C preheated washing buffer (0.02 M NaCl; 0.02 M Tris/HCl; 5 mM EDTA; 0.01% SDS; AppliChem GmbH, Darmstadt, Germany) for 10 to 15 min to remove unbound probes from the samples.

Finally, the slide was dipped into ice cold distilled H_2O for 3 s, dried and stored at -20 °C in the dark until further processing.

As positive controls various pure, actively growing cultures were used: *E. coli* (DSM 1116), *Cl. tyrobutyricum* (DSM 2637) for bacterial detection and *Methanosaeta concilii* (DSM 6752; DSMZ GmbH, Braunschweig, Germany) and *Methanospirillum hungateii* Mh1 (Department of Microbial Ecology, Limnology and General Microbiology, University of Konstanz) for archaeal detection.

The detection of fluorescently labeled cells was performed on the Olympus BX51 fluorescent microscope (Olympus, Hamburg, Germany) at a 600-fold magnification using the filter set WU (excitation 330 - 385 nm, emission >420 nm) for DAPI detection, the filter set NIBA (excitation 470 - 495 nm, emission 510 - 550 nm) for FITC detection and the filter set Cy3 (excitation 510 - 560 nm, emission 573 - 647 nm) for Cy3 detection. Images of the samples were taken with a digital Olympus DP72 camera applying the software cell F (Olympus, Hamburg, Germany) for each filter set. Afterwards, the fluorescently labeled archaeal and bacterial cells were counted from randomly taken images for about 1,000 DAPI stained cells for each triplicate of samples as described above.

For **PI analysis**, fresh leachate samples of the LBR 1, 2 and 3 (LBR 65 °C) were analyzed in triplicate on day 0, 7, 15 and 21. In detail, 100 µL of leachate was washed with 1x PBS (pH 7.4) and centrifuged at 15,000 x g for 5 min. The pellet was resuspended in 1 mL 1x PBS (pH 7.4) and 20 µL of PI solution (1 mg mL^{-1}, Invitrogen, Darmstadt, Germany) was added. The sample was incubated for 10 min in the dark. Briefly, the sample was centrifuged at 15,000 x g for 5 min and the pellet was resuspended in 1 mL 1x PBS (pH 7.4). 10 µL of the sample were applied per well on a 10-well Teflon-coated slide. The slide was dried and also stained with DAPI as described above. Microscopical detection and counting of cells was performed as described above.

Table 2.1 Primers and probes used for the polyphasic analyses of the two-phase biogas systems

Primer	Sequence (5'-3')	Target	Amplicon size	Target site according to *E. coli*	Method	Reference	Supplier
27f-Cy5	Cy5-AGAGTTTGATCMTGGCTCAG	Bacteria	approx. 899	8 - 27	TRFLP	Lane, 1991; Sipos et al., 2007	b
926MRr	CCGTCAATTCMTTTRAGTTT			926 - 947		Weisburg et al., 1991; Despres et al., 2007	b
Ar109f-Cy5	Cy5-ACKGCTCAGTAACACGT	Archaea	approx. 803	109 - 125	TRFLP	Großkopf et al., 1998	b
Ar912r	CTCCCCCGCCAATTCCTTTA			912 - 931		Lueders & Friedrich, 2000	b
27f	AGAGTTTGATCMTGGCTCAG	Bacteria	approx. 899	8 - 27	*rrs* gene library	Lane, 1991; Sipos et al., 2007	b
926MRr	CCGTCAATTCMTTTRAGTTT			926 - 947		Weisburg et al., 1991; Despres et al., 2007	b
Ar109f	ACKGCTCAGTAACACGT	Archaea	approx. 803	109 - 125	*rrs* gene library	Großkopf et al., 1998	b
Ar912r	CTCCCCCGCCAATTCCTTTA			912 - 931		Lueders & Friedrich, 2000	b
T7	TAATACGACTCACTATAGGG	pGem®-T vector	variable	-	*rrs* gene library	Promega GmbH	c
SP6	ATTTAGGTGACACTATAG					Promega GmbH	c
304f	GACGCATGTTGGACATATTAAAGC	TRF 304	151	194 - 219	qPCR	this study	b
304TaqMan	6-Fam-TAAAGGCCCACCAAGGCGACGA-Tamra			281 - 302		this study	b
304r	AGTTTGGGCCGTGTCTCAGT			341 - 360		this study	b
Bac338f	ACTCCTACGGGAGGC	Bacteria	468	338 - 354	qPCR	Yu et al., 2005	c
Bac516TaqMan	TGCCAGCAGCCGCGGTAATA			516 - 536		Yu et al., 2005	c
Bac805r	GACTACCAGGGTATCTAATC			785 - 805		Yu et al., 2005	c
EUB388 (pB-00159)[a]	CY3-GCTGCCTCCCGTAGGAGT-CY3	Bacteria	-	-	DOPE-FISH	Amann et al., 1990	d
EUB388 II (pB-00160)[a]	CY3-GCAGCCACCCGTAGGTGT-CY3	Bacteria	-	-	DOPE-FISH	Daims et al., 1999	d
EUB388 III (pB-00161)[a]	Cy3-GCTGCCACCCGTAGGTGT-Cy3	Bacteria	-	-	DOPE-FISH	Daims et al., 1999	d
Arch915 (pB-00027)[a]	FITC-GTGCTCCCCCGCCAATTCCT-FITC	Archaea	-	-	DOPE-FISH	Stahl & Amann, 1991	d
UNIV1390 (pB-00327)[a]	FITC-GACGGGCGGTGTGTACAA	Bacteria & Archaea	-	-	FISH	Zheng et al., 1996	d
UNIV1390 (pB-00327)[a]	Cy3-GACGGGCGGTGTGTACAA	Bacteria & Archaea	-	-	FISH	Zheng et al., 1996	d
NON338 (pB-000243)[a]	FITC-ACTCCTACGGGAGGCAGC	No organism	-	-	FISH	Wallner et al., 1993	d
NON338 (pB-000243)[a]	Cy3-ACTCCTACGGGAGGCAGC	No organism	-	-	FISH	Wallner et al., 1993	d

[a], accession number as indicated by probeBase (Loy et al., 2007)

[b], Biomers.net GmbH, Ulm, Germany; [c], Eurofins MWG GmbH, Ebersberg, Germany; [d], Metabion International AG, Martinsried, Germany

-, no amplification

3 RESULTS

3.1 Operation of the two-phase leach-bed biogas systems

The two-phase biogas systems have been operated throughout the whole experiment by M. Schönberg with the support of C. Joost. The temperature of each LBR of the three identically constructed biogas systems was increased stepwise from 55 up to 75 °C by 5 °C increments, while the temperature of each AF was kept constant at 55 °C throughout the experiment. Each temperature regime consisted of three 21-day fermentations to allow the microbial community to adapt to the increased temperatures. To each system, rye silage with an average pH of 4.20 ± 0.06, an ODM content of 17.55 ± 0.73% and a COD of 204.88 ± 9.75 g per kg (Table 3.1) was supplied. In contrast to that, the straw material used had higher pH, ODM and COD values (Table 3.1). After 21 days of fermentation, the digestate showed reduced COD values (Table 3.1), resulting from the degradation of the substrate. Process parameters, such as pH, ODM, COD, concentration of intermediates and total ammonia nitrogen, were provided by the analytical chemistry work group at the ATB. Biogas and methane yield and degradation rate of biomass was calculated and provided by M. Schönberg for further data interpretation

During the increase in temperature in the LBR, the pH in the three biogas systems was nearly constant with values between 7.52 ± 0.36 (LBR) and 7.95 ± 0.11 (AF; Table 3.2). Furthermore, the concentration of total ammonia nitrogen and free ammonia in the AFs of the three systems ranged from 0.85 ± 0.05 to 1.00 ± 0.11 g per L and from 0.21 ± 0.02 to 0.27 ± 0.04 g per L, respectively, during the whole experiment (Table 3.2), indicating no strong alterations.

Table 3.1 Analytical parameters (ODM, pH and COD) of substrates and digestates

	pH	ODM (%)	COD (g kg^{-1})
Rye silage[a]	4.20 ± 0.06	17.55 ± 0.73	204.88 ± 9.75
Winter barley straw	7.58	81.39	894.84
Wheat straw	7.42	81.89	875.80
Compost material	8.17	14.55	212.22
Digestate[b]	9.17 ± 0.16	11.14 ± 1.31	139.14 ± 26.17

[a], average of eight rye silage samples

[b], average of three biogas reactor systems at each temperature regime

However, several parameters, such as the biogas yield (Table 3.3), differed markedly during the temperature increase in the three biogas systems. The amount of biogas at an LBR temperature of 55, 60 and 65 °C was almost constant with values from 605.09 ± 2.73 to 618.90 ± 4.87 L per kg_{oS}. At 70 °C, the biogas yield decreased by 30% in the three biogas systems. After the bioaugmentation with compost (LBR 70 °C), an increase in the biogas yield of 15 to 21% was obtained for the three reactor systems, leading to average biogas yields of 516.23 ± 2.93 L per kg_{oS}. However, the positive effect of the bioaugmentation with compost on the biogas yield did not persist at higher LBR temperatures of 75 °C. Here, the average biogas yield was reduced to 397.20 ± 16.65 L per kg_{oS}.

The mean methane concentration of the biogas differed between 48.99 ± 6.45% and 61.99 ± 4.47% during temperature increase in the LBRs (Table 3.3). Regarding the two phases of the subject biogas systems separately, certain differences in the methane yield and content occurred between LBR and AF (Table 3.3). In all experimental runs, the methane content obtained for the AF ranged between 70 and 81% and for the LBR between 21 and 46%.

Simultaneously with the changes in the biogas yield at 70 °C, the degradation rate of the substrate also decreased in the three reactor systems (Table 3.3). Between 55 and 65 °C, a high degradation of ODM was achieved with values between 80.31 ± 1.39% and 65.40 ± 5.23%. Then, the degradation rate changed to 39.80 ± 3.60% at 70 °C, to 48.95 ± 2.85% after bioaugmentation at 70 °C and to 32.47 ± 3.05% at 75 °C also indicating a positive effect of the bioaugmentation with compost, which could not persist at higher temperatures.

The impact of the temperature increase in the LBRs on the intermediates produced was shown using the first reactor system as example (Figure 3.1). However, the other

two reactor systems revealed similar concentrations of the intermediates. At an LBR temperature of 55 to 65 °C, the maximal acetic acid concentration in the leachate samples was relatively high with 6.69 g per L, whereas the other intermediates such as n-butyric acid (0.96 g L^{-1}), propionic acid (1.32 g L^{-1}) and valeric acid (0.18 g L^{-1}) showed lower maximum concentrations. Above 65 °C, the maximal concentrations of acetic acid (Figure 3.1 B) and n-butyric acid (Figure 3.1 B) decreased strongly to 4.65 g per L and 0.25 g per L, respectively. In contrast, the propionic acid concentration still reached maximum concentrations of 0.93 g per L (Figure 3.1 D), showing less reduction. The concentration of the valeric acid remained nearly constant with maximal values of 0.14 g per L (Figure 3.1 E).

However, the highest concentration of the intermediates was measured during the first nine days of the 21-day fermentation independent of the LBR temperature regime. Interestingly at 70 °C, the degradation of acetic acid was prolonged in comparison to lower LBR temperatures. This effect was reduced after the bioaugmentation, but reappeared at 75 °C. In contrast to the carboxylic acids, the concentration of alcohols, i.e. ethanol and propanol, was slightly increased by the temperature increase in the LBR (Figure 3.1 F). At 75 °C, an alcohol concentration with a mean value of 0.15 g per L was measured during the first five days of the fermentation. At lower temperatures, the alcohol concentration was below the detection limit of 0.02 g per L in most cases.

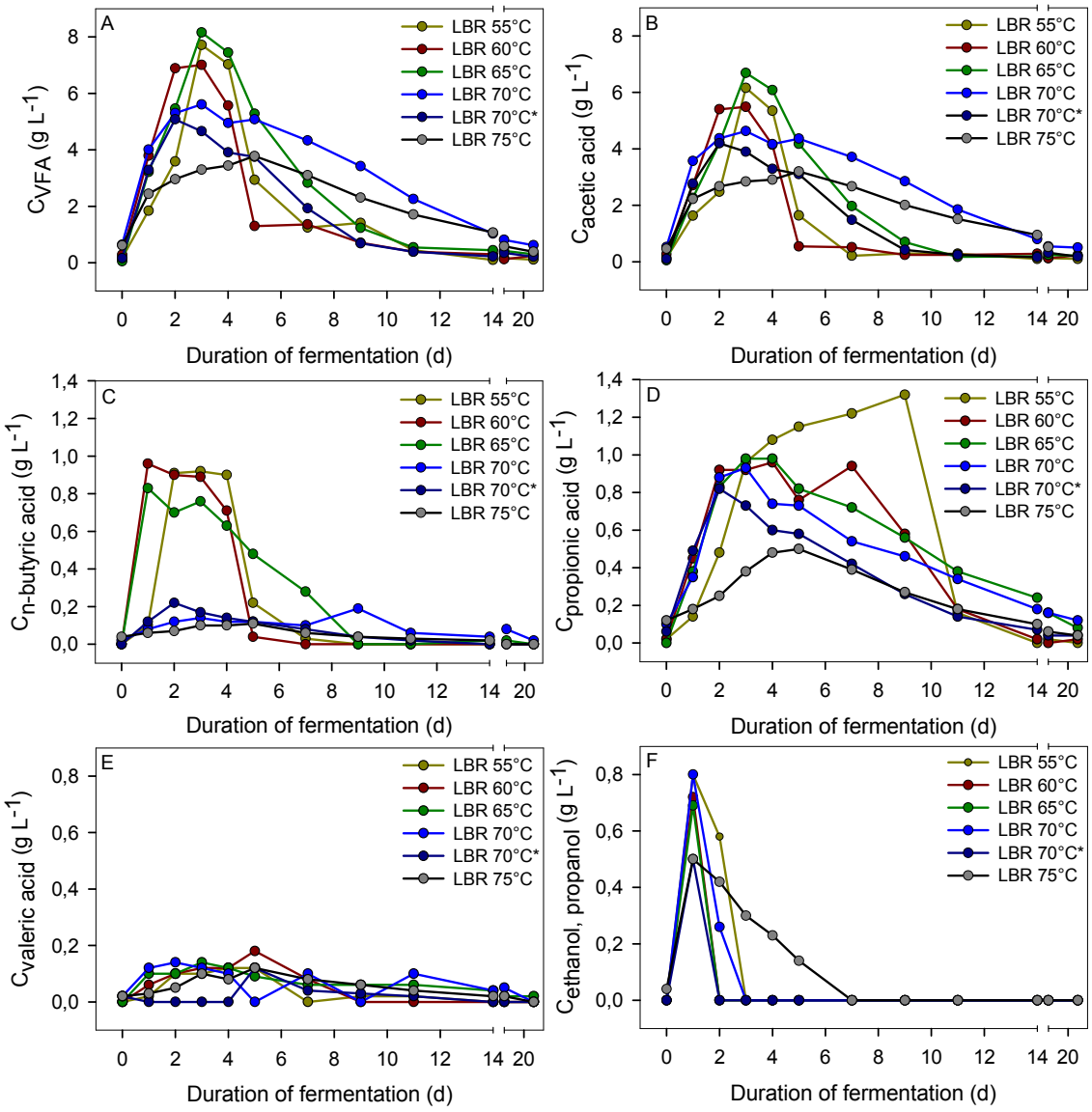

Figure 3.1 Concentration of total VFA (A), acetic acid (B), n-butyric acid (C), propionic acid (D), valeric acid (E) and ethanol and propanol as sum (F) shown for the first leach-bed reactor system during the 21-day fermentation process at all specified temperature regimes

Table 3.2 Process parameters of the three two-phase biogas systems

Temperature LBR reactor	pH[a] (LBR; AF)	NH_4-N[a] (g L^{-1}) (AF)	NH_3[a,b] (g L^{-1}) (AF)	Maximum VFA[a] ($g_{HAc\ eq.}$ L^{-1}) (LBR; AF)	Maximum COD[a] (g L^{-1}) (LBR; AF)
55 °C	7.52 ± 0.36; 7.80 ± 0.19	1.00 ± 0.11	0.24 ± 0.06	7.73 ± 0.64; 5.03 ± 0.71	17.89 ± 1.41; 14.89 ± 1.29
60 °C	7.56 ± 0.40; 7.95 ± 0.11	0.94 ± 0.09	0.27 ± 0.04	7.23 ± 0.71; 4.20 ± 1.26	17.65 ± 1.32; 14.68 ± 2.19
65 °C	7.43 ± 0.48; 7.89 ± 0.09	0.98 ± 0.06	0.24 ± 0.05	8.87 ± 0.62; 4.07 ± 1.88	19.42 ± 1.34; 12.37 ± 1.79
70 °C	7.54 ± 0.27; 7.88 ± 0.07	0.97 ± 0.11	0.24 ± 0.05	6.38 ± 0.87; 1.34 ± 0.73	18.93 ± 1.13; 9.00 ± 1.54
70 °C*	7.58 ± 0.24; 7.91 ± 0.06	0.99 ± 0.18	0.25 ± 0.06	5.12 ± 0.13; 1.01 ± 0.16	17.49 ± 1.19; 9.50 ± 0.87
75 °C	7.53 ± 0.25; 7.89 ± 0.09	0.85 ± 0.05	0.21 ± 0.02	3.99 ± 0.29; 0.74 ± 0.05	18.73 ± 0.87; 8.69 ± 0.67

[a], average values and standard deviation of the three biogas systems at one LBR temperature regime
[b], free ammonia was calculated accoding to Anthonisen and coworkers (1976)
70 °C*, analysis after bioaugmentation with compost; LBR, leach-bed reactor; AF, anaerobic filter reactor

Table 3.3 Biogas and methane yield and degradation rate of the three two-phase biogas systems

Temperature LBR reactor	Total biogas yield[a,b] (L kg_{OS}^{-1})	Total methane content[b] (%)	Methane content[b] (%)		Methane yield[a,b] (L kg_{OS}^{-1})		Degradation rate of ODM[b,d] (%)
			LBR	AF	LBR	AF	
55 °C	618.90 ± 4.87	50.54 ± 0.48	44.78 ± 0.99	69.99 ± 1.67	213.62 ± 11.61	99.17 ± 12.23	80.31 ± 1.39
60 °C	605.09 ± 2.73	54.62 ± 0.80	46.36 ± 0.95	72.89 ± 2.45	193.17 ± 3.07	137.32 ± 3.50	78.10 ± 0.85
65 °C	610.09 ± 1.45	49.70 ± 0.35	40.40 ± 0.44	77.27 ± 0.77	184.28 ± 3.18	118.95 ± 4.17	65.40 ± 5.23
70 °C	427.16 ± 17.71	48.99 ± 6.45	32.32 ± 8.72	79.15 ± 0.92	87.68 ± 19.66	121.20 ± 15.01	39.80 ± 3.60
70 °C*	516.23 ± 2.93	49.25 ± 1.17	34.80 ± 1.95	77.92 ± 0.85	119.42 ± 6.28	134.79 ± 3.89	48.95 ± 2.85
75 °C	397.20 ± 16.65	61.99 ± 4.47	21.00 ± 9.90	80.80 ± 1.21	28.55 ± 6.95	202.14 ± 19.51	32.47 ± 3.05

[a], gas yield normalized to 0 °C and 1,013 hPa
[b], average values and standard deviation of the three biogas systems at one LBR temperature regime
[d], degradation rate of ODM was corrected by the non-degradable lignin fraction
70 °C*, analysis after bioaugmentation with compost; LBR, leach-bed reactor; AF, anaerobic filter reactor

3.2 Analysis of bacterial and archaeal *rrs* gene sequences

3.2.1 Bacterial community composition in the LBR

The bacterial community composition was analyzed by two *rrs* gene libraries constructed from samples derived from the LBR at 55 and 75 °C. A total number of 76 (LBR 55°C) and 74 (LBR 75°C) *rrs* gene sequences were obtained, representing 30 and 17 bacterial OTUs, respectively.

Not only the number of OTUs, but also the composition of the bacterial community changed strongly during the temperature increase in the LBR. A pairwise comparison of the *rrs* gene libraries results revealed Bray-Curtis similarity values of 0.57 calculated for the OTUs and 0.21 calculated for the *rrs* sequences. This supports the findings of strong alterations within the bacterial community analyzed at an LBR temperature of 55 and 75 °C.

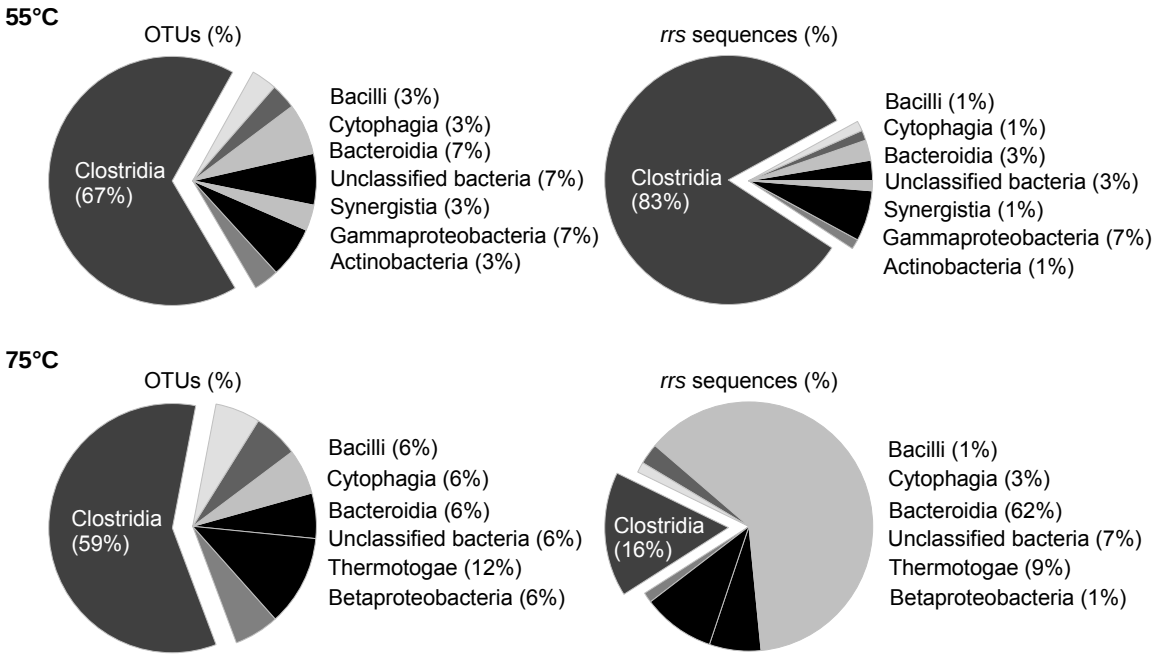

Figure 3.2 Results of the bacterial *rrs* gene sequence analyses of the LBR at 55 and 75 °C. The distribution of OTUs and *rrs* sequences obtained is indicated at class level.

During temperature increase in the LBR, the bacterial community changed from being Clostridia-dominated towards a more even distribution of Bacteroidia, Clostridia and Thermotogae. More specifically, members of the Clostridia were prevalent with 67% of OTUs and 83% of *rrs* sequences at 55 °C (Figure 3.2). At 75 °C, members of the Clostridia were strongly reduced accounting for 59% of OTUs and 16% of *rrs* sequences. Simultaneously, the number of *rrs* sequences assigned to the Bacteroidia class increased strongly from 3% to 62% after the temperature increase to 75 °C in the LBR.

Additionally, the results also showed that *rrs* sequences assigned to the Actinobacteria, Gammaproteobacteria and Synergistia classes, which were detected at lower levels at 55 °C, were absent at 75 °C (Figure 3.2). Contrarily, *rrs* sequences related to the Betaproteobacteria and particularly to the Thermotogae, which were absent at 55 °C, showed a relative abundance at 1% and 9% at 75 °C, respectively (Figure 3.2).

3.2.2 Archaeal community composition in the AF

The archaeal community composition was determined by the construction of an *rrs* gene library analyzing the packing's biofilm derived from the AF at an LBR temperature of 55 °C. A total number of 88 *rrs* sequences were analyzed, representing 12 archaeal OTUs.

About 50% of OTUs were assigned to the Methanobacteriales order and within this order to the *Methanobacterium* and *Methanothermobacter* genera (Figure 3.3). Further, Methanomicrobiales and Methanosarcinales were also identified with 33% and 17% of OTUs, respectively. The analysis of the *rrs* sequences revealed Methanobacteriales (52% of *rrs* sequences), followed by Methanosarcinales (30%) and Methanomicrobiales (18%) as prevalent archaeal orders (Figure 3.3). At the genus level, *Methanothermobacter* (38% of *rrs* sequences) and *Methanoculleus* (17%) followed by *Methanobacterium*, *Methanosarcina* and *Methanosaeta* (each 15%) were detected.

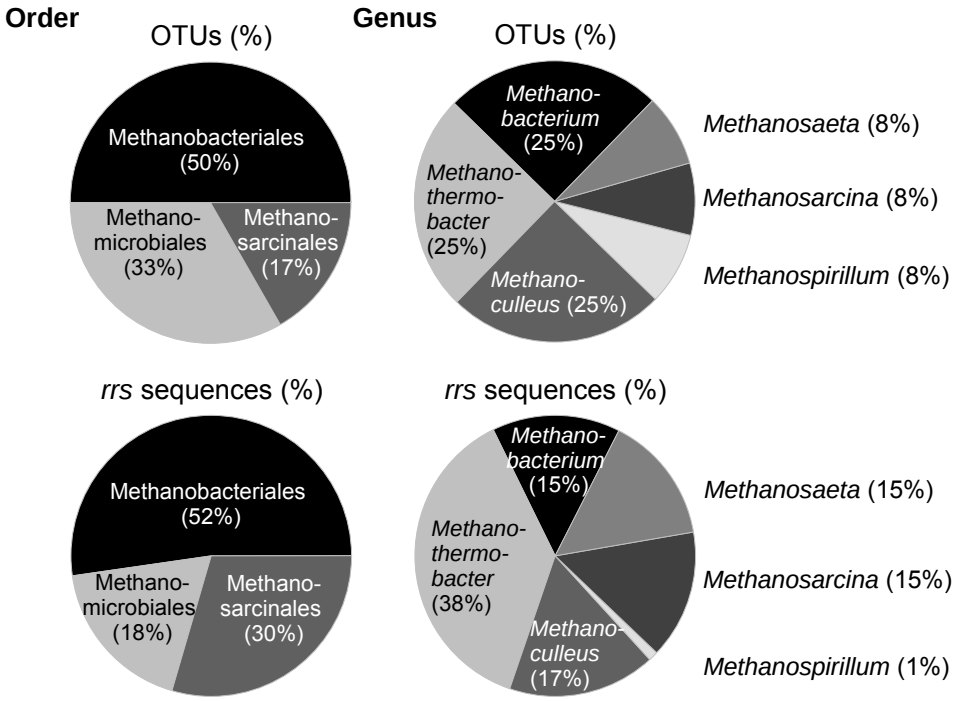

Figure 3.3 Results of the archaeal *rrs* gene sequence analyses of the packing's biofilm derived from the AF at an LBR temperature of 55 °C. The distribution of OTUs and *rrs* sequences is indicated at order and genus level.

3.2.3 Statistical analyses of the *rrs* gene libraries

The three *rrs* gene libraries were statistically analyzed calculating different parameters (Table 3.4). Two parameters, Good's coverage and the Chao-I estimator, were calculated in order to evaluate the coverage of microbial diversity. The results showed high coverage values (Good, 1953) for the bacterial *rrs* gene library at 75 °C and for the archaeal *rrs* gene library accounting for 85 and 95%, respectively (Table 3.4). Only the bacterial *rrs* gene library, constructed for the sample derived from the LBR at 55 °C, showed a lower coverage with 68%.

The Chao-I estimator values (Chao, 1987), which indicate the extrapolated number of OTUs, supported the findings of the coverage results (Table 3.4). The difference between the extrapolated OTU values and the identified OTUs for the bacterial *rrs* gene library at 55 °C differed strongly, supporting the lower coverage of the underlying

microbial community. The Chao I values calculated for the two other *rrs* gene libraries (Bacteria, 75 °C and Archaea, 55 °C) were more similar to the OTU values obtained.

Table 3.4 Statistical parameters of the archaeal and bacterial *rrs* gene libraries

		OTUs identified	Good's coverage[a] (%)	Shannon diversity index[a]	Simpson diversity index	Evenness	Chao-I estimator[a]
Bacteria	LBR 55 °C	30	68.42	2.74	0.89	0.51	168 (73 - 476)[b]
Bacteria	LBR 75 °C	17	85.14	1.63	0.60	0.30	31 (20 - 80)[b]
Archaea	AF 55 °C	12	95.45	1.94	0.81	0.58	14 (12 - 28)[b]

[a], based on the OTUs obtained
[b], confidence values (95% bootstrap)

To estimate the diversity of the bacterial and archaeal community, the Shannon (Shannon & Weaver, 1963) and Simpson indices (Simpson, 1949) were calculated (Table 3.4). Both indices showed that the highest diversity could be expected for the bacterial community at an LBR temperature of 55 °C. Furthermore, the parameter Evenness that was also calculated gave information about the distribution of the OTUs obtained (Lloyd & Ghelardi, 1964; Hill, 1973). A value of 1 indicates an equal distribution of OTUs. A low value indicates a strong prevalence of a specific OTU. In the case of the bacterial *rrs* gene library at 75 °C, one OTU (Bacteroidia) was strongly increased as indicated by the low Evenness value (Table 3.4).

3.3 Characterization and monitoring of the microbial community by TRFLP analyses

3.3.1 Establishment and optimization of TRFLP assays for bacterial and archaeal community analyses

Application of different DNA extraction methods

Four different methods were applied to evaluate the bias caused by DNA extraction. Two DNA extraction kits were used, which both induced cell lysis by mechanical force (sample FP and PS), whereas the third protocol, a step by step protocol, was based on chemical (SDS) and enzymatic (lysozyme) cell lysis (sample ST). The fourth protocol, step by step DNA extraction with an additional beating step, combined the chemical and enzymatic lysis with a mechanical treatment (sample STB).

All methods resulted in DNA, which was applicable for *rrs* gene amplification and downstream bacterial TRFLP analysis. A pairwise comparison of the TRFLP profiles obtained from the duplicates of each DNA extraction revealed rather high Bray-Curtis similarity values of 0.91 to 0.94 indicating reproducible results. Only the duplicate samples extracted by the PowerSoil® DNA Isolation Kit showed a slightly lower Bray-Curtis similarity with 0.84 (Table 3.5).

Table 3.5 Bray-Curtis similarity values of the bacterial TRFLP profiles of four DNA extraction methods. All samples were analyzed in duplicate.

	ST	STB	FP	PS
ST	0.94	0.73 ± <0.01	0.81 ± <0.01	0.75 ± 0.05
STB	0.73 ± <0.01	0.94	0.79 ± 0.03	0.82 ± 0.01
FP	0.81 ± <0.01	0.79 ± 0.03	0.91	0.78 ± 0.01
PS	0.75 ± 0.05	0.82 ± 0.01	0.78 ± 0.01	0.84

ST, step by step DNA extraction protocol; STB, step by step DNA extraction protocol with beating; FP, FastDNA® Spin Kit for Soil; PS, PowerSoil® DNA Isolation Kit

Furthermore, the comparison of TRFLP profiles derived from the four DNA extraction methods showed only slight differences, resulting in rather high Bray-Curtis similarity values between 0.73 and 0.82 (Table 3.5).

These findings were also supported by analyzing the stacked bar diagram of the bacterial TRFLP profiles obtained from the different DNA extraction protocols (Figure 3.4). Here differences, particularly between the PS duplicates, were also detected. Furthermore, the relative abundance of TRFs varied between the four DNA extraction methods. For instance, TRF 1 showed a higher relative abundance when extracted with a DNA protocol, including a mechanical treatment step (Figure 3.4). Despite these differences in the relative abundance of individual TRFs, all four DNA extraction methods resulted in the same 16 prevalent TRFs.

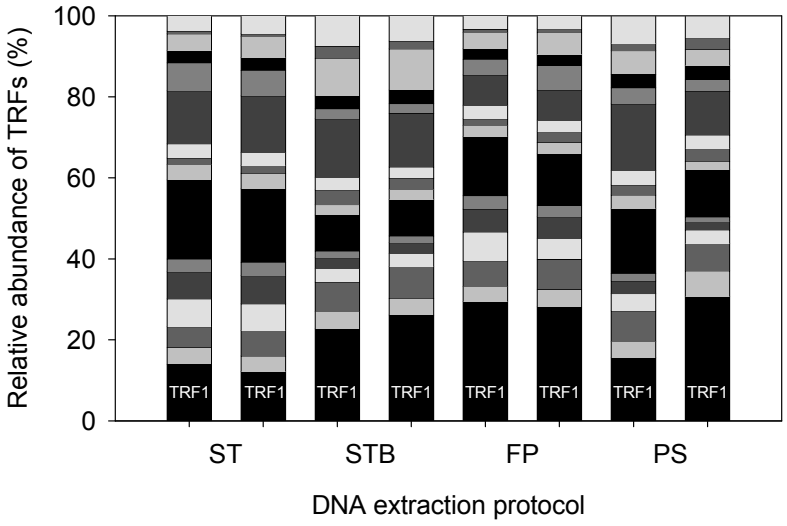

Figure 3.4 Bacterial TRFLP profiles obtained by four different DNA extraction protocols using digestate of the two-phase biogas reactor. TRFs above 2% of the total fluorescence intensity are shown. All samples were analyzed in duplicate. ST, step by step DNA extraction protocol; STB, step by step DNA extraction protocol with beating step; FP, FastDNA® Spin Kit for Soil; PS, PowerSoil® DNA Isolation Kit

Finally, the STB protocol was used for metagenomic analysis, resulting in high molecular weight DNA with high concentrations. The FastDNA® Spin Kit for Soil was applied for the other methodical approaches, resulting in reproducible TRFLP profiles and also in higher DNA concentrations than the PowerSoil® DNA Isolation Kit.

Optimization of PCR protocols and evaluation of primer sets

Different bacterial and archaeal reverse primer sets were tested by applying the TRFLP approach. This resulted in rather similar bacterial and archaeal TRFLP profiles independent of the primer sets applied. For instance, a comparison of TRFLP profiles obtained from two biogas samples amplified with each of the five bacterial primer sets (27f and 926r, 926Rr, 926RMr, 16S, 1492r) revealed high Bray-Curtis similarities of 0.88 ± 0.02 and 0.86 ± 0.04, respectively. Furthermore, the prevalent TRFs above 1% of the total fluorescence intensity were detected with all bacterial primer sets mentioned. However, the primer-set (27f, 926MRr) with two degenerated bases in the reverse primer was used as standard due to the higher number of potential targets in comparison to e.g. the reverse primer 926r without degenerated basis as assumed after applying the RDP probe match tool (Cole et al., 2009).

The comparison of the TRFLP results obtained after applying three archaeal primer sets (Ar109f and Ar912, Ar915, Ar958) also showed similar results (Bray-Curtis value of 0.80 ± 0.04) independent of the primer set used. The number of TRFs with fluorescence intensities above 1% varied slightly between 12 and 14. The primer set used in this study (Ar109f, Ar912r) resulted in the highest number of archaeal TRFs.

Additionally, the impact of cycle numbers was also evaluated, applying the bacterial TRFLP assay. The results showed an increase in TRFs of 29%, comparing 15 and 35 PCR cycles. Due to the fact that an increased cycle number may increase the risk of PCR biases, such as raised chimeric sequences (v. Wintzingerode et al., 1997), 25 and 28 PCR cycles were chosen for the bacterial and archaeal DNA amplification, respectively.

Evaluation of restriction enzymes

For an in-depth characterization of the microbial community, a good resolution of the inherent diversity resulting in a diverse and heterogenic TRFLP profile is essential. To evaluate the optimal restriction enzyme(s) for the biogas samples analyzed in this study, different enzymes and their combinations were tested.

For example, the results of three different enzymes (*Hae*III, *Hin*6I and *Msp*I) and their combinations are shown representing the bacterial community (Figure 3.5). The single enzyme digests resulted in a lower resolution of the bacterial community (total number

of TRFs: 42 ± 8.5) than the approach with two enzymes (54 ± 3.6 TRFs). The combination of the restriction enzymes *Msp*I and *Hin*6I were identified as most valuable showing a good resolution of the TRFLP profile and a high number of TRFs. Although the combination of *Hae*III and *Msp*I resulted in slightly more TRFs, the resolution obtained by using these enzymes was less due to the fact that some fragments are separated close to each other. This impedes the interpretation and identification of TRFs.

The optimization steps of the archaeal TRFLP assay were performed according to the steps described for the bacterial TRFLP assay, showing the best resolution after *Alu*I digestion.

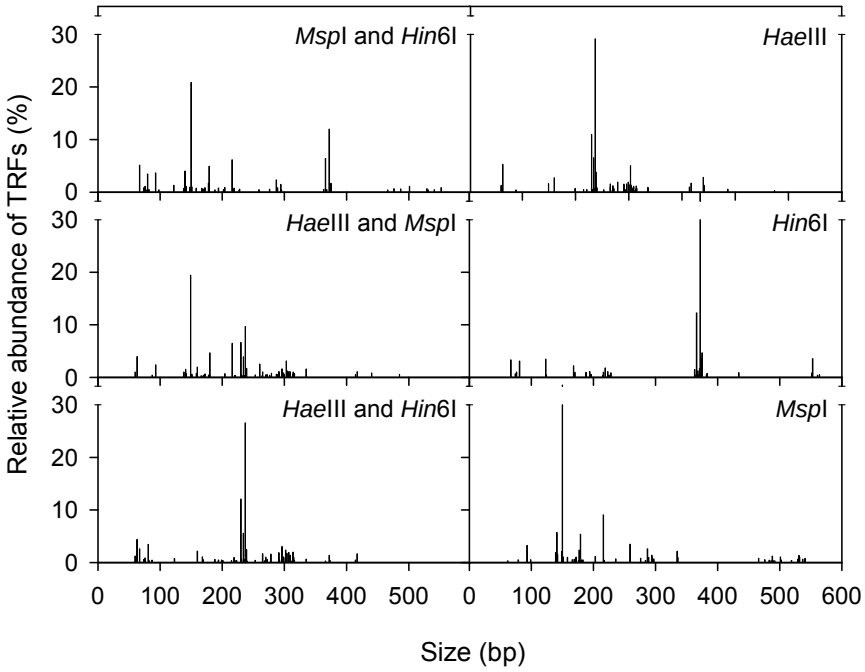

Figure 3.5 TRFLP profiles obtained by the use of different restriction enzymes and their combinations analyzing the bacterial community derived from the digestate. The average TRFLP profiles of duplicate samples are shown.

Reproducibility of the TRFLP analyses

All TRFLP analyses were conducted in triplicate samples based on three independent DNA extractions of the same biogas reactor sample. To give an idea of the reproducibility within the triplicates measured, the prevalent TRFs with at least 2% of

the total fluorescence intensity are shown with standard deviations as example (Figure 3.6).

The standard deviation of the triplicate samples varied between 0.1 and 5.8%, which was not obviously affected by the intensity or by the size of TRFs. Due to the fact that triplicate samples consisted of independent DNA extractions, PCR, digestion and separation steps, these standard deviations were rather low and proved reliability and reproducibility of the method applied. The triplicate TRFLP profiles are shown as average values without standard deviation in the result section of this study to keep the clarity of the diagrams.

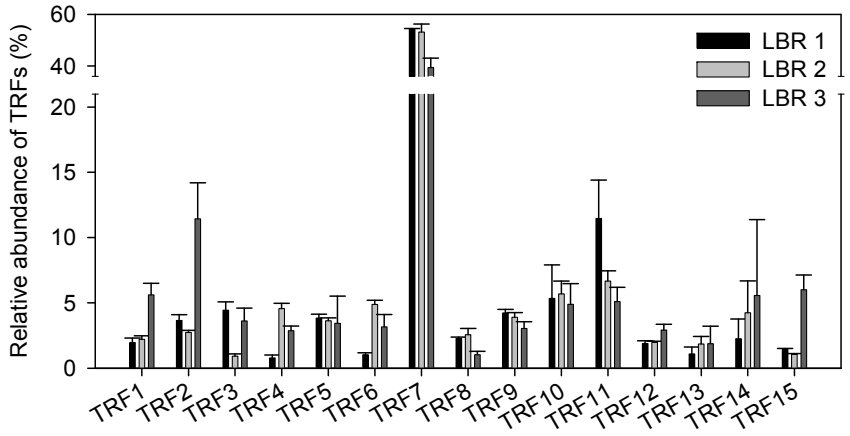

Figure 3.6 Triplicate TRFLP samples indicated with standard deviation. Digestate samples of the three identically constructed LBRs were analyzed by the TRFLP method applying the bacterial assay. TRFs above 2% of the total fluorescence intensity are shown.

Comparison of TRFLP profiles based on TRF height and area

In the literature, the analysis of TRFLP data is based on the TRF height or area. To evaluate the potential difference between these two data processing methods, a comparison between TRFLP results based on the TRF height and area was conducted. The TRFLP profiles obtained were similar, when focusing on the prevalent TRFs with relative abundances of more than 2% of the total fluorescence intensity (Figure 3.7). Only slight variations occurred in the relative abundance of the TRFs identified, indicating no obvious preference for the analysis of TRF by height or area. This is also supported by the high Bray-Curtis similarity values (0.89 - 0.94) obtained for samples

focused on the TRF height and area. However, due to the fact that the threshold for linear measurement is based on the TRF height on the GeXP Genetic Analysis System, the analysis of the TRFLP data was also conducted on the basis of the TRF height.

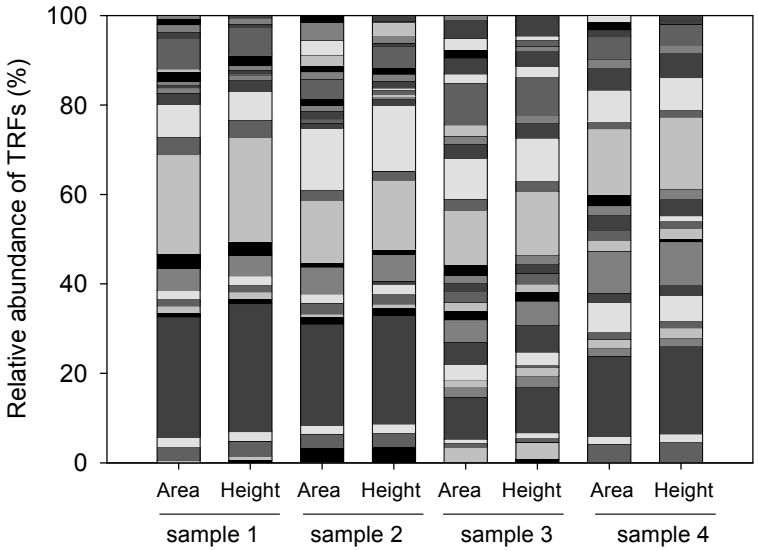

Figure 3.7 Comparison of TRF profiles based on TRF area and height. Biogas samples were analyzed by the bacterial TRFLP assay. TRFs above 2% of the total fluorescence intensity are shown.

3.3.2 Identification of terminal restriction fragments

The affiliation of TRFs (Table 3.6) was identified by constructing and analyzing bacterial and archaeal *rrs* gene sequences. The bacterial TRFs, which could be assigned to taxonomic groups, represented approximately 60 to 70% of the TRFLP profiles (TRFs >3% of the total fluorescence intensity) depending on the sample analyzed. Several of these TRFs showed the highest sequence similarity to members of the Clostridia class, as indicated by NCBI BLAST search against the NCBI nr database and by RDP classification. Members of other taxonomic groups, such as Bacteroidia or Thermotogae, were also identified.

In contrast to that, the assigned archaeal TRFs represented an even higher percentage of the TRFLP profiles accounting for up to 95%. The phylogenetic assignment of these archaeal TRFs revealed members of the Methanobacteriales, Methanosarcinales and Methanomicrobiales orders. In one case, the assignment of the archaeal TRFs was ambiguous. The *rrs* sequences of *Methanobacterium*, *Methanoculleus* and *Methanosaeta* resulted in a TRF with 107 bp length (Table 3.6).

Further, it must be noted that not all TRFs could be assigned to taxonomic groups due to the absence of corresponding sequences in the *rrs* gene libraries. Furthermore, the phylogenetic assignments of the *rrs* gene sequences to sequences retrieved from the NCBI nr database showed maximum identities between 85 and 100% indicating at least in part a distant relationship. Particularly, the assignment of the bacterial *rrs* sequences to reference sequences in the NCBI nr database showed rather low sequence identities, whereas the archaeal sequences revealed sequence identities to database sequences of at least 97%. This is also true for the assignment of *rrs* sequences applying the RDP classifier. Sequences with a sequence identity below 90% to reference sequences of the NCBI nr database, could only be assigned to higher taxonomic levels, such as family or order, using the RDP classifier. In contrast to that, the assignment of archaeal sequences also showed higher sequence similarities by means of the RDP classification. However, due to the differences in the taxonomy of NCBI and RDP, differences in the assignment of sequences occurred, notably at lower taxonomic levels (Table 3.6).

In the following descriptions of the TRFLP results, the affiliation of TRFs is based on the NCBI taxonomy due to the fact that the results of the metagenomic analyses obtained from CARMA (phylogenetic assignment and functional analysis) are also based on the NCBI taxonomy.

Table 3.6 Affiliation of archaeal (A) and bacterial (B) TRFs according to the NCBI and RDP taxonomy

	NCBI taxonomy				RDP taxonomy
TRF	NCBI nr database entry with the highest similarity[a]	Accession number	Query coverage (%)[b,c]	Maximum identity (%)[b,c]	Sequence assignment using the RDP Naive Bayesian rRNA Classifier[c,d]
A 107	*Methanobacterium beijingense* str. 4-1	AY552778	99 - 100	97 - 98	*Methanobacterium* 100%
	Methanoculleus bourgensis str. MS2	NR_042786	99	97 - 98	*Methanoculleus* 100%
	Methanosaeta concilii str. GP-6	CP002565	99 - 100	99 - 100	*Methanosaeta* 100%
A 337	*Methanothermobacter wolfeii* str. DSM 2970	NR_040964	100	100	*Methanothermobacter* 100%
A 339	*Methanothermobacter crinale* str. Tm2	HQ283273	99 - 100	98 - 99	unclassified Methanobacteriaceae (*Methanobacterium* 72%)
A 430	*Methanoculleus bourgensis*	AB065298	99	100	*Methanoculleus* 100%
	Methanoculleus chikugoensis str. MG62	NR_028152	99	98	
	Methanoculleus bourgensis str. MS2	NR_042786	99	100	
A 628	*Methanosarcina* str. 2214B	AB300208	99	99	*Methanosarcina* 100%
B 76	*Thermoanaerobacter* inferii str. AK15	EU262599	99	87	unclassified Firmicutes (*Fervidicola* 39%)
B 95	Bacteroidales str. 28bM	GU129116	57 - 61	87 - 96	unclassified Bacteroidetes (*Cesiribacter* 20%)
B 139	*Bacillus* str. TP-84	AJ002154	99	89	unclassified Bacillales (*Ureibacillus* 50%)
B 141	*Dethiobacter alkaliphilus* str. AHT 1	NR_044205	96	88	*Dethiobacter* 92%
B 151	*Clostridium* str. 6-31	FJ808611	86 - 88	87 - 89	unclassified Clostridiales (*Desulfitibacter* 24 - 26%)
B 161	*Clostridium orbiscindens* str. 17	GU968170	93	85	unclassified Ruminococcaceae (*Anaerotruncus* 36%)
B 167	*Clostridium* str. 6-16	FJ808609	93 - 94	96 - 99	*Clostridium* III 96 - 100%
B 194	*Fervidobacterium* str. CBS-2	EF222229	99 - 100	97 - 98	*Fervidobacterium* 100%
B 214	*Acetomicrobium faecale* type str. DSM 20678	FR749980	94 - 99	94 - 98	*Acetomicrobium* 100%
B 217	*Clostridium thermocellum* str. ATCC 27405	CP000568	99 - 100	91 - 94	*Clostridium* III 76 - 100%
B 221	*Acetomicrobium faecale* type str. DSM 20678	FR749980	96 - 99	95 - 98	*Acetomicrobium* 100%
B 228	*Haloplasma contractile* str. SSD-17B	NR_044362	97	86	unclassified Bacteria (*Haloplasma* 58%)
B 291	Clostridiales str. 24-4c	HQ452852	99	85	unclassified Ruminococcacae (*Saccharofermentans* 19%)
B 304	*Defluviitalea saccharophila* str. LIND6LT2	HQ020487	98	89 - 91	unclassified Lachnospiraceae (*Sporobacterium* 38%)

[a], nucleotide BLAST search against the NCBI non-redundant (nr) database without uncultured environmental sequences using the megablast algorithm (last access July 2012)
[b], values indicated by BLAST analysis against NCBI nr database
[c], ranged values are obtained by analyzing mutiple *rrs* gene sequences
[d], RDP Classifier version 2.5 (May 2012), a confidence value of at least 80% was used for phylogenetic assignment, genera indicated in brackets had a confidence value of ≤ 80%

3.3.3 Similarity of the bacterial community in the three biogas systems

The similarity of the bacterial community within the three biogas systems was compared at the beginning of the experiment (LBR 55 °C) by analyzing digestate samples with the TRFLP method.

The comparison of the TRFLP profiles from samples derived from the three biogas systems showed high similarity values of 0.92 to 0.95 (Chao-Jaccard) and 0.73 to 0.83 (Bray-Curtis; Table 3.7), indicating a similar bacterial community. Beside the quantity of TRFs, the Bray-Curtis similarity index also includes the relative abundance of TRFs, whereas the Chao-Jaccard similarity also includes the unseen shared species of two samples. However, a reduced Bray-Curtis value indicates more variations within the relative abundance of TRFs than within the number of TRFs.

Both similarity indices indicated a similar bacterial community at the beginning of the whole experiment. Further analyses at higher LBR temperatures (LBR 70 °C) revealed that the bacterial community changed in the same manner in all three biogas systems during the temperature increase in the LBR (cf. 3.3.6).

Table 3.7 Similarity indices for the bacterial TRFLP profiles of digestate samples taken from the three biogas reactors

Bray-Curtis	LBR1	LBR2	LBR3	Chao-Jaccard	LBR1	LBR2	LBR3
LBR1	0.90 ± 0.05	0.83 ± 0.04	0.73 ± 0.04	LBR1	0.97 ± 0.02	0.93 ± 0.01	0.92 ± 0.01
LBR2	0.83 ± 0.04	0.91 ± 0.03	0.75 ± 0.03	LBR2	0.93 ± 0.01	0.98 ± 0.00	0.95 ± 0.01
LBR3	0.73 ± 0.04	0.75 ± 0.03	0.82 ± 0.05	LBR3	0.92 ± 0.01	0.95 ± 0.01	0.97 ± 0.01

LBR1 - 3, leach-bed reactors of the three biogas reactor systems

3.3.4 Impact of the substrate-attached bacterial community on the bacterial community in the biogas reactor

The bacterial community attached to the surface of the substrates (silage and straw) was analyzed and compared with samples derived from the 21-day fermentation process at LBR temperatures of 55, 60 and 65 °C. This analysis was performed in the context of the Bachelor thesis of C. Nolte (2011).

The results showed that the bacterial community in the two-phase biogas reactor was not affected by the substrate-attached bacterial community (Figure 3.8). Hence, during the ongoing digestion process, most TRFs which were dominantly detected in substrate samples were not identified in the leachate samples derived from different time points of the fermentation process. After 21 days of fermentation, the bacterial community of the digestate showed almost no similarity to the original substrate-attached community. Only two TRFs were detected after 21 days of fermentation, which had also been identified in the community profile of the substrate supplied.

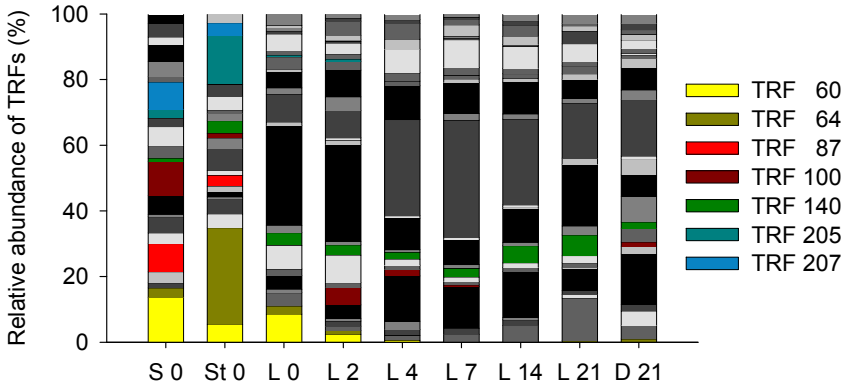

Figure 3.8 Impact of the substrate-attached bacterial community on the bacterial community in the biogas system. TRFs derived from the 21-day fermentation process at 65 °C with florescence intensities above 3% are shown. Colored bars represent major TRFs in the substrates. S 0, silage on day 0; St 0, straw material on day 0; L 0 - 21, leachate at different time points of fermentation; D 21, digestate at the end of the fermentation (data based on the Bachelor thesis of Nolte, 2011)

A pairwise comparison of the TRFLP profiles obtained from the substrate (silage and straw) and the leachate and digestate samples based on the Bray-Curtis and

Chao-Jaccard indices confirmed these findings. The similarity values were extremely low with 0.02 ± 0.01 to 0.24 ± 0.06, indicating a different bacterial community attached to the substrate in comparison to the bacterial community in the biogas reactor system during the 21 days of fermentation.

3.3.5 Changes in the bacterial community in the LBR during the fermentation of one load of substrate

The bacterial community dynamics were monitored by analyzing the leachate and digestate of the LBR at different time points during the 21-day fermentation process and at the end of the fermentation for each temperature regime of the LBR, applying the TRFLP method. Parts of this analysis were performed in the context of the Bachelor thesis of C. Nolte (2011).

LBR temperature of 55 and 60 °C

A similar bacterial community composition was observed at the beginning (day 0) and the end (day 21) of the fermentation process, whereas in the middle phase, strong changes occurred, particularly after 7 days of fermentation (Figure 3.9 A, B; Appendix Figure 7.1 A, B). This indicated that the bacterial community was subject to cyclic alterations during the digestion of one load of substrate (silage and straw) at LBR temperatures of 55 and 60 °C. The strongest alterations occurred slightly after the detection of the highest VFA concentration in the leachate.

These findings of cyclic changes in the bacterial community were supported by the results of the Bray-Curtis similarity analyses, which revealed high similarity values of 0.79 ± 0.02 (55 °C) and 0.75 ± 0.05 (60 °C) after a pairwise comparison of the leachate derived from day 0 and 21. Furthermore, a pairwise comparison of the leachate derived from day 0 and 7 showed low Bray-Curtis similarity values with 0.28 ± 0.03 (55 °C) and 0.48 ± 0.04 (60 °C), respectively.

All prevalent TRFs of these TRFLP profiles were assigned to members of the Clostridia class, independent of the alterations within the bacterial community (Figure 3.9 A, B).

More specifically, at the beginning and at the end of the fermentation process at 55 and 60 °C, one TRF (TRF 151) dominated the TRFLP profiles. In between, the bacterial community composition varied strongly during both the fermentation at 55 and 60 °C, particularly after 7 days. It was here that the TRF 151 (*Clostridium*) decreased strongly and TRF 217 (*Clostridium*) and TRF 304 (*Defluviitalea*) at 55 °C and TRF 167 (*Clostridium*) and TRF 304 (*Defluviitalea*) at 60 °C prevailed.

LBR temperature of 65 °C

The changes in the bacterial community in the LBR operated at 65 °C were also tracked by TRFLP analyses. In contrast to the former analysis, the fermentation process was also analyzed on days 4, 9 and 11 to obtain further insights into the alterations in the bacterial community.

Here, the first strong alterations within the bacterial community occurred on day 4 (Figure 3.9 C, Appendix Figure 7.1 C). It was here that the highest concentration of VFA was measured. A comparison of the TRFLP profiles derived from days 0 and 2 with those from day 4 showed Bray-Curtis values of 0.43 ± 0.04 and 0.55 ± 0.06, indicating alterations within the bacterial community.

Between days 4 and 14, the bacterial community showed lower alterations. This is supported by higher Bray-Curtis similarity values between 0.73 ± 0.10 and 0.79 ± 0.07. Here, TRF 151 (*Clostridium*), which had been prevalent before, was strongly reduced and suppressed by the emergence of TRF 167, followed by TRFs 84, 170 and 228. Apart from TRFs 84 and 170, which were of unknown phylogenetic affiliation, TRF 167 revealed the highest sequence similarity to a member of the *Clostridium* genus (Figure 3.9 C). In contrast to that, the assignment of TRF 228 showed the highest sequences similarity to the *Haloplasma* genus (unclassified bacteria).

At the end of the 21-day digestion process, slight alterations within the bacterial community reappeared. Accordingly, the pairwise comparison of samples from day 21 with those from day 14 showed slightly reduced Bray-Curtis values of 0.63 to 0.65 ± 0.05.

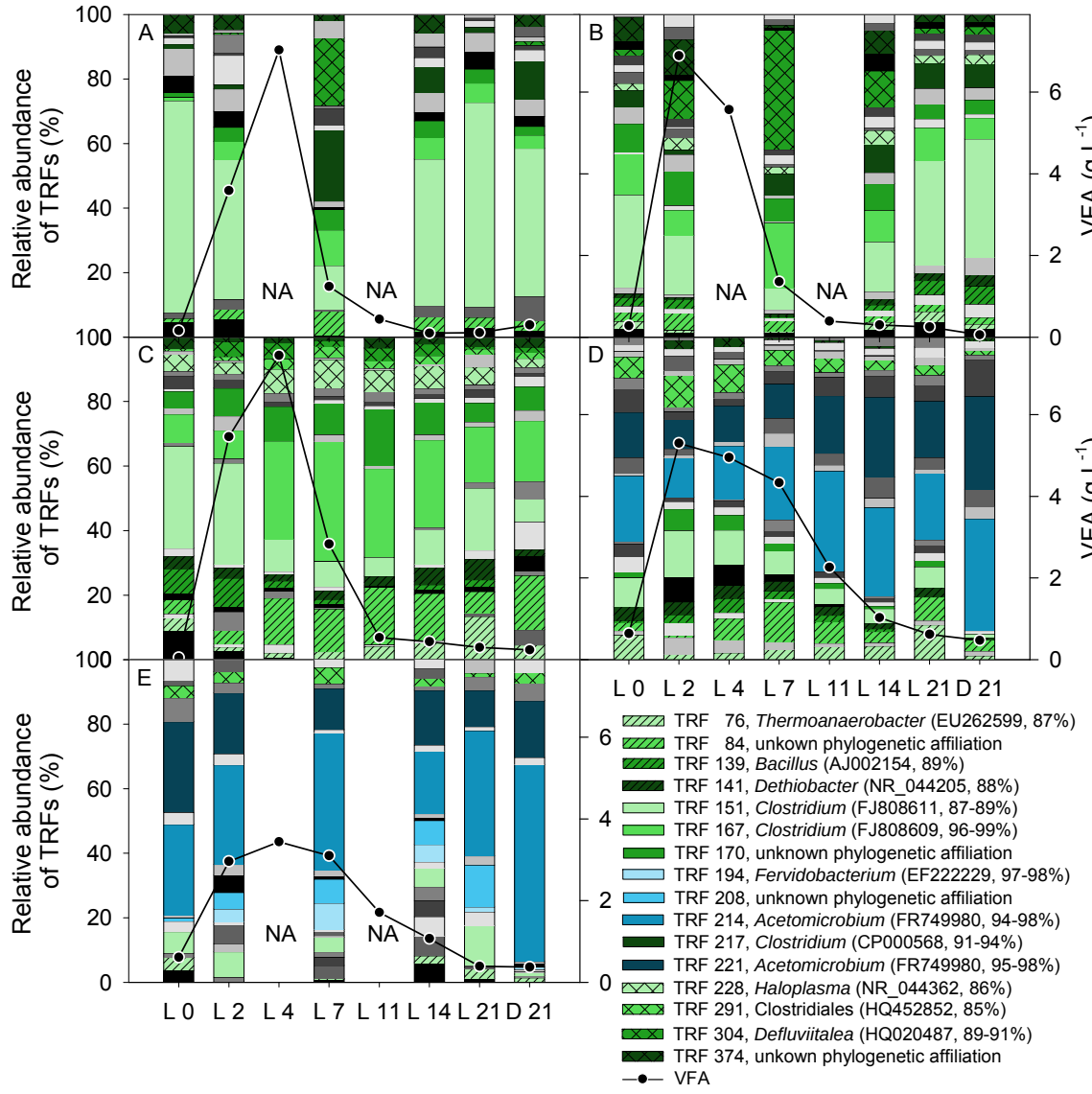

Figure 3.9 Bacterial community dynamics and VFA concentration during the 21-day fermentation of one load of substrate at LBR temperatures of 55 °C (A), 60 °C (B), 65 °C (C), 70 °C (D) and 75 °C (E). TRFs above 3% of the total fluorescence intensity are shown. Sequence accession number and identity of the TRF affiliations are indicated in brackets (cf. Table 3.6). L 0 - 21, leachate at different time points of fermentation; D, digestate at the end of the fermentation; NA, not analyzed (data of B, C and D based on the Bachelor thesis of Nolte, 2011)

LBR temperature of 70 and 75 °C

The bacterial community was also subject to alterations at LBR temperatures of 70 and 75 °C (Figure 3.9 D, E; Appendix Figure 7.1 D, E). The first changes already occurred after two days of fermentation. On days 2 and 4, the highest VFA concentrations were detected in both fermentations. The pairwise comparison of the leachate samples derived from days 0 and 2, based on the Bray-Curtis similarity, resulted in values of 0.52 ± 0.04 (70 °C) and 0.60 ± 0.02 (75 °C). This indicates differences within the bacterial community already at the start of the digestion process. Afterwards, the composition of the bacterial community changed successively until the end of the 21-day fermentation.

Despite these changes, the TRF 214, followed by TRF 221, dominated the TRFLP profiles during the whole digestion process at 70 and 75 °C (Figure 3.9 D, E). The TRFs 214 and 221 showed the highest sequence similarity to a member of the Bacteroidia class (*Acetomicrobium*). At 70 °C, TRFs, which had been prevalent at lower LBR temperatures, were also detected in higher abundances, such as TRF 151 (*Clostridium*) and TRF 84 (unknown phylogenetic affiliation). At 75 °C, TRF 194, which was assigned to the *Fervidobacterium* genus (Thermotogae), was detected for the first time (Figure 3.9 D, E).

3.3.6 Impact of temperature increase on the bacterial community in the LBR

To determine the bacterial community changes in the LBR as a consequence of the temperature increase, the bacterial TRFLP profiles were compared for two different time points of the fermentation at each temperature regime of the LBR.

Substantial alterations in the bacterial community were observed after temperature increase from 65 to 70 °C (Figure 3.10). Up to 65 °C, the bacterial community consisted mostly of members belonging to the Clostridia class. Above 65 °C, members of the Bacteroidia, Clostridia and Thermotogae classes dominated the bacterial community within the LBR. These changes in the bacterial community were supported by the results of a pairwise comparison based on the Bray-Curtis similarity. The

similarity values calculated for TRFLP profiles derived from samples at 65 and 70 °C ranged between 0.38 ± 0.01 and 0.45 ± 0.02.

In detail, this TRFLP analysis resulted in a total number of 31 TRFs. At 55 and 60 °C, the community profiles showed only slight variations (Figure 3.10). The prevalent TRFs at these temperatures, i.e., TRFs 151, 167, 217 and 304 showed the highest sequence similarity to members of the Clostridia class. At 65 °C, slight changes in the bacterial community were detected (Figure 3.10). For instance, the relative abundance of the TRFs 84 and 167 were increased, whereas other TRFs decreased (TRF 304) or disappeared (TRF 217).

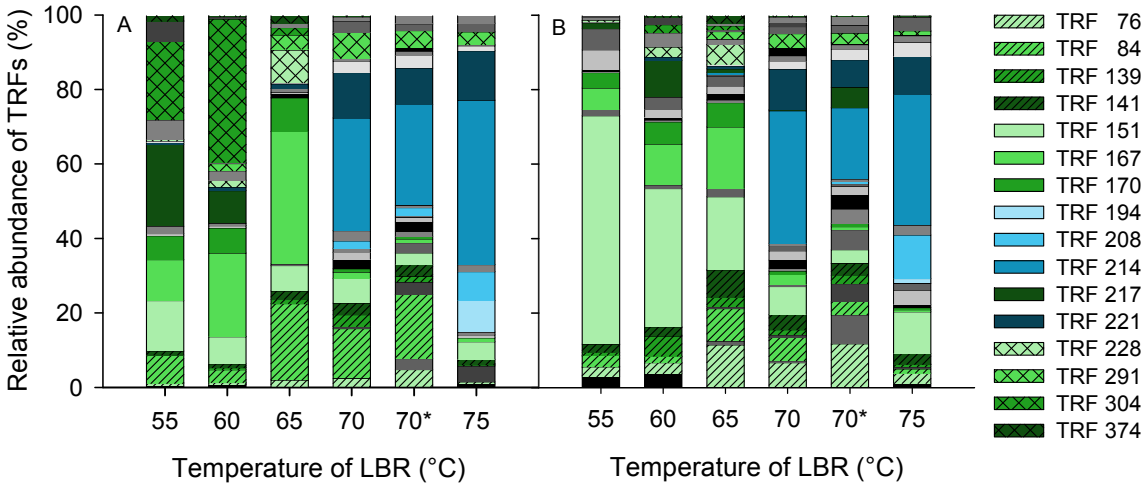

Figure 3.10 Impact of temperature increases in the LBR (55 - 75 °C) on the bacterial community composition in the LBR. Bacterial TRFLP profiles of leachate samples from the LBR on day 7 (A) and 21 (B) are shown. Phylogenetic affiliation of TRFs as indicated in Table 3.6. TRFs above 3% of the total fluorescence intensity are shown. *, analysis after bioaugmentation with compost

After temperature increase to 70 °C, fundamental alterations in the bacterial community were observed (Figure 3.10). Some TRFs, such as TRFs 167 and 304 decreased strongly or disappeared, whereas three fragments (TRFs 208, 214 and 221) were detected for the first time. TRF 214 (*Acetomicrobium*) was the prevalent fragment at 70 and 75 °C with relative abundances up to 44%. Additionally at 75 °C, another TRF appeared (TRF 194), which was assigned to the *Fervidobacterium* genus (Thermotogae).

The TRFLP profiles of samples derived from the fermentation after the bioaugmentation with compost at 70 °C showed two new TRFs (TRFs 147, 183) as well as already known TRFs at higher abundances (e.g., TRFs 76, 79, 84, 86, 152, 172 and 177). Some of these TRFs were also detected in the TRFLP profiles derived from the compost sample. However, the major TRFs of the compost sample (e.g., TRFs 151, 181, 206) were not enriched in the TRFLP profiles derived from the biogas samples after bioaugmentation.

Impact of temperature increase on the bacterial community in the three biogas systems

The second and third two-phase biogas systems were also analyzed at LBR temperatures of 65 and 70 °C (each on day 7) to confirm the bacterial community changes in the LBR of the first biogas system (Figure 3.11).

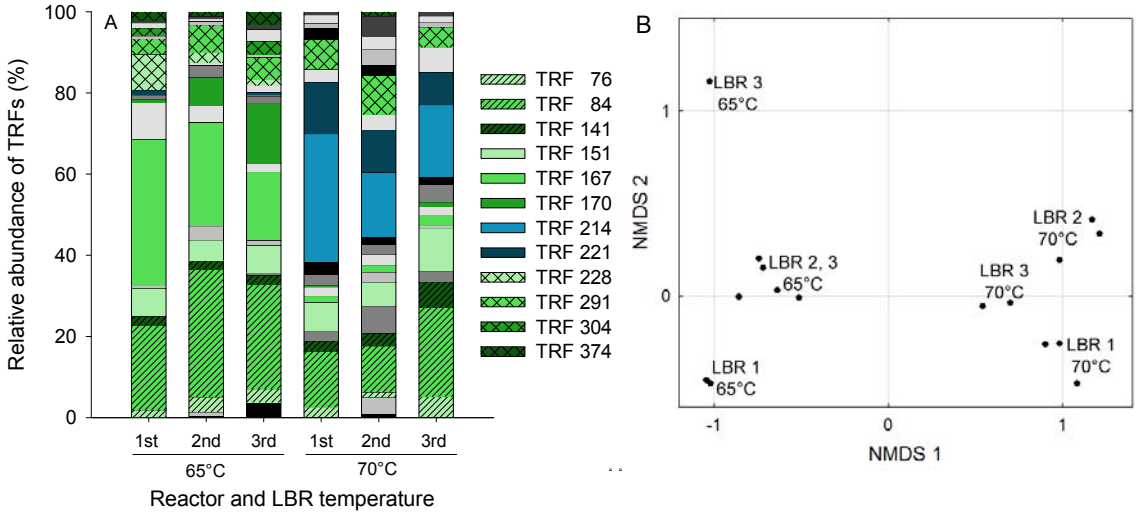

Figure 3.11 TRFLP profiles (A) and NMDS plot of TRFLP profiles (B) obtained from the three biogas reactors at LBR temperatures of 65 and 70 °C (day 7). Phylogenetic affiliation of TRFs as indicated in Table 3.6. TRFs above 3% of the total fluorescence intensity are shown. Stress value of NMDS analysis is 0.032.

In the two identically constructed systems, the same alterations in the bacterial community from being Clostridia-dominated towards being dominated by members of the Bacteroidia and Clostridia classes were detected. These alterations were also supported by the pairwise comparison based on the Bray-Curtis similarity, showing

rather low similarity values of 0.41 ± 0.05 between TRFLP profiles derived from 65 and 70 °C. These Bray-Curtis similarity values were the basis for the NMDS plot (Figure 3.11.) also supporting the strong change of the bacterial community between 65 and 70 °C in all three reactor systems (Figure 3.11).

Direct response of the bacterial community in the LBR to the temperature increase to 70 °C

Samples of the two-phase biogas reactor were normally taken at the earliest after one fermentation period of 21 days to enable the adaption of the bacterial community to the increased temperature. Here, to track the direct response of the bacterial community to the temperature increase to 70 °C, the fermentation was directly analyzed after this temperature increase.

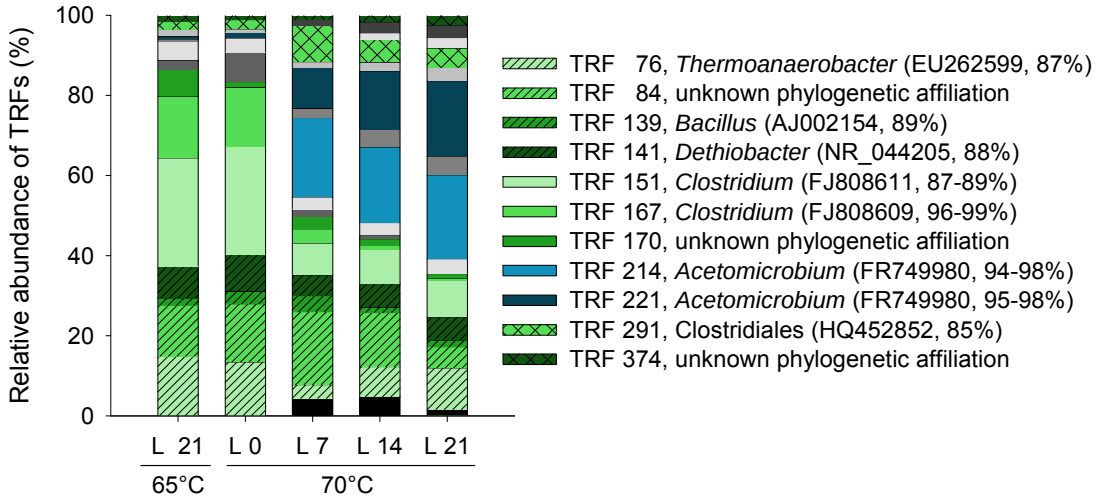

Figure 3.12 Direct response of the bacterial community in the LBR to the temperature increase of 70 °C. TRFLP profiles of leachate samples are shown. Sequence accession number and identity of the TRF affiliations are indicated in brackets (cf. Table 3.6). TRFs above 3% of the total fluorescence intensity are shown. L 0 - 21, leachate at different time points of fermentation

A clear change in the bacterial community in the LBR was already observed after 7 days of fermentation at an LBR temperature of 70 °C (Figure 3.12). In detail, the TRFs 214 and 221 (*Acetomicrobium*), which were dominantly detected at 70 °C, were already prevalent after 7 days of fermentation at 70 °C (Figure 3.12). The relative

abundance of these TRFs increased slightly until the end of the fermentation on day 21. The emergence of these TRFs suppressed the detection of TRFs 76, 151 and 167 (all assigned to Clostridia), which had dominated at the start of the fermentation directly after temperature increase to 70 °C (Figure 3.12).

3.3.7 Impact of temperature increase on the bacterial community in the AF

Besides the obvious role of the bacterial community in biomass degradation in the LBR, the bacterial community may also play a major role in the AF interacting with hydrogenotrophic archaea in syntrophy. To evaluate the impact of the temperature increase on the bacterial community in the AF, this community was also analyzed (Figure 3.13).

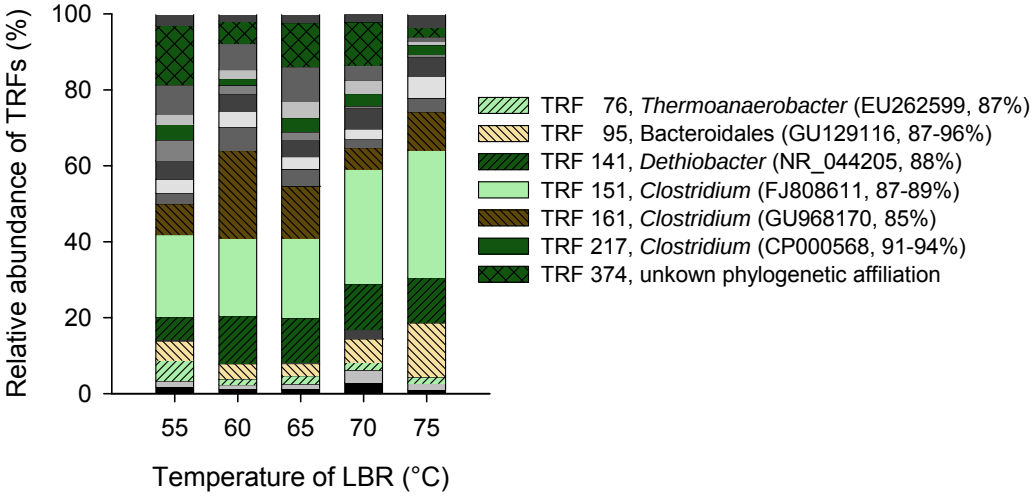

Figure 3.13 Bacterial community attached to the AF packings during temperature increases in the LBR from 55 to 75 °C. Sequence accession number and identity of the TRF affiliations are indicated in brackets (cf. Table 3.6). TRFs above 3% of the total fluorescence intensity are shown.

Altogether, only slight variations were detectable in the bacterial community in the AF during the temperature increase in the LBR. This is supported by the Bray-Curtis

similarity values for these TRFLP profiles, ranging between 0.60 ± 0.09 and 0.77 ± 0.05.

During the whole experiment, the TRF 151 (*Clostridium*), followed by TRF 161 (*Clostridium*), TRF 141 (*Dethiobacter*), TRF 374 (unknown phylogenetic affiliation) and TRF 95 (Bacteroidia) were the most prevalent bacterial TRFs in the AF (Figure 3.13). Most of these TRFs were also detected as prevailing in the LBR except for TRF 161, which was detected for the first time. The TRFs 151, 161 and 141 were assigned to members of the Clostridia class, indicating a prevalence of Clostridia in the AF. Only TRF 95 showed the highest sequence similarity to a member of the Bacteroidia class.

3.3.8 Changes in the archaeal community in the AF during the fermentation of one load of substrate

In contrast to the dynamics of the bacterial community within the 21-day fermentation of one load of substrate, the archaeal community in the AF altered less as indicated for the LBR temperature regime of 55°C (Figure 3.14 A). The pairwise comparison (Bray-Curtis index) of the TRFLP profiles from AF samples at different time points of the fermentation showed rather high similarities between 0.70 ± 0.06 and 0.83 ± 0.01. At all time points, the TRF 339, showing the highest sequence similarity to the hydrogenotrophic *Methanothermobacter* genus, was prevalently detected (Figure 3.14 A). Beside this strain, another member of the strict hydrogenotrophic *Methanothermobacter* genus (TRF 337) was identified (Figure 3.14 A). In contrast, strict acetoclastic (*Methanosaeta* sp., TRF 107) or mixotrophic methanogens (*Methanosarcina* sp., TRF 628) formed the minority within the TRFLP profiles of leachate samples derived from the AF at an LBR temperature of 55 °C (Figure 3.14 A).

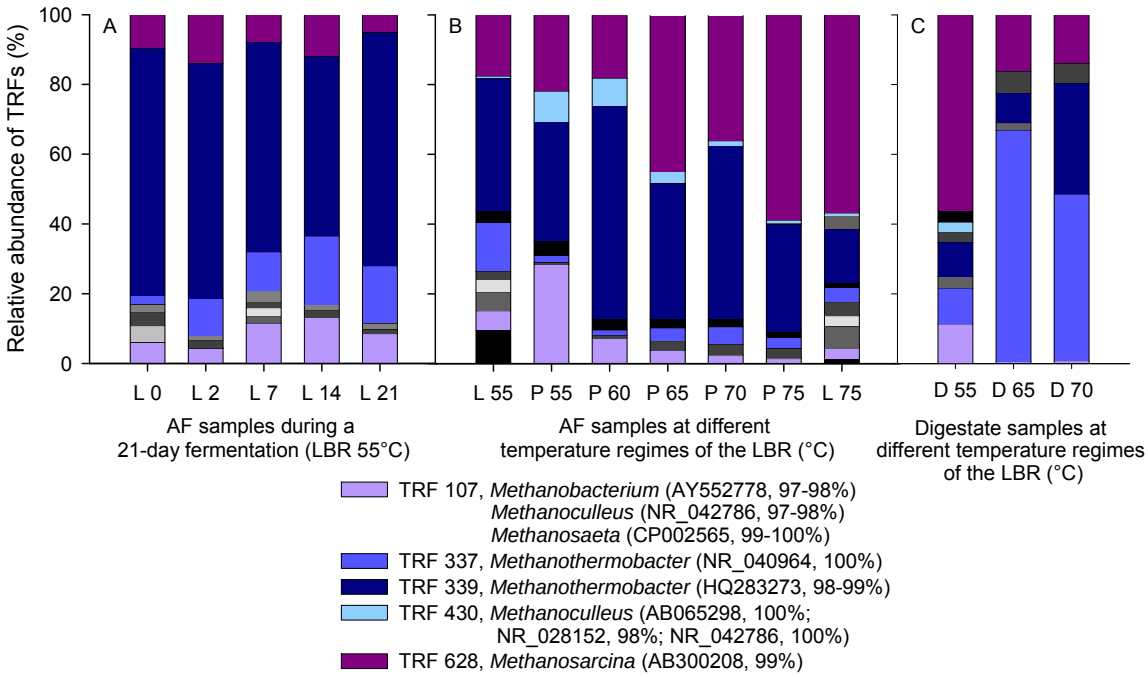

Figure 3.14 Changes in the archaeal community composition during the experimental runs. Archaeal TRFLP profiles were obtained for AF samples during the 21-day fermentation of one load of substrate at an LBR temperature of 55 °C (A), for AF samples (day 21) during temperature increases in the LBR (55 - 75 °C, B) and for digestate samples at different temperature regimes of the LBR (C). Sequence accession number and identity of the TRF affiliations are indicated in brackets (cf. Table 3.6). TRFs above 3% of the total fluorescence intensity are shown. L 0 - 21, leachate at different time points of fermentation; L 55 & 75, leachate at LBR temperatures of 55 and 75 °C; P 55 - 75, packing at different temperature regimes of the LBR; D 21, digestate at the end of fermentation; D 55, 65 & 70, digestate at different temperature regimes of the LBR

3.3.9 Impact of temperature increase on the archaeal community in the AF

During the increase in the LBR operation temperature, the temperature of the AF remained constant at 55 °C. To monitor the archaeal community during temperature increase in the LBR, the biofilm on the packing's surface derived from the AF was

analyzed at the end of each LBR temperature regime. Further, leachate samples of the AF at an LBR temperature of 55 and 75 °C were also analyzed for comparative analysis.

The archaeal TRF 339, assigned to *Methanothermobacter* (Methanobacteriales), and TRF 628, assigned to *Methanosarcina* (Methanosarcinales), were most prevalent during the whole experiment, showing an uneven progress (Figure 3.14 B). A pairwise comparison between packing samples derived from 55 to 75 °C based on the Bray-Curtis similarity revealed values equal or higher than 0.66 ± 0.03, indicating slight changes in the archaeal community.

At 55 °C, the archaeal community of the packing's biofilm consisted mostly of members of the strict hydrogenotrophic Methanobacteriales, whereas species belonging to the mixotrophic Methanosarcinales dominated the archaeal community at 75 °C (Figure 3.14 B). This is also true for the leachate samples analyzed at LBR temperatures of 55 and 75 °C.

In addition to these TRFs, further fragments were identified in the archaeal TRFLP profiles. For instance, TRF 107, which was also prevalent, but only in the AF packing at an LBR temperature of 55 °C (Figure 3.14 B), was assigned to members of the Methanobacteriales, Methanomicrobiales and Methanosarcinales (Figure 3.14 B). Additionally, TRFs 337 and 430, assigned to Methanobacteriales and Methanomicrobiales, respectively, were less frequently detected or not detected in all samples (Figure 3.14 B).

3.3.10 Impact of temperature increase on the archaeal community in the LBR

The archaeal community in the LBR was also monitored during temperature increase (Figure 3.14 C). As shown for the bacterial community, the temperature increase had also an impact on the archaeal community in the LBR. Here, a shift from mixotrophic to hydrogenotrophic methanogens was detected during temperature increase.

In detail, at an LBR temperature of 55 °C, the archaeal community profile was dominated by *Methanosarcina* (TRF 628). Strict hydrogenotrophic methanogens, such as *Methanothermobacter* (TRFs 337 and 339), were detected at lower level. At LBR temperatures of 65 and 70 °C, the TRFLP profiles revealed a strong reduction of *Methanosarcina*. Instead, TRFs assigned to the *Methanothermobacter* genus (TRF 337) were identified at higher abundances. Interestingly, this TRF was detected only rarely in the TRFLP profiles from the AF.

3.4 454-pyrosequencing of microbial metagenomes

Four different biogas reactor samples were analyzed by 454-pyrosequencing in order to determine the microbial community and the genetic potential for e.g., carbohydrate degradation. Digestate samples were taken from the LBR at 55, 65 and 70 °C (D 55, D 60, D 70). The fourth sample was derived from the packing's biofilm of the AF (P 55) at an LBR temperature of 55 °C.

Table 3.8 454-pyrosequencing parameters of four different samples derived from the two-phase biogas system

	Packing of AF LBR/AF 55 °C (P 55)	Digestate of LBR LBR 55 °C (D 55)	Digestate of LBR LBR 65 °C (D 65)	Digestate of LBR LBR 70 °C (D 70)
Metagenomic sequences	248,775	303,493	309,589	315,387
Sequenced bases (bp)	97,884,221	120,496,674	124,456,333	127,974,741
Average read length (bp)	393	397	402	406
GC content (%)	8.0 - 80.9	0.0 - 80.0	11.6 - 84.2	12.8 - 81.4

bp, base pairs

The 454-pyrosequencing run resulted in 1,177,244 metagenomic sequences with an average read length of 400 bases (Table 3.8). The sequence information obtained comprised 470,811,969 bases for all samples. The metagenomic sequences were phylogenetically and functionally characterized, using the MetaSams platform 0.99 (Zakrzewski et al., 2013).

Phylogenetic assignment of metagenomic sequences by RDP classifier and CARMA

The phylogenetic assignment of metagenomic sequences was conducted using the RDP classifier and the CARMA tool. A total of 3,473 metagenomic sequences were identified encoding parts of the 16S rRNA (Table 3.9), which represented only 0.29 ± 0.09% of the total metagenomic sequences. In contrast to the analysis of the *rrs* sequences, the analysis of metagenomic sequences representing functional genes (so-called environmental gene tags, EGTs) encompassed 303,514 EGTs, applying CARMA. This represented 25.67 ± 1.83% of the total metagenomic sequences (Table 3.9).

Table 3.9 Number of metagenomic sequences and the number of sequences assigned to taxonomic groups applying the RDP classifier and CARMA. For description of samples refer to Table 3.8.

	P 55	D 55	D 65	D 70	Distribution (%)
Metagenomic sequences	248,775	303,493	309,589	315,387	100
Identified *rrs* sequences using RDP	495	771	946	1,261	0.29 ± 0.09
Identified EGTs using CARMA	59,492	75,131	80,124	88,767	25.67 ± 1.83
Identified pEGTs using CARMA	56,532	72,048	76,537	85,579	24.58 ± 1.89

EGT, environmental gene tag; pEGT, prokaryotic environmental gene tag

Altogether, approximately 70% of metagenomic sequences remained unassigned, which indicated that a certain number of additional species are involved in the biogas fermentation process. However, the majority of assignable metagenomic sequences (*rrs* sequences and EGTs) belonged to the Bacteria domain independent of the phylogenetic analysis or the metagenomic sample (Table 3.10).

A total ranging from 88.9% (P 55) to nearly 100% (D 70) of *rrs* sequences (RDP classifier), encoding parts of the 16S rRNA, were assigned to Bacteria. The CARMA results showed that 69.8% (P 55) to 95.0% (D 70) of EGTs, encoding functional genes, were assigned to Bacteria. Independent of the applied phylogenetic assignment method, the sample derived from the packing of the AF showed a reduced number of Bacteria, whereas the number of metagenomic sequences assigned to Archaea was clearly enriched with 11% (RDP) and 25% (CARMA). Simultaneously, the digestate samples showed slightly increasing assignments to Bacteria and a slight decrease in Archaea during LBR temperature increase.

A minor percentage of EGTs was assigned to Eukaryota using the CARMA tool (Table 3.10). At a reactor temperature of 55 °C, EGTs belonging to Eukaryota were identified with an average percentage of 3.9% (P 55, D 55). At higher LBR temperatures, Eukaryota were detected with 1.4 to 2.0% of EGTs.

Table 3.10 Distribution of phylogenetic assignments of *rrs* sequences and EGTs to taxonomic groups applying the RDP classifier and CARMA. For description of samples refer to Table 3.8.

Domain	Distribution of phylogenetic assignments (%)							
	P 55		D 55		D 65		D 70	
	RDP	CARMA	RDP	CARMA	RDP	CARMA	RDP	CARMA
Bacteria	88.9	69.8	97.9	91.6	99.0	93.6	99.9	95.0
Archaea	11.1	25.2	2.1	4.3	1.0	3.8	0.1	3.3
Eukaryota	-	4.1	-	3.6	-	2.0	-	1.4
Others	-	0.9	-	0.5	-	0.6	-	0.3

3.4.1 Phylogenetic assignment of metagenomic sequences to Bacteria

Phylogenetic assignment of metagenomic sequences to Bacteria by RDP classifier and CARMA

The number of identified bacterial classes differed depending on the applied phylogenetic assignment methods. Whereas the CARMA tool revealed approximately 25 bacterial classes within all samples, the RDP classifier showed a descending diversity of Bacteria from 11 (P 55) to 3 (D 70) classes during LBR temperature increase.

The majority of metagenomic sequences were assigned to Bacteria and herein most prevalently to the Clostridia class, followed by the Bacilli, Thermotogae and Gammaproteobacteria classes independent of the metagenomic sample or the applied phylogenetic assignment method (Figure 3.15). During the LBR temperature increase, a slight reduction of members belonging to the Clostridia was only detected for the results derived from the RDP classifier. Simultaneously, the number of metagenomic sequences assigned to the Bacilli class increased, indicating alterations induced by the temperature increase.

More specifically, Clostridia, the prevalent class, was detected in 16.2% of *rrs* sequences by the RDP classifier and 19.4% of prokaryotic EGTs (pEGTs) by the CARMA tool in the methanogenic biofilm sample (P 55; Figure 3.15). In contrast, the digestate samples revealed higher percentages of Clostridia between 24.4 to 31.9% of *rrs* sequences by RDP and 36.2 to 44.7% of pEGTs by CARMA.

Bacilli were the next prevalent class. The digestate samples revealed an increasing occurrence from 0.1 to 4.0% of *rrs* sequences (RDP) and 6.8 to 9.5% of pEGTs (CARMA) during the LBR temperature increase from 55 to 70 °C (Figure 3.15). In the sample derived from the AF, Bacilli were less detected with 0.4% (RDP) and 4.5% (CARMA).

Members of the Thermotogae class were most frequently identified at an LBR temperature of 55 °C (P 55, D55) accounting for 1.2 to 1.8% by both, the RDP and CARMA analysis (Figure 3.15). At higher temperatures, members of the Thermotogae were less abundant or not detected.

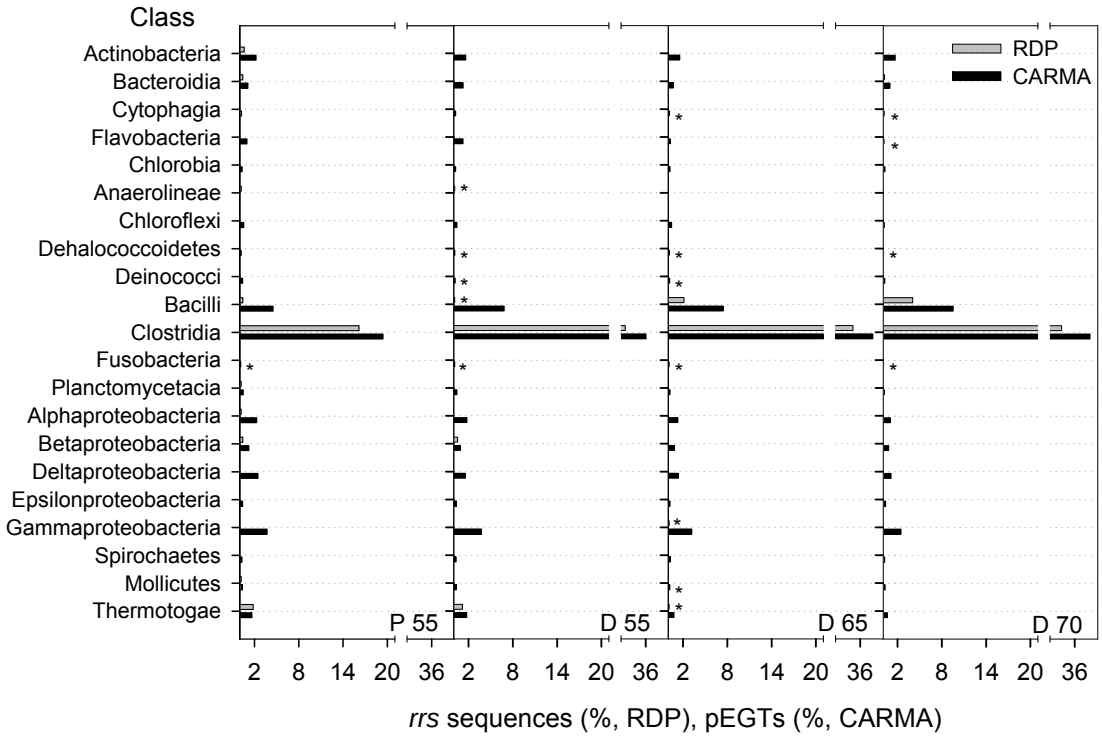

Figure 3.15 Phylogenetic assignment of metagenomic sequences to Bacteria using the RDP classifier (grey) and CARMA (black) showing the prevalent bacterial classes. For description of samples refer to Table 3.8. pEGTs, prokaryotic environmental gene tags; *, abundance ≤ 0.2% of *rrs* sequences or pEGTs

Furthermore, the CARMA analysis revealed a presence of Gammaproteobacteria from 2.5 to 3.7% of pEGTs in all samples. In contrast, the RDP classifier found members of the Proteobacteria, such as Betaproteobacteria, to a minor extent and only at 55 °C (Figure 3.15). In addition, members of other classes, such as Actinobacteria, Bacteroidia, Flavobacteria and Cytophaga occurred with relative abundances of 2.2%, 1.3%, 1.3% and 0.3%, respectively (Figure 3.15).

According to the assignment of metagenomic sequences to classes, *Clostridium* and *Bacillus* were the most prevalent bacterial genera in all metagenomic samples as revealed by CARMA (Figure 3.16 A). In the digestate samples, a slight reduction of members of the *Clostridium* genus occurred (20.4 - 17.3%) along with an increase in members of the *Bacillus* genus (2.5 - 4.7%), particularly after a temperature increase to 70 °C. In addition, also *Caldicellulosiruptor* (0.3 - 1.7%) and *Alkaliphilus* (1.1 - 1.6%) were detected with increasing proportions in the digestate samples during the LBR temperature increase.

In the sample derived from the packing's biofilm from the AF, 4.1% of pEGTs were assigned to the *Clostridium* genus, followed by *Pelotomaculum* (1.1%), *Petrotoga* (0.9%) and *Syntrophomonas* (0.8%; Figure 3.16 A).

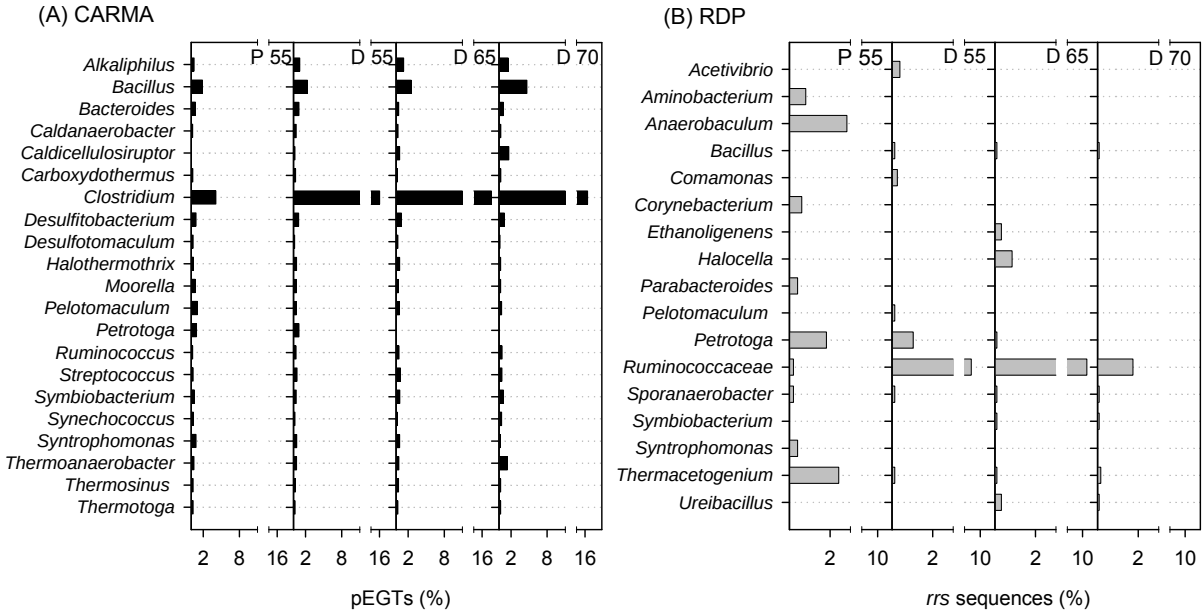

Figure 3.16 Phylogenetic assignment of metagenomic sequences to Bacteria using CARMA (A) and the RDP classifier (B) showing the prevalent bacterial genera. The *rrs* sequences assigned to Ruminococcaceae could not be classified at genus level. For description of samples refer to Table 3.8. pEGTs, prokaryotic environmental gene tags

In contrast to that, the RDP classifier revealed slightly different results (Figure 3.16 B). In the sample derived from the AF, *Anaerobaculum* (2.8%), *Thermacetogenium* (2.4%) and *Petrotoga* (1.8%) were detected prevalently. In the digestate samples, Ruminococcaceae, which could not be assigned to a genus, were classified as dominant with 6.4% (D 55), 11.7% (D 65) and 1.7% (D 70) of *rrs* sequences, indicating a strong decrease at an LBR temperature of 70 °C. Notably, members of the *Clostridium* genus were not identified in all samples by the RDP classifier, which may be due to different applied taxonomies. Further genera such as *Bacillus*, *Petrotoga* and *Thermacetogenium* were less frequently detected (≤ 1% of *rrs* sequences) in the digestate samples by the RDP classifier (Figure 3.16 B).

Phylogenetic assignment of EGTs having a predicted function in carbohydrate degradation

The Pfam database provides a broad range of protein families. Using the Pfam analysis, carbohydrate degrading enzymes were identified in all samples and subsequently assigned to taxonomic groups. In total 27 protein families representing glycoside hydrolases (GH), e.g., 'GH family 5' (e.g., cellulase, PF00150) and 'GH family 10' (e.g., xylanase, PF00331) were selected for this analysis (Appendix Table 7.1 A).

The assignment of EGTs having a predicted function in carbohydrate degradation to taxonomic groups (Figure 3.17) also revealed strong differences between the sample from the AF and the digestate samples from the LBR. This supports the findings of the previous phylogenetic assignment based on *rrs* sequences (RDP classifier) and all identified EGTs (CARMA). Furthermore, an alteration of the bacterial community during temperature increase from 65 to 70 °C was detectable. The results of the digestate samples revealed Clostridia, Bacilli, Gammaproteobacteria and Bacteroidia as prevalent bacterial classes but with varying abundances (Figure 3.17). Whereas the number of EGTs assigned to Clostridia remained relatively constant within the three digestate samples, Gammaproteobacteria were reduced by 40% after the temperature increase to 70 °C. On the other hand at 70 °C, the assignment of EGTs to Bacilli and Chloroflexi was increased twofold, whereas Bacteroidia increased threefold, supporting the strong emergence of Bacteroidia as revealed by the TRFLP analysis.

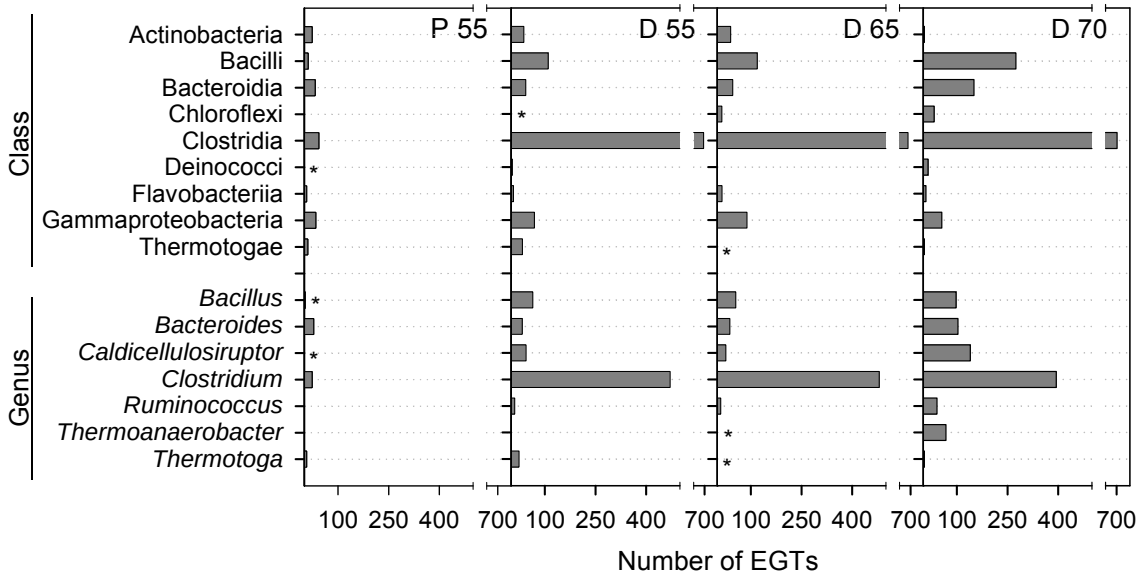

Figure 3.17 Phylogenetic assignment of EGTs encoding carbohydrate degrading enzymes as revealed by CARMA. Only prevalent taxonomic groups of class and genus level are shown. EGTs of D 55, D 65 and D 70 are normalized to an equal amount of total metagenomic sequences. For description of samples refer to Table 3.8. EGTs, environmental gene tags; *, detected with ≤ 3 EGTs

At genus level, *Clostridium* was also prevalently detected in the digestate samples at LBR temperatures of 55 to 70 °C (Figure 3.17). In addition, the *Bacillus*, *Caldicellulosiruptor* and *Bacteroides* genera also showed carbohydrate degrading potential. At 70 °C, *Clostridium* was slightly reduced, whereas *Caldicellulosiruptor*, *Bacteroides* and *Bacillus* strongly increased by a factor of up to 5 (Figure 3.17). Furthermore, *Thermoanaerobacter* and *Ruminococcus* genera were also identified as showing carbohydrate degrading potential.

In contrast to the digestate samples, the number of EGTs with a predicted function in carbohydrate degradation was strongly decreased in the methanogenic biofilm sample of the AF (Figure 3.17). This small number of EGTs was assigned to the Clostridia, Gammaproteobacteria, Bacteroidia and Actinobacteria classes. At the genus level, *Bacteroides*, followed by *Clostridium* and *Thermotoga* were identified.

3.4.2 Genetic potential for the degradation of plant-derived biomass

Plant-derived biomass is composed of cellulose, hemicellulose and lignin. The degradation of lignin, the most recalcitrant component, is realized principally by white-rot fungi under aerobic conditions. Only few bacterial strains were identified showing a lignin degrading potential (Bugg et al., 2011). To determine the genetic potential of the microbial community for lignin degradation, Pfam protein families encompassing enzymes with lignin degrading activity were analyzed (Table 3.11).

Laccases and peroxidases are essential ligninolytic enzymes. Laccase enzymes, catalyzing the oxidation of aromatic and non-aromatic compounds (Claus, 2004), belong to the multicopper oxidases protein family (PF00394, PF07731, PF07732 and PF02578). Only the protein family PF02578 was identified in the metagenomic samples with increasing tendency during temperature increase in the LBR (Table 3.11). A taxonomic assignment of EGTs encoding the Pfam PF02578 resulted in bacterial groups, such as *Alkaliphilus*, *Syntrophobacter* and *Clostridium*.

Furthermore, peroxidases, heme-containing enzymes, are also essential for lignin degradation (Reddy & D`Souza, 1994). The corresponding protein family PF00141 was not detected in the metagenomic samples (Table 3.11). Further, the protein family glyoxal oxidase (PF07250), essential for the extracellular lignin degradation (Whittaker et al., 1999), was identified in marginal ranges only at higher LBR temperatures of 65 and 70 °C (Table 3.11), indicating that lignin degrading enzymes were less abundant in this biogas system.

Table 3.11 Pfam analysis of lignin degrading enzymes applying CARMA. For description of samples refer to Table 3.8.

Pfam accession	Protein family	P 55 (EGTs)	D 55[a] (EGTs)	D 65[a] (EGTs)	D 70[a] (EGTs)
PF00394	Multicopper oxidase	0	0	0	0
PF07731	Multicopper oxidase	0	0	0	0
PF07732	Multicopper oxidase	0	0	0	0
PF02578	Multicopper polyphenol oxidoreductase laccase	39.00	40.99	53.04	66.26
PF00141	Peroxidase	0	0	0	0
PF07250	Glyoxal oxidase N-terminus	0	0	2.41	1.58

[a], identified EGTs are normalized to an equal amount of total metagenomic sequences

In contrast, EGTs encoding protein families, which encompass enzymes with degradation activity for other plant-derived polysaccharides (e.g., cellulose) and for oligo- and disaccharides, were identified in higher amounts in the metagenomic samples (Table 3.12). The analysis of the genetic potential for these carbohydrate degrading enzymes suggests a defined carbohydrate degrading potential for each metagenomic sample, representing different microbial communities.

Table 3.12 Most prevalent GH families of the metagenomic samples as derived from the Pfam analysis by CARMA. For description of samples refer to Table 3.8.

Samples	Pfam accession	GH family	Selection of GH activities[a]	EGTs[b]
P 55	PF03065	GH 57	A-amylase, 4-α-glucanotransferase, α-galactosidase	79
	PF02056	GH 4	A-glucosidase, α-galactosidase, 6-phospho-β-glucosidase	72
	PF04616	GH 43	B-xylosidase, arabinanase, xylanase	55
	PF02837	GH 2	B-galactosidase, β-mannosidase, β-glucuronidase	51
	PF01915	GH 3	B-glucosidase, xylan 1,4-β-xylosidase	43
	PF03636	GH 65	A,α-trehalase, maltose phosphorylase	34
D 55	PF00759	GH 9	Endoglucanase, cellobiohydrolase, β-glucosidase.	221
	PF00331	GH 10	Endo-1,4-β-xylanase, endo-1,3-β-xylanase	199
	PF01915	GH 3	B-glucosidase, xylan 1,4-β-xylosidase	187
	PF04616	GH 43	B-xylosidase, arabinanase, xylanase	161
	PF00150	GH 5	Cellulase, glucan β-1,3-glucosidase, endo-β-1,4-xylanase, cellulose β-1,4-cellobiosidase	116
	PF02056	GH 4	A-glucosidase, α-galactosidase, 6-phospho-b-glucosidase	96
D 65	PF00331	GH 10	Endo-1,4-β-xylanase, endo-1,3-β-xylanase	221
	PF01915	GH 3	B-glucosidase, xylan 1,4-β-xylosidase	191
	PF04616	GH 43	B-xylosidase, arabinanase, xylanase	184
	PF01055	GH 31	A-glucosidase, α-xylosidase	166
	PF00150	GH 5	Cellulase, glucan β-1,3-glucosidase, endo-β-1,4-xylanase, cellulose β-1,4-cellobiosidase	129
	PF00759	GH 9	Endoglucanase, cellobiohydrolase, β-glucosidase	112
D 70	PF01055	GH 31	A-glucosidase, α-xylosidase	438
	PF04616	GH 43	B-xylosidase, arabinanase, xylanase	360
	PF01915	GH 3	B-glucosidase, xylan 1,4-β-xylosidase	335
	PF00331	GH 10	Endo-1,4-β-xylanase, endo-1,3-β-xylanase	328
	PF01229	GH 39	B-xylosidase	219
	PF02837	GH 2	B-galactosidase, β-mannosidase, β-glucuronidase	177

[a], activities of GH families were retrieved from the CAZY (carbohydrate-active enzymes) database (Cantarel et al., 2009)
[b], EGTs are normalized to an equal amount of total metagenomic sequences
GH, glycoside hydrolase

In the methanogenic sample P 55, the prevalent protein families, such as the GH families 4 (PF03065), 43 (PF04616) and 3 (PF01915), comprising e.g., α-galactosidase, xylanase and β-glucosidase, showed a lower abundance in comparison to GH families of the digestate samples derived from the LBR (Table 3.12). Nevertheless, a genetic potential for enzymes having polysaccharide degrading activity (e.g., cellulose or xylan degradation) was also detected in the microbial community in the AF.

In contrast, the metagenomic digestate samples revealed GH families with higher abundances (Table 3.12). GH families, such as 10 (PF00331), 3 (PF01915), 43 (PF04616) and 5 (PF00150) were identified prevalently in the digestate samples derived from the LBR at 55 and 65 °C. These GH families encompass enzymes, such as β-xylanase, β-glucosidase, β-xylosidase and cellulase, which are mainly involved in the degradation and processing of polysaccharides, such as xylan and cellulose. At 70 °C, the GH families 31 (PF01055), 43 (PF04616), 3 (PF01915), 10 (PF00331) and 39 (PF01229) were most prevalent with even increased abundances. These most prevalent GH families mainly comprise enzymes, such as α- and β-xylosidase, β-glucosidase and xylanase, which are also relevant for the breakdown of polysaccharides, such as xylan and cellulose.

Furthermore, to assess differences in the genetic potential of the microbial communities in the different reactor compartments and at different LBR temperatures, a comparison of the abundances of specific GH families was performed (Figure 3.18). To do this, GH protein families obtained through Pfam analysis, representing enzymes involved in plant-derived biomass degradation were compared.

The comparison of the most prevalent GH families revealed the strongest difference for the sample of the AF in comparison to the digestate samples of the LBR (Figure 3.18). Almost all of the GH families analyzed were decreased in the metagenomic sample from the AF. In the digestate samples of the LBR, the strongest changes were observed in the LBR sample after the temperature increase to 70 °C, which is in accordance with the previous TRFLP and phylogenetic assignment results.

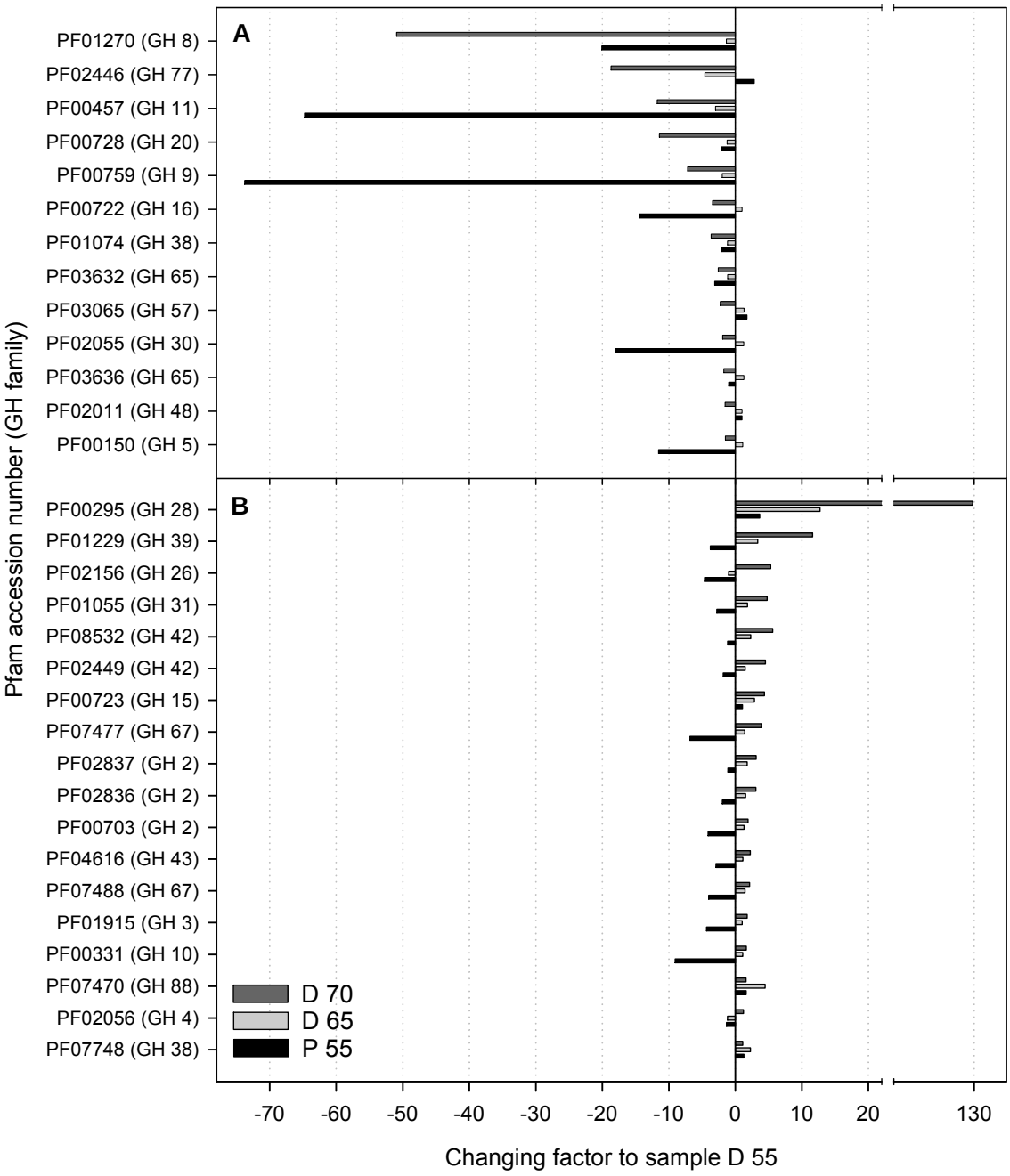

Figure 3.18 Differences in GH family abundances between the metagenomic samples P 55, D 65 and D 70 and the digestate sample derived from the LBR at 55 °C (D 55). Changing factor shows the decreased GH family abundances in the digestate samples (A) and the increased GH family abundances in digestate samples (B) during temperature increase. The most prevalent GH families (number of EGTs identified >50) are shown as derived from the Pfam analysis by CARMA. For description of samples refer to Table 3.8. GH, glycoside hydrolase

In detail, the digestate samples derived from the LBR at 70 °C, but also at 65 °C, revealed decreasing abundances of some GH families with polysaccharide degradation activity in comparison to the digestate sample taken at an LBR temperature of 55°C (Figure 3.18 A). For instance, the GH protein families 8 (PF01270) and 11 (PF00457), involved in the degradation of xylan, were strongly decreased particularly at LBR temperatures of 70 °C. Further GH families, representing enzymes with poly-, di- or monosaccharide degradation and processing activity, were also less frequently detected at higher LBR temperatures. For instance, the abundance of the protein families GH 9 (PF00759) and 38 (PF01074) was strongly reduced.

The possibility of assigning the EGTs, which encode these protein families, to taxonomic groups gives insights into the changes in the microbial community. Interestingly, the assignment of EGTs, encoding the GH families 8, 9, 11 and 38 mentioned above, revealed a decrease in members of the Firmicutes and particularly a decrease of members belonging to the Clostridia class.

In contrast to these findings, the digestate samples derived from the LBR at 65 °C and particularly from the LBR at 70 °C also revealed higher abundances of specific GH families in comparison to the digestate sample at 55°C (Figure 3.18 B). Protein families, such as the GH families 28 (PF00295), 39 (PF01229), 26 (PF02156) and 31 (PF01055) were particularly more abundant in the sample derived from the LBR at 70 °C. Some of these protein families encompass pectinolytic enzymes (GH 28), enzymes, which are involved in the degradation and the processing of xylan (GH 26, 31, 39) as well as further enzymes for the breakdown of polysaccharides (GH 31).

The taxonomic assignment of EGTs, encoding GH 28, revealed that the strong increase in the GH family 28 at an LBR temperature of 70 °C was mainly caused by the emergence of members of the Bacteroidetes phylum. In contrast to that, the assignment of EGTs, encoding the GH family 39, revealed an emergence of Proteobacteria (mainly Alphaproteobacteria) and Firmicutes (mainly Clostridia). Further, an increase of Firmicutes (Clostridia), Bacteroidetes, Proteobacteria and Chloroflexi was also detected for the GH families 26 and 31 during temperature increase through the phylogenetic assignment of the corresponding EGTs.

3.4.3 Phylogenetic assignment of metagenomic sequences to selected pathogens

Phylogenetic assignment of metagenomic sequences to selected pathogens by CARMA

Pathogens residing in agricultural biogas reactors may present risks for plants, animals and humans due to the usage of digestate as fertilizer. Selected plant pathogens, such as *Agrobacterium tumefaciens*, *Clavibacter michiganensis*, *Ps*. *syringae*, *Ralstonia solanacearum* and *Xanthomonas campestris*, were identified in marginal amounts with less than 0.02% of pEGTs each (Figure 3.19). Furthermore, pathogens responsible for infections in potatoes, such as *Synchytrium endobioticum, Rhizoctonia solani*, *Helminthosporium solani* but also other plant pathogens, such as *Fusarium oxysporum* and *Sclerotinia sclerotiorum* were not identified in the metagenomic samples.

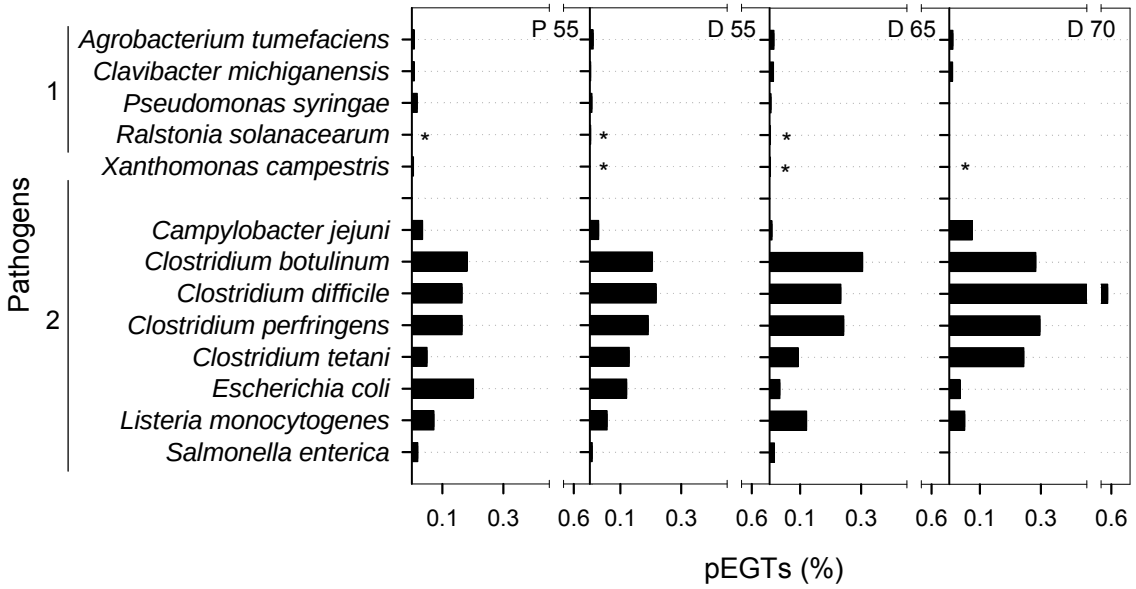

Figure 3.19 Phylogenetic assignment of pEGTs to selected plant (1) and human or animal pathogens (2) as revealed by CARMA. For description of samples refer to Table 3.8. *, pEGTs with an relative abundance <0.05‰

Animal and human pathogens belonging to the *Campylobacter*, *Clostridium*, *Escherichia*, *Listeria* and *Salmonella* genera were also analyzed using CARMA (Figure 3.19). The assignment of pEGTs to these pathogens was higher with up to 0.6%

(*Cl*. *difficile*, Figure 3.19) in comparison to the plant pathogens. However, this still indicated a minor abundance of putatively pathogen-associated pEGTs. The occurrence of some species, such as *E*. *coli*, *L*. *monocytogenes* and *Salm*. *enterica*, was reduced at an LBR temperature of 70 °C. On the other hand, the detection of pathogenic *Clostridium* species or *Camp*. *jejuni* was slightly increased in the digestate sample at an LBR temperature of 70 °C.

Genetic potential for pathogenicity as revealed by Pfam analysis

The analysis of EGTs matching Pfam protein families representing toxins or virulence factors was performed focusing only on selected animal and human pathogens. Altogether, only 0.02% of the 1,177,244 metagenomic sequences (Table 3.13) showed similarities to selected protein families (Appendix Table 7.2), possessing pathogenicity in animals and humans. This means that the majority of these pathogen-associated protein families were represented by less than 6 EGTs.

For instance, the β-1,4-N-acetyl-galactosaminyltransferase family (PF06306) of *Camp*. *jejuni*, which is required for the GT1a ganglioside mimic synthesis and therefore associated with the Guillain-Barré syndrome (Gilbert et al., 2000), was only marginally detected at a temperature of 55 °C (Table 3.13). This is also true for the heat-labile enterotoxin of *E*. *coli* (PF01375, PF01376) and for the *Clostridium* neurotoxin (PF07953), which is composed of the tetanus neurotoxin and different serotypes of the botulinum neurotoxin (Punta et al., 2012).

Other protein families were also detected to a marginal extent at higher reactor temperatures of 65 and 70 °C (Table 3.13). For instance, the *Campylobacter* major outer membrane protein family (PF05538), which may be involved in the adaption to host environments (Zhang et al., 2000), but also some *Clostridium*-associated protein families were detected. The protein families of the *Cl*. *botulinum* HA-17 protein (PF05588), a hemagglutinin subcomponent, which is part of the L toxin, a progenitor toxin of the *Cl*. *botulinum* type D str. 4947 (Kouguchi et al., 2002) were also identified marginally at 70 °C. The same is true for the ADP-ribosyltransferase exoenzyme protein family (PF03496). This enzyme, found in clostridial species, such as *Cl*. *perfringens*, acts on actin, leading to lethal and dermonecrotic reactions in mammals (Tsuge et al., 2003). Furthermore, EGTs assigned to the heat-stable

enterotoxin ST (PF02048) of *E. coli* were also identified at temperatures of 70 °C (Table 3.13).

Whereas these pathogen-associated protein families were detected with less than 6 EGTs, the Holin protein family (PF05105) was identified with slightly higher abundances in all samples (Table 3.13). The Holin protein family includes the protein TcdE/UtxA, which is involved in toxin secretion in *Cl. difficile* (Tan et al., 2001). Further, this family also includes other proteins, which are involved in bacterial lysis and virus dissemination (Punta et al., 2012).

Table 3.13 Assignment of EGTs matching with toxin-associated Pfam families. For description of samples refer to Table 3.8.

Putative pathogen	Pfam accession	Protein family	P 55	D 55[a]	D 65[a]	D 70[a]
Campylobacter jejuni	PF05538	*Campylobacter* major outer membrane protein	0.0	0.0	0.8	0.8
Campylobacter jejuni	PF06002	A-2,3-sialyltransferase (CST-I)	0.0	0.0	0.8	0.0
Campylobacter jejuni	PF06306	B-1,4-N-acetylgalactosaminyltransferase (CgtA)	0.0	2.5	0.0	0.0
Clostridium botulinum	PF05588	*Clostridium botulinum* HA-17 protein	0.0	0.0	0.8	2.4
Clostridium sp.	PF07953	*Clostridium* neurotoxin, N-terminal receptor binding	0.0	2.5	0.0	0.0
Clostridium sp.	PF08470	Nontoxic nonhaemagglutinin C-terminal	1.0	0.0	0.0	0.0
Clostridium sp.	PF03495	Clostridial binary toxin B/anthrax toxin PA	0.0	1.6	0.8	0.0
Clostridium difficile	PF05105	Holin family	39.0	33.6	44.2	52.8
Clostridium perfringens	PF03496	ADP-ribosyltransferase exoenzyme	0.0	3.3	0.0	3.9
Escherichia coli	PF01375	Heat-labile enterotoxin α chain	1.0	0.0	0.0	0.0
Escherichia coli	PF01376	Heat-labile enterotoxin β chain	0.0	5.7	0.0	0.0
Escherichia coli	PF02048	Heat-stable enterotoxin ST	0.0	0.0	0.0	2.4
Escherichia coli, *Shigella flexneri*	PF06109	Haemolysin E (HlyE)	0.0	0.8	1.6	0.0

[a], identified EGTs are normalized to an equal amount of total metagenomic sequences

3.4.4 Phylogenetic assignment of metagenomic sequences to Archaea

Phylogenetic assignment of metagenomic sequences to Archaea by RDP classifier and CARMA

In the metagenomic samples, the methanogenic archaeal orders Methanosarcinales, Methanobacteriales, Methanomicrobiales and Methanococcales were identified (Figure 3.20).

Most assignments to these Archaea were obtained in the packing's biofilm from the AF at an LBR temperature of 55 °C. Here, Methanosarcinales prevailed with 7.3% of pEGTs as revealed by CARMA and 5.3% of *rrs* sequences by the RDP classifier. In addition, members of the Methanobacteriales (6.9% CARMA, 4.2% RDP) and Methanomicrobiales (2.5% CARMA, 1.4% RDP) were also detected. Members of the Methanococcales were less frequently detected with 0.85% of pEGTs (CARMA).

In contrast to these results, the TRFLP analysis and the *rrs* gene library results revealed a prevalence of the Methanobacteriales order at an LBR temperature of 55 °C.

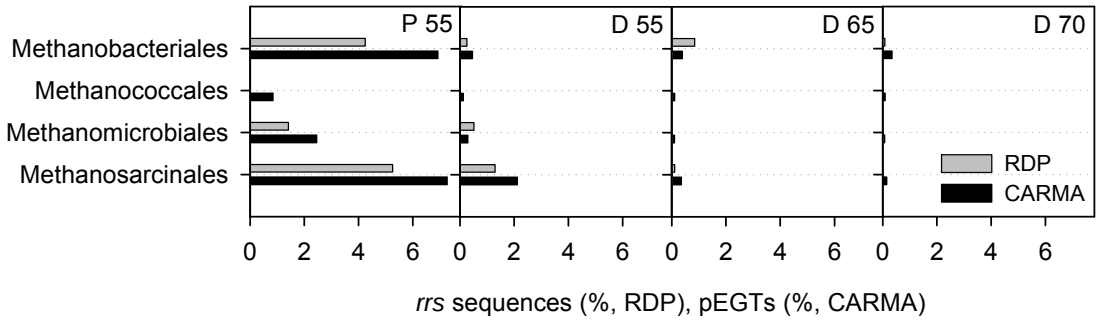

Figure 3.20 Phylogenetic assignment of metagenomic sequences to Archaea using CARMA (black) and the RDP classifier (grey) showing the prevalent archaeal orders. For description of samples refer to Table 3.8. pEGTs, prokaryotic environmental gene tags

At genus level, *Methanosarcina*, *Methanothermobacter* and *Methanobacterium* were most prevalent in the sample of the AF (Figure 3.21). Interestingly, the CARMA tool revealed *Methanosarcina* and *Methanothermobacter* as most prevalent, whereas the RDP classifier revealed *Methanosarcina* and *Methanobacterium* as dominant genera.

These differences are probably caused by the use of different taxonomies. Whereas the RDP classifier is based on the taxonomy proposed by Garrity and coworkers (2007), CARMA is based on the NCBI taxonomy.

However, in contrast to the AF sample, the digestate samples showed a strongly reduced number of archaeal assignments (Figure 3.20), particularly at higher LBR temperatures. At an LBR temperature of 55 °C, members of the Methanosarcinales were identified with 2.1% of pEGTs (CARMA) and 1.3% of *rrs* sequences (RDP). At higher LBR temperatures of 65 and 70 °C, less than 1% pEGTs or *rrs* sequences (CARMA and RDP) were classified to methanogenic archaea in the digestate samples. However, Methanobacteriales was the major archaeal order at these higher temperatures.

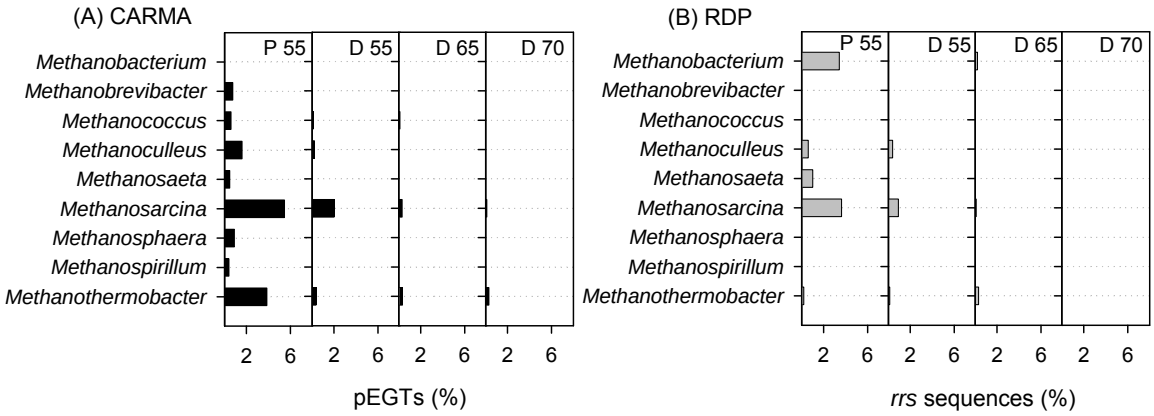

Figure 3.21 Phylogenetic assignment of metagenomic sequences to Archaea using CARMA (A) and the RDP classifier (B) showing the prevalent archaeal genera. For description of samples refer to Table 3.8. pEGTs, prokaryotic environmental gene tags

Phylogenetic assignment of EGTs having a predicted function in methanogenesis

Protein families relevant for methanogenesis were identified and subsequently assigned to taxonomic groups (Figure 3.22). In total 27 protein families, e.g. 'methyl-coenzyme M reductase subunits' (PF02249, PF02745, PF02241, PF02783) were selected for this analysis (Appendix Table 7.1 B).

The assignment of methanogenic Pfam protein families to taxonomic groups differed slightly from the previous phylogenetic assignment of metagenomic sequences by RDP and CARMA. Here, in the biofilm sample derived from the AF, Methanobacteriales (182 EGTs), followed by Methanosarcinales (126 EGTs), were prevalently identified

(Figure 3.22), as indicated by the TRFLP and *rrs* gene library analyses. According to this, the genera *Methanothermobacter* and *Methanosarcina* were dominantly detected in the packing sample derived from the AF at 55 °C.

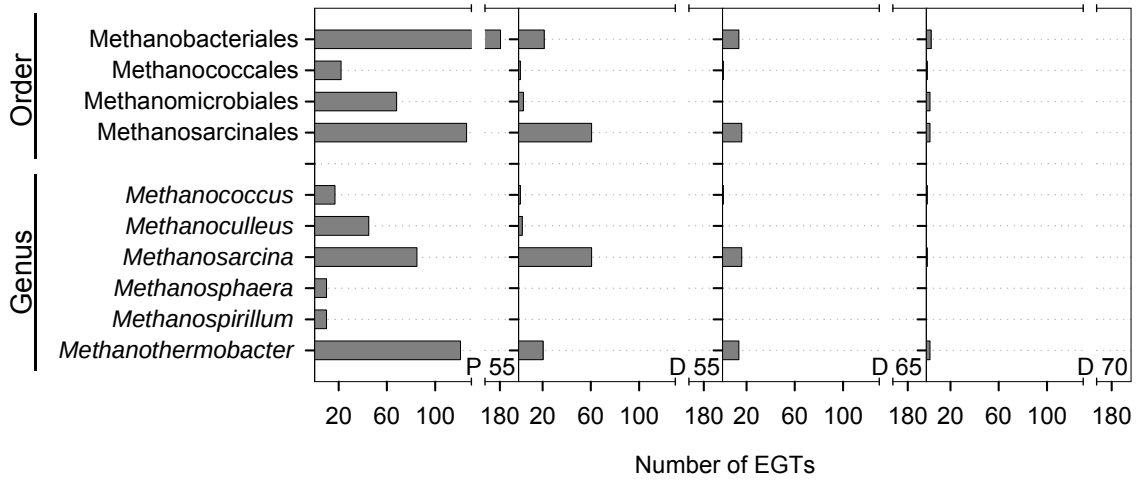

Figure 3.22 Phylogenetic assignment of EGTs encoding methanogenic enzymes as revealed by CARMA. Only major groups of the class and genus level are shown. EGTs of D 55, D65 and D 70 are normalized to an equal amount of total metagenomic sequences. For description of samples refer to Table 3.8. EGTs, environmental gene tags

In contrast to that, the digestate samples showed similar results to the phylogenetic assignment by RDP and CARMA (Figure 3.22). In the digestate sample at an LBR temperature of 55 °C, Methanosarcinales as well as Methanobacteriales were identified, but at higher temperatures hardly any methanogenic protein family was detected.

3.5 Quantification of bacterial *rrs* genes

QPCR analysis allows the detection and quantification of specific microorganisms in various habitats. In this study, the quantification of Bacteria and of a putatively process-relevant bacterium was performed. This bacterium was detected as prevalent species

after one week of fermentation in the LBR at 55 to 60 °C as shown by TRFLP and *rrs* gene library analyses (cf. Figure 3.9 or 3.10). Hence, it can be assumed that this bacterium plays an important role in the anaerobic degradation process at thermophilic temperatures. Its corresponding *rrs* sequence has the accession number HE804843 and resulted in the TRF 304 after TRFLP analysis. The NCBI BLAST analysis of this sequence showed the highest sequence similarity to *Defluviitalea saccharophila* str. LIND6LT2 (Defluviitaleaceae, Clostridiales, Jabari et al., 2012) with 89 to 91%. This indicates a more distant taxonomical relation to the target microorganism. In contrast, the RDP classifier assigned the target sequence HE804843 to the Lachnospiraceae with a confidence level of 93 to 94%, which represents another family within the Clostridiales order.

To monitor this putatively process-relevant bacterium, a specific TaqMan primer set (primer set 304), comprising the forward and reverse primer as well as the TaqMan probe, was developed.

3.5.1 Specificity of the primer set 304

The TaqMan primer set 304 developed in this study was analyzed for target-strain specificity and potential false positive or negative results. To identify potential false negative results, the *rrs* gene libraries constructed were analyzed for mismatches to the primer set 304. Only one sequence (out of 16), which resulted in a TRF 304 after TRFLP analysis, revealed a mismatch to the 304r reverse primer. However, one mismatch of the target sequence to the reverse primer should not seriously affect the binding of the whole primer set 304.

To identify potential false positive results, further sequences of the *rrs* gene libraries were screened for potential binding sites of the primer set 304. In the *rrs* gene libraries (excluding *rrs* sequences resulting in TRF 304), two sequences with a potential false positive binding site were found for the 304r primer and the TaqMan304 probe. However, a false positive amplification is rather unlikely due to the fact that the corresponding forward primer of the primer set 304 did not bind to these sequences. All other sequences in the bacterial *rrs* gene libraries showed at least 8 mismatches to the

primer set 304, as confirmed after sequence alignment. Particularly the forward primer seemed to be highly specific, whereas the TaqMan probe and particularly the reverse primer were less specific.

To gain more detailed information on potential false positive results, the NCBI Primer BLAST tool and the RDP probe match tool were used for comparison (last access November 2012). The primer BLAST analysis of the primer set 304 against the NCBI nr database (limited to Bacteria) resulted in 46 sequences matching the primer set 304 (Table 3.14). However, most of these sequences from uncultured bacteria showed a high sequence similarity of 99 to 100% to the target sequence (HE804843), indicating a very close relation. Furthermore, some of these highly similar sequences also stemmed from thermophilic anaerobic digesters. Additionally, a primer BLAST search of the primer set 304 against the archaeal NCBI nr database showed only potential binding sites within one sequence with five mismatches each to the 304f and 304r primer.

When applying the RDP probe match tool, similar results to those described above were obtained. When analyzing the target specificity of the forward and reverse primer 304, 24 sequences plus 15 sequences derived from this study (resulting in TRF 304) were identified to have no mismatch to the primers. These 39 sequences clustered within the unclassified Lachnospiraceae group, as assumed for the target sequence HE804843 by RDP classification. Hence, these sequences showed high sequence similarities of up to 100% to the target sequence also indicating a very close relation. These sequences partially agree with the sequences shown in Table 3.14.

Furthermore, 48 matches of the 304f and 304r primers to RDP database sequences were obtained when using the RDP probe match tool enabled for three mismatches. Only five out of 293,554 sequences belonging to the Bacteroidetes group (accession numbers: FJ930387, GU230430, HQ478279, FJ745267, GU584663) and two out of 123,596 sequences (accession numbers: EU645078, EU645198) belonging to the unclassified Bacteria were identified as having only three mismatches to the target sequence. However, these sequences showed additionally 2 to 4 mismatches to the TaqMan probe, which indicated that the risk of a false positive amplification is rather low.

Hence, the primer set 304 seemed to be specific for a small group of unclassified Lachnospiraceae, closely related to the target sequence HE804843, which was prevalently identified during the thermophilic fermentation process.

Table 3.14 Uncultured or environmental sequences retrieved from the primer BLAST search against the NCBI nr database (last access November 2012) showing no mismatch to the primer set 304. Retrieved sequences showed high sequence similarities to the target sequence (TRF 304; HE804843) of primer set 304.

Hit	Accession number	Microorganism	Source	Sequence similarity to target sequence
1	DQ887970	Uncultured bacterium clone B55_K_B_F05	Thermophilic anaerobic solid waste bioreactor	99%
2	HQ183761	Uncultured *Bacillus* sp. clone De247	Leachate sediment	99%
3	FN994058	Uncultured bacterium str. MS14339-B088	Long-term biogas completely stirred tank reactor	99%
4	AM947511	Uncultured bacterium clone 2d_1FB3	Anaerobically digested sludge	99%
5	JF795000	Uncultured bacterium clone T4	Anoxic bulk soil	99%
6 - 21	JN708647, -717, -724, -805, -820, -847, -871, -879, -884, -898, -921, -924, -935, -950, -979, -997	Uncultured bacterium clones	Thermophilic anaerobic digester	99 - 100%
22 - 46	JQ100075, -0621, -6376, -6551, -7804; JQ110262, -0839, -1744, -6707; JQ120796, -3515, -6358, -6445, -9279; JQ130054, -6180, -8776; JQ148181; JQ161845, -5666, -6328, -7478, -8540, -8577, -9911	Uncultured bacterium clones	Anaerobic sludge digester	99 - 100%, 2x97%, 1x95%

3.5.2 Quantification of Bacteria and a putatively process-relevant bacterium

Parameters suited to assess the efficiency of the qPCR analysis (PCR efficiency, R^2 and slope of the calibration curve), were within the limits stated by Zhang and Fang (2006), indicating reliable results. Furthermore, all results of the analyzed samples were within the calculated limits of detection and quantification (cf. 2.6).

During temperature increase in the LBR from 55 to 75 °C, the number of bacterial *rrs* copies was reduced by almost one log (Figure 3.23 A). More specifically between 55 and 65 °C, the number of the bacterial *rrs* copies per mL leachate was consistent with an average number of $1.3 \pm 0.5 \times 10^{11}$. At 70 °C, the number of the bacterial *rrs* copies was reduced to $3.6 \pm 0.1 \times 10^{10}$ per mL leachate. After the bioaugmentation with

compost, which introduced new thermophilic microorganisms, the bacterial *rrs* copy number was slightly increased to 4.3 ± 0.8 x 10^{10} per mL leachate. This effect did not persist at 75 °C. Here, a further reduction of the bacterial *rrs* copy number was detected, accounting for 2.8 ± 0.5 x 10^{10} copies per mL leachate.

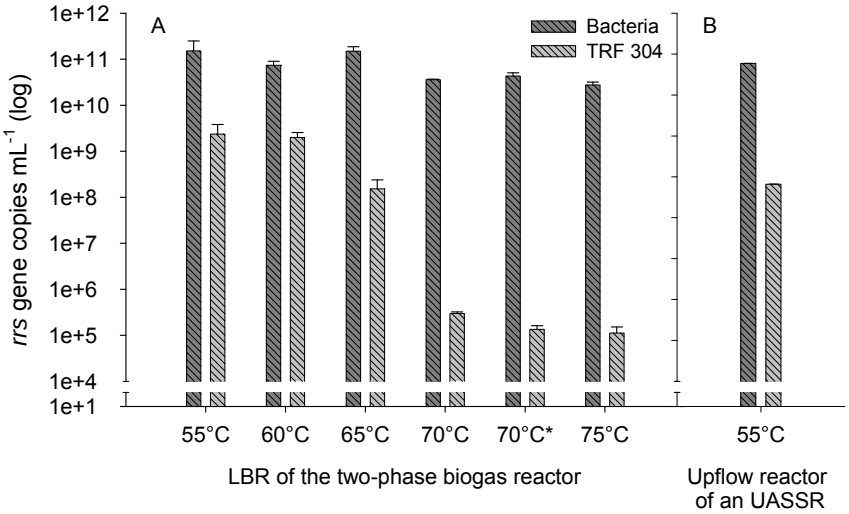

Figure 3.23 Quantification of Bacteria and bacteria, resulting in TRF 304, by qPCR analysis. Leachate samples of the LBR of the two-phase biogas system at temperatures from 55 to 75 °C were analyzed (A). Leachate samples derived from the upflow reactor of a thermophilic upflow anaerobic solid-state reactor (UASSR, 55 °C) were employed for comparison (B). The standard deviation represents the results of three measurements. 70 °C*, analysis after bioaugmentation with compost

The analysis of bacteria, resulting in TRF 304 after TRFLP analysis and representing a small group of the unclassified Lachnospiraceae, was performed using the primer set 304. The number of the *rrs* copies was reduced by 4 logs during temperature increase in the LBR (Figure 3.23 A), indicating a sensitivity of these bacteria to temperatures above 65 °C. This supported the findings of the TRFLP analysis, where the TRF 304 was absent in TRFLP profiles derived from samples at 70 and 75 °C.

However, up to an LBR temperature of 60 °C, these bacteria were identified prevalently. At temperatures of 55 and 60 °C, they were detected with 2% (55 °C) and 3% (60 °C) of the total bacterial *rrs* copies, accounting for 2.4 ± 1.5 x 10^{9} and 2.0 ± 0.5 x 10^{9} *rrs* copies per mL leachate, respectively. At 65 °C, the number of *rrs* copies was reduced by one log to 1.5 ± 0.9 x 10^{8}, representing now only 0.1% of the

total bacterial *rrs* copies. From 70 °C on, the number of *rrs* copies was strongly reduced by 4 orders of magnitude to 1.1 ± 0.4 x 10^5 to 3.0 ± 0.2 x 10^5 copies per mL. It was here that these bacteria accounted for less than 0.001% of the total bacterial *rrs* copies. Furthermore, an effect of bioaugmentation on the abundance of these bacteria was not detected.

To prove that bacteria, resulting in TRF 304, also inhabit other thermophilic biogas reactor systems, a thermophilic upflow anaerobic solid-state reactor (UASSR, 55 °C) was also analyzed (Figure 3.23 B). The results showed a number of 6.6 ± 0.03 x 10^8 *rrs* copies per mL leachate for these bacteria, representing 0.1% of the total bacterial *rrs* copies within the UASSR. Although the relative abundance of these bacteria, was lower in the thermophilic UASSR, these results proved that they also inhabit other thermophilic biogas systems.

3.6 Microscopical analyses of the microbial biogas community

Microscopical analyses were commonly used to quantify the total number of cells, Bacteria and Archaea. Therefore, DAPI staining of microbial cells and DOPE-FISH analysis were conducted. Furthermore, fresh leachate samples were also analyzed by PI staining identifying cells with reduced membrane integrity. Parts of this chapter were performed in the context of the Diploma thesis of C. Krumrei (2010).

3.6.1 Fluorescence *in situ* hybridization and total cell count analyses

Total cell count analysis was carried out after sampling the LBR leachate at all LBR temperature regimes (55 - 75 °C). This increase in operation temperature in the LBR led to a reduction in cell densities by almost one log as determined by DAPI staining (Figure 3.24 A), which is in accordance with the qPCR results.

At 55 °C, an average of 2.7 ± 0.6 x 10^{10} cells per mL was detected. A slight reduction of the total cell count was observed after an LBR temperature increase to 60 °C. At 60 and 65 °C, a total of 1.6 to 1.7 ± 0.2 x 10^{10} cells per mL was determined (Krumrei, 2010). The further increase in the LBR temperature to 70 °C led to a reduced cell count of 6.2 ± 1.3 x 10^{9} cells per mL. The following bioaugmentation showed no positive effect on the cell densities. After the bioaugmentation at 70 and 75 °C, the average total cell count was lower than before with 4.6 ± 1.1 x 10^{9} cells per mL.

The DOPE-FISH analysis was performed for the first three temperature regimes of the LBR (55 - 65 °C, Figure 3.24 A; Krumrei, 2010). The hybridization rate achieved for this analysis was very low at less than 30%, although different optimization steps were performed in the context of a Diploma thesis of Krumrei (2010). On the other hand, the hybridization rate of the pure cultures, such as *E. coli* (DSM 1116), *Cl*. *tyrobutyricum* (DSM 2637) and *Methanospirillum hungatii str.* Mh1, was high between 80 and 100%.

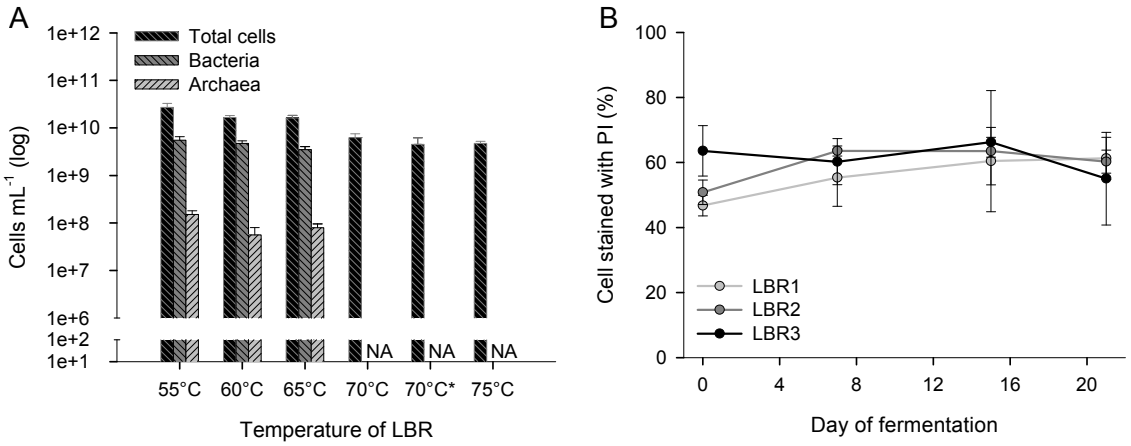

Figure 3.24 Total cell counts and DOPE-FISH results during temperature increase (A), percentage of cells stained with PI during 21 days of fermentation at 65 °C (B). NA, not analyzed; 70*, analysis after compost bioaugmentation (data based on the Diploma thesis of Krumrei, 2010)

However, no strong alterations of bacterial and archaeal cells were detected between LBR temperatures of 55 and 65 °C. The number of bacterial cells as determined by DOPE-FISH remained almost stable representing 20.4 to 28.2% of the total cell count. In contrast, the archaeal cells represented only 0.3 to 0.6% of the total cell count, which indicated that archaeal cells represented only a small part of the microbial community.

3.6.2 Propidium iodide analysis

PI is a fluorescent dye that intercalates in RNA and DNA. It can only enter in microbial cells with reduced membrane integrity. PI staining was performed analyzing fresh leachate samples of the three LBRs at 65 °C without a previous treatment.

During the 21-day fermentation at 65 °C, the number of microbial cells that were stained was nearly constant and ranged between 53.7 ± 4.9% on day 0 and 63.4 ± 10.2% on day 15 (Figure 3.24 B; Krumrei, 2010), indicating a high number of cells with reduced membrane integrity.

4 DISCUSSION

4.1 Methodical aspects

As the majority of microorganisms are not yet cultivable, culture-independent methods are of major importance for gaining insights into different microbial habitats due to the fact that these methods overcome the strong limitations concerning cultivation efficiency. In the following sections, the advantages of the key methods applied as well as potential drawbacks are discussed.

4.1.1 DNA extraction

An effective DNA extraction is of major importance for culture-independent, DNA-based molecular analyses. A well known problem is the variable lysis efficiency of microbial cells. Different lysis procedures are known for extracting DNA from microbial cells, such as the application of chemical compounds (e.g., SDS), enzymes (lysozyme) and mechanical (e.g., beating step with silica or glass beads) or physical (e.g., freeze and thaw cycles) treatment.

Four different DNA extraction methods were compared with respect to their efficiency and reproducibility. Two DNA extraction kits (FastDNA® Spin Kit for Soil, PowerSoil® DNA Isolation Kit), including a beating step, and a step-by-step protocol, including lysozyme and SDS for lysis, with and without an additional beating step were applied.

The snapshot of the bacterial diversity obtained after using the four DNA extraction protocols was the same, focusing on TRFs with more than 2% of the total fluorescence intensity. Only the relative abundance of TRFs varied between the four DNA extraction methods. Changes within the relative abundance of the microbial community after different DNA extractions have been reported by different authors also analyzing fingerprint profiles (e.g., Krsek & Wellington, 1999; Sun et al., 2012). However, to secure a high lysis efficiency of microbial cells, the DNA extraction protocols with a mechanical treatment step (FastDNA® Spin Kit for Soil and step-by-step protocol) were used in this study, resulting in highly reproducible results. DNA extraction protocols with a mechanical treatment step were shown to be efficient methods as indicated by Bergmann and coworkers (2010) and Vanysacker and coworkers (2010).

A further challenge is the DNA extraction from biofilms attached to heterogenic crop material, such as the digestate. Several studies have applied chemical (e.g. Chen & Stewart, 2000), enzymatic (e.g. Johansen et al., 1997; Böckelmann et al., 2003) or physical (e.g. Mott et al., 1998; Rochex et al., 2009) treatment for detaching biofilms. However, using the whole plant material for DNA extraction, as performed in this study, minimizes the potential loss of microbial cells, which is in accordance with other studies (e.g., McEniry et al., 2008; Wang et al., 2010).

4.1.2 TRFLP analysis

The TRFLP method is a valuable tool for the monitoring of microbial communities. It is a high-through-put method, which allows a higher resolution of DNA fragments (Marsh, 1999) and therefore an improved comparison of samples in contrast to other fingerprinting methods, such as the DGGE analysis. Hence, this method has been widely used for gaining insights into different environmental habitats, such as soil (e.g., Lueders & Friedrich, 2000; Singh et al., 2006; Blackwood & Buyer, 2007; Ulrich et al., 2008; Enwall & Halin, 2009; Cao et al., 2012), marine (e.g., Denaro et al., 2005; Pereira et al., 2006; Dang et al., 2009; Opatkiewicz et al., 2009; Kim et al., 2011) or lake habitats (e.g., Chan et al., 2005; Kim et al., 2011; Bai et al., 2012; Bhattarai et al., 2012).

In agreement with all PCR-based techniques, which include the construction of gene libraries, the TRFLP method can be affected by PCR biases, such as sequence errors through misincorporation or the formation of chimeric sequences (v. Wintzingerode et al., 1997). To optimize the PCR step, the influence of the number of PCR cycles on the TRFLP profile was analyzed. The number of TRFs was increased by 29% comparing the bacterial TRFLP assay after 15 and 35 PCR cycles, respectively. This increase in the TRF number might be influenced by the emergence of chimeric sequences, which increased by higher cycle numbers (v. Wintzingerode et al., 1997). Chimeric sequences can be generated between two different targets with high sequence similarity during DNA amplification. To lower the risk of chimera production during PCR, the number of PCR cycles for *rrs* gene amplification was kept to 25 (for bacterial analyses) and 28 (for archaeal analyses), respectively.

In addition, the impact of different bacterial and archaeal reverse primers on the amplification of the *rrs* gene was analyzed by the TRFLP method. Each bacterial and archaeal primer set reflected almost the same community. However, primers designed for the amplification of Bacteria and Archaea do not equally comply with the two most important criteria: to be specific for the designated target and also general enough to amplify all target sequences (Schütte et al., 2008). This may lead to a distorted representation of the microbial diversity; an important fact of all PCR-based methods.

Another important issue is the occurrence of pseudo-TRFs after TRFLP analysis. Pseudo-TRFs can be produced by PCR and the subsequent restriction enzyme digest. The formation of single strand DNA (ssDNA) sequences during PCR can reproducibly lead to pseudo-TRFs. These ssDNA sequences can form secondary dsDNA structures, which are recognized as target by restriction enzymes in the digestion step leading to false fragments (Egert & Friedrich, 2003). To identify such pseudo-TRFs, a construction of a gene library is required, as performed in this study. Pseudo-TRFs showed no corresponding sequences in the *rrs* gene libraries constructed from the same environmental samples. In this study, no corresponding *rrs* sequences were identified for the bacterial TRFs 84, 208 and 374, which indicated putative pseudo-TRFs.

The construction and analysis of such *rrs* gene libraries can also be used for the assignment of TRFs to taxonomic groups and has an advantage over a comparison of TRFs with *in silico* databases. *In silico* comparison bears the risk of false phylogenetic assignments of TRFs due to the discrepancy of *in silico* cut TRFs and TRFs measured

in a capillary gel electrophoresis. Variations of up to several base pairs can occur as reported by different authors (e.g., Liu et al., 1997; Kitts, 2001; Kaplan and Kitts, 2003; Bukovska et al., 2010). In this study, the measured TRF length varied up to 6.7 bp in comparison to the TRF length obtained after *in silico* cut of the respective *rrs* sequence. These differences result from separation with capillary gel electrophoresis, which is not only affected by the length of the DNA fragment, but also by its GC content and the fluorescent dye attached to the DNA. To solve this issue, the *rrs* sequences were also analyzed with the capillary gel electrophoresis in this study, which proved a reliable assignment of TRFs obtained from environmental samples. In only one case, the phylogenetic assignment of archaeal TRFs was ambiguous. Three different archaeal *rrs* sequences, which were most similar to *Methanobacterium*, *Methanoculleus* and *Methanosaeta*, resulted in the archaeal TRF 107. However, other archaeal TRFs, showing a higher abundance than TRF 107 and also the bacterial TRFs could be assigned unambiguously.

Another important point is the application of appropriate enzymes. Further, the use of more than one enzyme can increase the resolution of the TRFLP approach. In this study, two restriction enzymes *Hin*6I and *Msp*I were used, showing the best resolution for the diverse bacterial community. Engebretson and Moyer (2003) tested 18 restriction enzymes, showing a resolution of up to 70% of OTUs obtained in a community modeled with more than 50 OTUs. Hence, the TRFLP method can reflect the majority of a microbial community and therefore it is a valuable tool for comparative community analyses. Nevertheless, it must be kept in mind that the most dominant TRF of a TRFLP profile does not necessarily represent the most dominant microorganism in the microbial community. This is particularly true for analyses based on genes, which are present as multiple copies in the genome, such as the *rrs* gene (Farrelly et al., 1995; Osborn et al., 2000) used in this study.

Although this method was introduced in 1997, the processing of TRFLP data is still not consistent in scientific studies. For instance, the analysis of the TRFLP data can be conducted on the basis of the TRF height or area. Different studies have been performed favoring the TRF height (Dunbar et al., 2001; Caffaro-Filho et al., 2007) or TRF area (Kitts, 2001; Sait et al., 2003). However, there are also some studies having no preference or showing positive and negative aspects for both, the TRF height and area based analysis (Lueders & Friedrich, 2003; Schütte et al., 2008). This was supported by the findings in this study showing no strong differences between the

TRFLP profiles analyzed on the basis of the TRF height or area. However, after data processing, TRFLP results are suitable for comparative analyses and therefore for the tracking of microbial community dynamics.

4.1.3 Metagenomic and bioinformatic analysis

Metagenomic studies, the so-called high-throughput DNA sequencing approaches, have been widely applied to study different habitats, such as the guts of mice and termites (e.g., Turnbaugh et al., 2006; Warnecke et al., 2007), soils (e.g., Leininger et al., 2006), but also mesophilic biogas systems (Krause et al., 2008a; Schlüter et al., 2008). In contrast to conventional DNA sequencing technologies, such as the Sanger dideoxy sequencing method, the 454-pyrosequencing technology allows a markedly increased sequence throughput at less cost and time (Margulies et al., 2005). Furthermore, the analysis of microbial metagenomes allows not only the characterization of microbial communities, but also the determination of the genetic potential for the expression of enzymes, such as carbohydrate degrading enzymes.

Another advantage is that this sequencing approach is not PCR-based and therefore is not affected by PCR biases. Nevertheless, 454-pyrosequencing can also lead to sequence errors. Huse and coworkers (2007) and Gilles and coworkers (2011) have analyzed the older GS20 system and the new GS FLX^{TM} Titanium system and obtained a sequencing error rate of 0.49% and 1.07%, respectively, which is to a greater extent linked to the presence of homopolymers (repetitive bases) in the sequence.

The phylogenetic assignment of hundreds of thousands metagenomic sequences to taxonomic groups remains a sophisticated bioinformatic effort. This assignment is based on a comparison of metagenomic sequences with entries in different databases and is therefore influenced by the content of such databases. Due to database limitations, only approximately 30% of the metagenomic sequences could be assigned to taxonomic groups with the phylogenetic characterization methods applied. Therefore, many metagenomic sequences remained unclassified indicating that a considerable number of additional species might be involved in the production of biogas.

The phylogenetic assignments of the RDP classifier and CARMA are based on two different taxonomies. The RDP classifier relies on the taxonomy proposed by Garrity and coworkers (2007), whereas CARMA based on the NCBI taxonomy (Wheeler et al., 2007; Finn et al., 2008; Krause et al., 2008b). For instance, *Cl*. *thermocellum* was classified to "Ruminococcaceae" by means of the RDP classifier, although the NCBI taxonomy assigned this species to Clostridiaceae. Therefore, the unclassified members of the family Ruminococcaceae, identified by means of the RDP classifier, correspond most probably to *Clostridium* species as revealed by CARMA, using the NCBI taxonomy.

Further differences between the results obtained from the RDP classifier and CARMA, particularly at genus level, could also be explained by the different taxonomies. For instance, the assignment of metagenomic sequences to archaeal genera revealed a high number of *Methanothermobacter* as determined by CARMA, but when analyzed by the RDP classifier *Methanobacterium* was more abundant.

Additionally, the assignment of metagenomic sequences by CARMA can also lead to an overestimation of specific taxa. Krause and coworkers (2008b) have reported that Proteobacteria were incorrectly assigned by a rate of 3.8%, using the CARMA software. The comparison of CARMA results with results of the *rrs* gene library analysis revealed Proteobacteria at 11% and 7%, respectively, supporting the results described by Krause and coworkers (2008b).

Providing these concerns are kept in mind, the study of microbial metagenomes by high-throughput sequencing is a promising tool for gaining detailed information about the microbial community and its genetic potential.

4.1.4 Quantification of microorganisms

The qPCR and the FISH method are commonly used for the quantification of microorganisms in different habitats, such as biogas reactors (e.g., Burrell et al., 2004; Yu et al., 2005, 2006; Blume et al., 2010; Krakat et al., 2010b; Nettmann et al., 2010).

In this study, two different TaqMan approaches were used for qPCR analyses. The use of such target specific approaches has clear advantages over dsDNA-intercalating fluorescent dyes, such as SYBR green (Sharkey et al., 2004; Zhang & Fang, 2006). The primer set 304 (TaqMan assay) developed in this study specifically targets a group of the unclassified Lachnospiraceae as classified by RDP. In contrast, the classification of the target sequence by NCBI revealed the highest sequence similarity to a member of the Defluviitaleaceae family. This is another example for a different assignment of the same *rrs* sequence using the RDP and NCBI taxonomies.

The DOPE-FISH method allows the quantification of microorganisms based on the microscopical detection of cells. However, the application of the FISH method for environmental samples is difficult. Studies on coastal water showed that less than 50% of total cells were visualized by FISH applying the EUB 338 probe (Pernthaler et al., 2002). In this study, the hybridization rate of probes by DOPE-FISH analysis was low (<30%) despite various optimization methods performed in the context of the Diploma thesis of Krumrei (2010). Impurities in environmental samples can infer the visualization of cells due to high background fluorescence as indicated for biogas samples by Nettmann and coworkers (2010). Further, it might be possible that some microbial groups, which were currently uncharacterized, were not targeted by the bacterial or archaeal probes used in this study. This was already detected for the EUB 338 probe a few years ago, which was then amended by the EUB II and III probes (Daims et al., 1999).

In addition, a low ribosomal content as suggested for marine Actinobacteria by Pernthaler and coworkers (2002) can also reduce the efficiency of probe hybridization. A fact that can also influence the hybridization rate of other FISH analyses. In this study, 50% of total cells were stained by PI indicating at least changes in the cell status. This might affect the hybridization of probes and therefore might be also an explanation for the low hybridization rate in this study.

4.2 Operation of two-phase leach-bed biogas systems

The leach-bed biogas systems analyzed in this study were phase-separated and optimized for the conversion of high-fiber substrate. During the whole experimental run, various parameters, such as biogas and methane yield, VFA concentration and degradation rate of ODM, were analyzed to monitor the performance of the systems.

4.2.1 Performance of the biogas systems during temperature increase

The three identically constructed two-phase biogas systems showed similar reactor performances. The parameters analyzed, such as the biogas yield, the pH, the concentration of VFA and ammonia, resulted in similar values, indicating a reproducible reactor performance of the three systems during the whole experimental run.

During temperature increase, no irreversible accumulation of VFA was determined, which otherwise could lead to an inhibition of microorganisms and particularly to a restriction of methanogenic archaea. Accordingly, the pH ranged between 6.6 and 8, which means favorable conditions for the degradation of plant-derived biomass. Hu and coworkers (2004) showed that the degradation efficiency of crystalline cellulose was the highest between pH values of 6.8 to 7.3.

In the range of 55 to 65 °C, the overall reactor performance was efficient with high total biogas and methane yields and high degradation rates. At temperatures of 70 °C, an abrupt change in the reactor performance, including a decrease in the biogas and methane yield and a decrease in the degradation rate, occurred. Studies on anaerobic digestion processes have revealed a positive influence of temperature on the production of methane from 20 to 60 °C (Ahring, 2003). Above a temperature of 60 °C, a reduced reactor performance has been observed (Ahring, 2003). Although the overall performance in the biogas system at 65 °C was still good and the total biogas yield remained nearly the same, the total methane yield already decreased slightly by 8% at this temperature. However, a strong reduction of the total biogas and methane yield

occurred at 70 °C with 29% and 37%, respectively, in comparison to the values obtained at 60 °C.

In order to stabilize the microbial community at this high temperature, a bioaugmentation with compost was performed at 70 °C. The 21-day fermentation after the bioaugmentation at 70 °C led to improvements in ODM degradation by 9% and biogas yield by 15 to 21%. A study of Neumann and Scherer (2011) also achieved an increase in biogas yield of 6% after bioaugmentation compost during continuous mesophilic fermentations.

The comparison of the bacterial community in this study before and after bioaugmentation revealed only slight changes, which did not completely explain the improved reactor performance in the two-phase biogas system. However, changes in the bacterial community might be occurred during the fermentation with compost, which still took effect on the 21-day fermentation process thereafter. However, the improvements achieved by the bioaugmentation were not maintained during a further temperature increase to 75 °C.

Nevertheless, repeated bioaugmentation with compost might be a valuable tool for the stabilization of thermophilic fermentative bacterial communities. Furthermore, addition of specialized bacteria, which are capable to degrade carbohydrates at higher temperatures, could lead to further improvements. The first studies in this direction have already been published by different authors (e.g., Bagi et al., 2007; Nielsen et al., 2007), who have inoculated several reactor types with *Caldicellulosiruptor*.

4.2.2 Phase-separation of the two-phase biogas system

Phase-separated biogas systems intend to separate process phases, such as hydrolysis and acidogenesis from methanogenesis. The analysis of the metagenomes derived from both the LBR and AF give first insights into the spatial distribution of the microbial community and hence the phase-separation of the biogas system analyzed.

The metagenomes studied here revealed strong differences in the microbial community composition. The genetic potential of bacteria for the expression of carbohydrate

degrading enzymes was strongly increased in the LBR in comparison to the AF. This is in accordance with their role in the hydrolysis of plant-derived biomass, which is supplied to the LBR. This finding supports the results obtained by Muha and coworkers (2011). Their mathematical model of the same two-phase biogas system indicated that the hydrolysis only takes place in the LBR when analyzing an LBR at 55 °C and an AF at 38 °C. Additionally, the authors assumed that acidogenesis and acetogenesis most probably take place in both reactor compartments (LBR and AF) in this two-phase biogas system.

Furthermore, a spatial distribution of methanogens responsible for methane production also occurred. The genetic potential for the expression of methanogenic enzymes was increased in the AF in comparison to the LBR. This led to a high methane content of 70 to 81% in the biogas obtained from the AF in comparison to the LBR (21 - 46% methane content). Hence, the intended spatial distribution of both the bacterial and archaeal community was achieved at least in parts in this phase-separated biogas system.

These findings also confirmed the results obtained by Talbot and coworkers (2010), who also identified a spatial distribution of the microbial consortium analyzing a plug-flow-type anaerobic bioreactor. Their study showed that acid producing bacteria as well as acetoclastic methanogens are mainly located in the hydrolysis/acidification stage of the reactor system.

4.3 Bacterial community in the two-phase biogas system

The composition of the bacterial community was analyzed to achieve an overview about the bacteria involved in the anaerobic digestion of plant-derived biomass and the subsequent conversion pathways. Furthermore, the changes in the bacterial community were monitored in detail during the fermentation of one load of substrate and at increasing temperatures in the LBR.

4.3.1 Dynamic changes in the bacterial community in the LBR during the 21-day fermentation

The bacterial community residing in the biogas system shifted in a cyclic pattern during the fermentation of one load of substrate at all LBR temperature regimes (55 - 75 °C). Thereby, the substrate-attached microbial community introduced by the batch-feeding every 21 days did not affect this dynamic bacterial community.

Changes in the bacterial community as a consequence of the anaerobic digestion process are already known for other biogas reactor systems. Some studies have shown that the bacterial community was highly dynamic in biogas systems, although the whole reactor performance remained stable (Fernandez et al., 1999; Chackhiani et al., 2004). Those studies analyzed small CSTRs (working volume <2 L), which were continuously fed with glucose at mesophilic or with cattle manure at thermophilic temperatures. An analysis of a continuous mesophilic biogas reactor with an increased working volume of 16 L, converting organic household waste, also showed alterations in the bacterial community after 44 and 90 days of fermentation (Cardinali-Rezende et al., 2009). Furthermore, Kampmann and coworkers (2012) have shown that the bacterial community composition in a mesophilic biogas system (working volume of 200 L) shifted after changes in the pH.

This is also true for the bacterial community in this study. The maximal concentration of VFA was achieved during the first nine days of the fermentation. Simultaneously, the pH decreased slightly in the LBR due to the VFA produced, but not below 6.6. Within these nine days, the strongest alterations in the bacterial community were detected, particularly at LBR temperatures from 55 to 65 °C. In this temperature range, different members of the Clostridia class prevailed as consequence of the anaerobic digestion process. For instance, the *Defluviitalea* genus (unclassified Lachnospiraceae as determined by RDP classifier, TRF 304) emerged at 55 and 60 °C simultaneously to the increase in VFA concentration and therefore may has a prominent role in the anaerobic digestion process. For this group, a qPCR primer set was developed in this study. Nevertheless, also other clostridial groups prevailed during the anaerobic digestion process (e.g., TRF 167, *Clostridium*), for which a development of biomarkers may also be of interest.

However, dynamic changes within the microbial community, as observed in this study, may be the most important feature of a well-functioning anaerobic digestion process, allowing coherent pathways for converting different intermediates into precursors to methanogenesis as proposed by Pycke and coworkers (2011). They analyzed full-scale mesophilic and thermophilic CSTRs and a mesophilic UASB and found differences in the bacterial composition by 20 to 40% within 15 days, indicating a highly dynamic system. The hypothesis of Pycke and coworkers (2011) was supported by the findings of this study that revealed the most prominent changes in the bacterial community at LBR temperatures of 55 to 60 °C, where the best reactor performances were achieved.

4.3.2 Composition and dynamics of the bacterial community in the LBR during temperature increase

The bacterial community was subject to alterations during temperature increases in the LBR from 55 to 75 °C as indicated by TRFLP, *rrs* gene library and metagenomic analyses.

Between 55 and 65 °C, members of the Clostridia were detected to be the dominant part of the bacterial community in the LBR. Several genera belonging to the class Clostridia were identified, indicating a high diversity within this class. *Clostridium* was the most prevalent genus, followed by various genera, such as *Alkaliphilus*, *Caldicellulosiruptor*, *Defluviitalea*, *Desulfitobacterium*, *Moorella*, *Pelotomaculum*, *Syntrophomonas* and *Thermoanaerobacter*.

Numerous *Clostridium* species are known for their cellulolytic activity (Felix & Ljungdahl, 1993; Bayer et al., 2004) and therefore for their potential key role in anaerobic biomass degradation. Furthermore, the study of McDonald and coworkers (2012) on anaerobic cellulose degradation showed that different members of the *Clostridium* III cluster were associated with high cellulose degradation. In addition, *Thermoanaerobacter* and *Caldicellulosiruptor* are also capable of degrading carbohydrates (De Vos et al., 2009). For instance, *Caldicellulosiruptor* increases the yield of methane after its addition to a thermophilic biogas fermenter as indicated by

Nielson and coworkers (2007). Further, species of the *Moorella* genus were also predicted to ferment cellulosic material (Karita et al., 2003) and produce acetate as fermentation end product (Drake & Daniel, 2004; De Vos et al., 2009).

Further degradation steps in the biogas formation process including oxidation of fatty acids or degradation of proteins may be carried out by *Syntrophomonas* and *Alkaliphilus*, respectively (McInerney et al., 1981; Takai et al., 2001), which were detected in all metagenomes.

Hence, members of the Clostridia class play a key role in the degradation of plant-derived biomass and the subsequent acido- and acetogenesis as mentioned in previous studies (e.g., Klocke et al., 2007; Krause et al., 2008a; Schlüter et al., 2008; Liu et al., 2009; Krakat et al., 2010b; Wirth et al., 2012).

Additionally, members of the Bacilli and Alpha-, Beta-, Gamma- and Deltaproteobacteria classes were also detected in the biogas system at 55 to 65°C but with lower abundances. Bacilli and Proteobacteria, in particular Deltaproteobacteria, were recently found in a mesophilic biogas systems supplied with fodder beet silage or maize silage (Klocke et al., 2007; Krause et al., 2008a). Members of the Thermotogae were also identified in this study at temperatures of 55 to 65 °C, but also with minor prevalence compared to Clostridia. *Petrotoga*, a genus of the Thermotogae class, was found particularly at thermophilic temperatures of 55 °C. Some members of this genus, such as *Petrotoga mobilis* are known to be fermentative and capable of degrading xylan (Lien et al., 1998).

The high diversity of Clostridia and other fermentative bacteria at temperatures of 55 to 65 °C resulted in high degradation rates of ODM leading to high biogas yields and efficient reactor performances.

After temperature increase to 70 °C, strong changes in the bacterial community and the reactor performance occurred. Bacterial community changes were detected within all three identically constructed biogas systems already after 7 days as determined by TRFLP analysis.

Members of the Clostridia class were reduced and partially replaced by a member of the Bacteroidia class, which was identified as being closely related to the *Acetomicrobium* genus as resulted from TRFLP and *rrs* gene analyses. Further, the metagenomic results also indicated an increase of the *Bacillus* (Bacilli), *Bacteroides* (Bacteroidia) and *Caldicellulosiruptor* (Clostridia) genera.

Acetomicrobium species (Bacteroidia) grow at temperatures up to 75 °C (Krieg et al., 2010). They degrade carbohydrates, such as glucose and cellobiose, which leads to the fermentation end products acetate, lactate, ethanol, CO_2 and H_2 (Krieg et al., 2010). In addition, species of the *Bacteroides* genus (Bacteroidia), identified by metagenomic analysis, are saccharolytic bacteria producing mainly succinate and acetate as fermentation end products (Krieg et al., 2010). In other studies, members of the Bacteroidia were only detected in mesophilic and not in hyperthermophilic fermentations. As example, Kongjan and coworkers (2011) did not identify Bacteroidia when analyzing a two-stage UASB reactor system at 70 and 50 °C, supplied with wheat hydrolysate. In contrast, some studies revealed Bacteroidetes as a prevalent part of the bacterial community, but only in mesophilic biogas systems (Klocke et al., 2007; Krause et al., 2008a; Schlüter et al., 2008; Liu et al., 2009; Kampmann et al., 2012).

In addition, the *Bacillus* genus showed a high diversity, including species capable of degrading carbohydrates (De Vos et al., 2009). Members of the *Caldicellulosiruptor* genus have their growth optima between 65 and 75 °C. Various carbohydrates serve as fermentable substrates leading to fermentation end products of acetate, ethanol, CO_2 and H_2 (De Vos et al., 2009).

Furthermore at an LBR temperature of 75 °C, a member of the Thermotogae (*Fervidobacterium* sp.) was detected in this two-phase biogas system by TRFLP analysis. Members of the *Fervidobacterium* genus use various hexoses for energy metabolism and produce lactate, CO_2, H_2, acetate as well as ethanol, but no butyrate (Patel et al., 1985; Cai et al., 2007).

In accordance with the changes in the bacterial community, the intermediate production changed in the biogas system at 70 °C. For instance, the concentration of the acetic acid and butyric acid was reduced. The fermentation end products of the bacteria prevalent at these temperatures may explain at least the strong reduction in n-butyric acid. Accordingly, it has been reported that a certain number of extreme thermophilic bacteria produce mainly acetate and H_2 as end products and less butyrate and propionate (Wiegel, 1992; Ahring, 2003).

Due to the fact that the intermediate butyrate can be converted into acetate (Wu et al., 1993), the decrease in n-butyric acid also affects the acetic acid producing bacteria. This could also explain the reduced acetic acid concentration at temperatures of

70 and 75 °C. A diminished consumption of the acetic acid by acid-consuming microorganisms, such as syntrophic acetate-oxidizing bacteria or acetoclastic methanogens, could also be assumed, due to a prolonged decomposition of acetic acid in the leachate derived from the LBR at 70 and 75 °C. Ahring and coworkers (2001) identified a disturbance in the proportion between acid-producing and acid-consuming microorganisms in CSTRs already at 65 °C.

These changes in the bacterial community at 70°C finally lead to a strong reduction in the performance of the two-phase biogas system.

4.4 Genetic potential for anaerobic digestion of plant-derived biomass

The microbial degradation of biomass conducted by different bacteria is the time-limiting step during the whole process of biomass conversion to methane. This study focused on the degradation of carbohydrates, an important part of the whole biomass degradation.

The lignin fraction of plant-derived biomass represents a source of energy, which is currently not used by the degradation process due to the anaerobic conditions. Lignin accounts for approximately 4% and 7% of the dry matter in the rye silage and straw material used, respectively. However, to get more insights into the whole genetic potential for carbohydrate degradation, the microbial potential for lignin degradation was also investigated.

Only a minor number of EGTs was assigned to the protein family PF02578 encoding multicopper polyphenol oxidoreductase laccases. Laccases seemed to play an important role in lignin degradation not only in white-rot and brown-rot fungi, but also in bacteria (Bugg et al., 2011). However, the assignment of EGTs, encoding enzymes grouped in this protein family, revealed *Alkaliphilus*, *Syntrophobacter* and *Clostridium*, which have not yet been associated with the degradation of lignin. Members of these genera are strict anaerobic bacteria using proteinaceous substrates (Takai et al.,

2001), propionate (Boone & Bryant, 1980) or various substrates (e.g., Sleat et al., 1984; Schnürer et al., 1996) for energy generation. In contrast, some studies have shown that bacteria, involved in the degradation of lignin, belong to the Actinomycetes, Alpha- and Gammaproteobacteria classes (e.g., Masai et al., 2007; Ahmad et al., 2010; Bugg et al., 2011). Among those, members of the *Streptomycetes*, *Sphingomonas* and *Pseudomonas* genera were identified. Although some metagenomic sequences could be assigned to these genera (e.g., to *Pseudomonas*), the genetic potential of the microbial community for lignin degradation in the biogas system analyzed was very low.

This supports the results of the study of Jaenicke and coworkers (2011), who have identified metagenomic sequences, which encode lignin degrading enzymes, only rarely in a mesophilic biogas system. In comparison to that, sequences, encoding cellulose degrading enzymes, were increased by a factor of 36 (Jaenicke et al., 2011). Other metagenomic studies on biogas communities have also revealed a high genetic potential particularly for carbohydrate degrading enzymes (Krause et al., 2008a; Schlüter et al., 2008; Jaenicke et al., 2011; Wirth et al., 2012). A broad genetic potential for the degradation of hemicelluloses and celluloses was also identified in the microbial community of this study.

Interestingly, although the GH family profiles differed at least slightly in the metagenomic samples analyzed in this study, GH families 3 and 43 were identified in all metagenomes among the five most abundant GH families. These GH families were also prevalently identified in metagenomes derived from a mesophilic and thermophilic biogas system supplied with straw and hay and a full-scale, mesophilic biogas system (Jaenicke et al., 2011; Rademacher et al., 2012; Hanreich, unpublished data). This may indicate a potential key role of the GH families 3 and 43 in biomass degradation independent of the biogas system analyzed. GH family 3 and 43 encompass enzymes, such as β-glucosidase, xylan 1,4-β-xylosidase and β-xylosidase, arabinanase, xylanase, respectively. These enzymes are involved in the breakdown of polymers, such as xylan and cellulose.

However, to deepen the insights into the differences of the genetic potential for carbohydrate degradation in the biogas system analyzed in this study, the abundance of each GH family of interest derived from the four metagenomes was compared. The GH families showed variations in abundance between the metagenomic samples. In the biofilm sample from the AF almost all GH families of interest were decreased by a

factor of up to 20 and in extreme cases by a factor of 70 in comparison to the LBR sample at 55 °C. Hence, the genetic potential for carbohydrate degradation seemed to be strongly reduced in the AF.

Furthermore, the samples from the LBR at 55 and 65 °C revealed the most similar GH family spectrum, indicating a comparable genetic potential for carbohydrate degradation of the inherent microbial community in the biogas reactor at these temperatures. In contrast, the metagenomic sample from the LBR at 70 °C showed stronger alterations. The minor abundance of specific GH families (e.g., GH 8, 11) at this temperature was mainly caused by a decrease of Firmicutes, particularly Clostridia, as indicated by the taxonomic assignment of the corresponding EGTs. On the other hand, the emergence of different GH families (e.g., GH 28, 39) was mainly caused by members of the Bacteroidetes phylum, but also by Firmicutes (Clostridia), Proteobacteria and Chloroflexi phyla. In particular the strong decrease of the number of Firmicutes (Clostridia*)* and the emergence of Bacteroidetes are in agreement with the alterations in the bacterial community after temperature increase to 70 °C as shown by TRFLP and *rrs* gene analyses.

Although the total number of EGTs assigned to selected GH families was the highest in the metagenomic sample at 70 °C, its composition and the assignment to taxonomic groups changed. This might be the reason for the strong decrease in the degradation rate of ODM at 70 °C. For instance, the GH families 9 and 5, encompassing the highest number of up to now identified cellulase genes (Schülein, 2000), were less prevalent at 70 °C. Furthermore at this temperature, the presence of GH family 11, encompassing the highest number of enzymes acting on xylan (Collins et al., 2005), was also reduced. Hence, the genetic potential for carbohydrate degradation of the bacterial community at hyperthermophilic temperatures was not as effective as the genetic potential of the thermophilic community, although GH families with polysaccharide-degrading activity were also detected.

The results clearly indicated that the prevalent GH families identified at 55 and 65 °C might be important for efficient carbohydrate degradation due to the fact that the highest biomass degradation was achieved at these temperatures. Hence these GH families may provide a basis for the development of specific marker systems for the monitoring of biogas reactors by qPCR analysis. Some studies have already focused on the detection of genes encoding GH families 5 and 48 by qPCR (Pereyra et al., 2010). Whereas the GH family 5 was identified with higher abundance in the

metagenomic samples at 55 and 65 °C, GH 48 was less frequently detected in this study and in the metagenome of a mesophilic biogas community (Jaenicke et al., 2010; Rademacher et al., 2012). However, the prevalently detected GH families 3 and 43 should also be considered for such a quantitative approach.

4.5 Putative pathogens in the two-phase biogas system

The presence of selected pathogens was analyzed to determine the potential risk for infections of plants, animals and humans through field application of digestate.

The phylogenetic assignment of metagenomic sequences to plant pathogens, such as *Clavibacter michiganensis*, *Ps*. *syringae* and *Ralstonia solanacearum*, was marginal in the thermophilic two-phase biogas system. Furthermore, other widespread plant pathogens, such as *Rhizoctonia solani* and *Sclerotinia sclerotiorum*, were not detected.

Other studies on this topic showed that plant pathogens did also not proliferate in mesophilic biogas systems. The results of a project study (FNR, 2012d) showed that different plant pathogens, such as *Rhizoctonia solani* and *Sclerotinia sclerotiorum*, were inactivated after a few days of fermentation at mesophilic temperatures as determined with culture-dependent methods. This was also confirmed by the study of Kaemmerer and coworkers (2008), who analyzed different plant pathogens after experimental and full-scale biogas fermentations. Furthermore, they showed that the ensiling process also has the potential to inactivate plant pathogens.

Further potential risks might be derived from pathogens infecting animals or humans. The number of metagenomic sequences, which could be assigned to potential animal or human pathogens was very low. Only the Holin protein family was identified in slightly higher abundances (PF05105). This family includes a protein, which is supposed to be involved in toxin secretion in *Cl*. *difficile* (Tan et al., 2001). Other protein families comprising pathogen-associated proteins were less frequently identified in the two-phase biogas system. This might be achieved by the high reactor temperatures and by the fact that the biogas system under study was supplied with

rye-silage and straw. Manure, a source of pathogens, such as *Cl*. *botulinum*, was only added in the beginning of the reactor start-up.

However, other studies on this topic have also shown a low risk of proliferation of potential pathogens even in mesophilic biogas systems supplied with manure. For instance, Dohrmann and coworkers (2011), who have investigated mesophilic and thermophilic biogas reactors supplied with different manures, did not detect pathogenic *Clostridium* species after analyzing the *rrs* gene. In addition, no evidence for a spreading of pathogens through digestate application was found by the study of Eikmeyer and coworkers (accepted), who analyzed the four metagenomes of this study and three further metagenomes from mesophilic biogas-producing communities. A further work of Goberna and coworkers (2011) revealed a complete disappearance in viable cells of *E*. *coli* and *Salmonella* sp. and a partial disappearance of *Listeria* sp., comparing fresh manure with manure fermented in a mesophilic biogas reactor. Another study of Iwasaki and coworkers (2011) compared samples from a mesophilic and thermophilic biogas plant, detecting viable numbers of the *Coli-aerogenes* (*Escherichia* - *Aerobacter*) and *Enterococcus* group only in the mesophilic biogas plant. However, a reduction in viable bacterial cells occurred during the subsequent anaerobic digestion. Hence, a sanitation effect due to increased temperatures, but also due to retention time might occur at least for specific bacterial groups.

In addition to that, Vinneras and coworkers (2006) indicated that the risk for an unintended distribution of pathogens via the gas of biogas systems or through the condensate water of gas pipes is also very low after applying culture-dependent methods.

These results indicated that the risk of an unintended proliferation of potential pathogens and therefore the risk for infections of plants, animal and humans after applying digestate to agricultural land is rather low. Nevertheless, to deepen the knowledge about the proliferation of pathogens in biogas systems and about temperature-dependent sanitation effects, further studies need to be performed applying culture-dependent methods or targeting specific genes of pathogens by qPCR. The metagenomic results obtained in this study might serve as basis for these studies.

4.6 Archaeal community in the two-phase biogas system

The production of methane is carried out by methanogenic archaea via three different pathways: the hydrogenotrophic, acetoclastic and methylotrophic pathways, using CO_2 and H_2, acetate, methanol or carbon monoxide. To elucidate a potential predominance of one of these pathways in the biogas reactor studied in this work, the composition of the archaeal community was analyzed by metagenomic, TRFLP and *rrs* gene library analyses.

4.6.1 Composition of the archaeal community in the LBR during temperature increase

The archaeal community in the LBR was analyzed for three different temperature regimes (55, 65 and 70 °C) by metagenomic and TRFLP analysis. At an LBR temperature of 55 °C, Methanosarcinales, i.e. *Methanosarcina*, were the most prevalent methanogenic archaea in the LBR. At temperatures higher than 65 °C, members of the Methanosarcinales order were less detected, indicating an inhibition of growth. This is in accordance with the findings that thermophilic *Methanosarcina* species, such as *Msr*. *thermophila*, grow at temperatures of up to 55 °C (Boone & Castenholz, 2001).

On the other hand, members of the Methanobacteriales, i.e. *Methanothermobacter*, were prevalently detected in the LBR at a temperature of 65 °C. At this temperature, the hydrogenotrophic pathway was obviously the prevalent one for methane production in the LBR. *Methanothermobacter* species have their growth optima between 55 and 65 °C (Boone & Castenholz, 2001), confirming the advantage of *Methanothermobacter* over *Methanosarcina* in the LBR at temperatures of 65 °C.

At even higher temperatures, the TRFLP profiles also revealed *Methanothermobacter* as prevalent. However, the metagenomic results indicated a strong growth inhibition of the methanogenic archaea due to the fact that hardly any EGT could be assigned to this taxonomic group. Although methanogens, such as members of the

Methanothermus and *Methanocaldococcus* genera, also grow at hyperthermophilic temperatures (Boone & Castenholz, 2001), the members of the genera identified, such as *Methanosarcina* and *Methanothermobater*, grew up to 55 and 65 °C, respectively, supporting the assumed inhibition at 70 °C. This can be supported by the methane yield obtained in the LBR. At 65 °C, the methane yield was reduced by 14%, whereas a reduction of 59% occurred at 70 °C in comparison to the methane yield obtained at 55 °C. Furthermore, at an LBR temperature of 75 °C, only minor amounts of methane were measured in the LBR.

4.6.2 Composition of the archaeal community in the AF

The archaeal community in the AF was tracked during the temperature increase in the LBR. At an LBR temperature of 55 °C, *Methanosaeta*, a strict acetoclastic methanogen, was detected with minor abundance in the AF. During the course of the experiment *Methanosaeta* was strongly reduced or not found in the AF, although the temperature of this reactor compartment, its pH and its concentration of free ammonia, remained constant. For instance, a total ammonia nitrogen concentration of 0.85 to 1.00 g per L and, due to the high temperature (55 °C) and the pH (7.80 - 7.95), a free ammonia concentration of 0.21 to 0.27 g per L were determined in the AF. Although *Methanosaeta* was found as predominant Archaea at total ammonia nitrogen concentrations of up to 1.5 g per L (Karakashev et al., 2005; Nettmann et al., 2010), they were not identified at free ammonia concentrations above 0.20 g per L in full scale biogas plants (Nettmann et al., 2010). In this study, *Methanosaeta* was identified at ammonia concentrations of 0.24 g per L in the AF at an LBR temperature of 55 °C. However, this concentration might restrict the further proliferation of *Methanosaeta* in the AF during the experimental runs. In addition, a VFA concentration of up to 5.03 g per L in the AF can also restrict *Methanosaeta* (Karakashev et al., 2005) and instead favor the prevalence of *Methanosarcina* or strict hydrogenotrophic archaea.

Hence, members of the Methanosarcinales and Methanobacteriales were the most prevalent orders in the AF independent of the LBR temperature and the analytical approach. The major genera were determined to be *Methanosarcina*, a mixotrophic

methanogen, and *Methanothermobacter* (*Methanobacterium* as determined by RDP classifier), a hydrogenotrophic methanogen. Furthermore, protein families, consisting of enzymes for both pathways, were identified in the AF at least at an LBR temperature of 55 °C. During the following temperature increase in the LBR, both genera (*Methanosarcina* and *Methanothermobacter*) showed an uneven progress in the AF.

Methanobacteriales, particularly *Methanothermobacter* (*Methanobacterium* as determined by RDP classifier), which was prevalently detected in the AF, showed a further increase at an LBR temperature of 70 °C. A study on a hyperthermophilic two-stage UASB reactor, which was conducted at 70 and 55 °C and supplied with wheat hydrolysate, also showed *Methanothermobacter* as prevalent (Kongjan et al., 2011). An explanation for the increase in the biogas system studied in this work might be that the concentration of VFA in the AF was clearly reduced at 70 °C and above. A reduced acetic acid concentration combined with a thermophilic temperature of 55 °C in the AF mean favorable conditions for acetate oxidizers acting with H_2-scavenging hydrogenotrophic archaea in syntrophy, having an advantage over the acetoclastic methanogens (Zinder & Koch, 1984; Ahring 1995). This syntrophic interaction can be conducted via interspecies H_2 transfer, which has been described for *Methanothermobacter* sp. and syntrophic oxidizing bacteria (Ishii et al., 2005).

Interestingly, *Methanosarcina* was also prevalent in the AF, particularly at higher LBR temperatures. Some studies on archaeal communities in biogas reactors revealed a high abundance of *Methanosarcina* (Methanosarcinaceae) in mesophilic and thermophilic systems supplied with manure as main component (Karakashev et al., 2005) or in thermophilic systems supplied with sludge (Lerm et al., 2012), but also in a mesophilic anaerobic digester supplied with wine distillation waste (Godon et al., 1997). Furthermore, an analysis of a thermophilic CSTR supplied with manure and maize silage showed a potentially time-dependent increase of *Methanosarcina* during 14-weeks of fermentation (Bergmann, unpublished data). Hence, *Methanosarcina* seemed to be widely distributed in various biogas systems. In contrast to the acetoclastic *Methanosaeta*, *Methanosarcina* can tolerate free ammonia concentrations of 0.45 g per L (Nettmann et al., 2010), which was underrun in the two-phase biogas system studied in this work.

Furthermore, *Methanosarcina* can utilize acetate, but also CO_2/H_2, methanol and carbon monoxide for methanogenesis. At hyperthermophilic temperatures in the LBR, the acetic acid concentration, which altered during the 21-day fermentation period from

0.04 to 0.82 g per L (0.7 to 13.7 mM) in the AF, fell below the threshold for acetate utilization of *Methanosarcina* in some cases. This threshold varies between 0.11 to 2.50 mM for *Methanosarcina* species from different anaerobic systems (Zinder, 1990; Jetten et al., 1992; Mladenovska & Ahring, 2000). It is therefore conceivable that *Methanosarcina* also utilized other methanogenic pathways than the acetoclastic one depending on the apparent supply of acetic acid or other precursors. This is also supported by the study of Karakashev and coworkers (2006), who have reported that the acetoclastic pathway was only present in mesophilic and thermophilic reactors when Methanosaetaceae were present. However, the use of CO_2/H_2 for the production of methane has not been described for cultivable *Methanosarcina* strains growing at thermophilic temperatures (Boone & Castenholz, 2001). Nevertheless, the potential use of all methanogenic pathways could mean a key advantage over the strict hydrogenotrophic methanogens in this reactor.

4.7 Syntrophic interactions of VFA-oxidizing bacteria and methanogens

A further important point already mentioned is the syntrophic interaction of certain bacteria with hydrogenotrophic methanogens, oxidizing acetate and other VFAs. The bacterial community identified in the AF might interact in syntrophy with H_2-scavenging methanogens.

During the temperature increase in the LBR, the bacterial community in the AF showed no strong alterations. Most of the prevalent bacterial TRFs that were identified in the AF by TRFLP analysis showed the closest assignment to members of the Clostridia class. The same is true for the metagenomic results, revealing a predominance of Clostridia in the AF. Furthermore, the assignment at genus level revealed a prevalence of *Clostridium*, *Anaerobaculum*, *Thermacetogenium* and *Petrotoga*, but also *Pelotomaculum* and *Syntrophomonas* as determined either by RDP or CARMA.

The *Clostridium* genus, predominantly found in the biogas system under study, is linked to the group of acetate-oxidizing bacteria (Schnürer et al., 1996). Certainly, the

acetate-oxidizing *Cl*. *ultunense* strain (NR_026531) grows at mesophilic and not at thermophilic temperatures and showed only low *rrs* sequence identities of 81 to 88% to TRF sequences assigned to the *Clostridium* genus (e.g., TRF 151, 161, 217). However, currently unknown clostridial strains might be involved in syntrophic acetate oxidation.

Members of the *Anaerobaculum* genus (Synergistia class) are not capable of fermenting acetate, although the fermentation of various organic acids has been reported (Rees et al., 1997; Menes & Muxi, 2002; Maune & Tanner, 2012). Therefore, syntrophic acetate oxidation in cooperation with hydrogenotrophic methanogens by members of the *Anaerobaculum* genus is rather unlikely. However, as members of this genus are capable of producing acetate, they might be involved in the supply of acetate for syntrophic oxidation. This might also be true for members of the *Petrotoga* genus, which are fermentative bacteria producing, for instance, acetate as fermentation product (Lien et al., 1998).

However, members of the *Thermacetogenium* genus were also prevalently identified in the AF. The type species *Thermacetogenium phaeum* oxidizes acetate in syntrophic association with *Mtb*. *thermautotrophicus* (Hattori et al., 2000). Due to the fact that members of both genera were prevalently detected in the AF, a syntrophic conversion of acetate to methane is likely.

Beside this potential syntrophic acetate oxidation, further syntrophic cooperations can be assumed. *Pelotomaculum*, which was identified by CARMA, can oxidize lactate, propionate and several alcohols in syntrophic cooperation with hydrogenotrophic methanogens (Imachi et al., 2002). Moreover *Syntrophomonas* oxidizes fatty acids under anaerobic conditions. This occurs in syntrophic association with H_2-scavengers, such as methanogens (McInerney et al., 1981).

4.8 Determination of cell densities of Bacteria and Archaea

The quantitative detection of Bacteria and Archaea was performed by means of qPCR, DAPI staining and DOPE-FISH analysis.

At LBR temperatures of 55 to 65 °C, the total cell count varied between 1.6 and 2.7 x 10^{10} per mL, whereas the number of Bacteria varied between 3.5 and 5.5 x 10^{9} per mL. At these temperatures, the number of the bacterial *rrs* gene copies was higher (1.3 x 10^{11} copies mL^{-1}), presumably due to multiple copy numbers of the *rrs* gene in cells. These results are in accordance with other quantitative studies in biogas reactors. Blume and coworkers (2010) have identified approximately 1 x 10^{9} to 1 x 10^{11} bacterial *rrs* gene copies per mL in their acidification experiment in a mesophilic, laboratory-scale CSTR supplied with maize silage. Nettmann and coworkers (2010) have detected lower total cell counts (1 - 9 x 10^{8} mL^{-1}), but also high bacterial *rrs* gene copy numbers of 1 to 9 x 10^{11} per mL, analyzing six agricultural biogas plants operated between 37 and 45 °C. The total cell counts detected in the study of Krakat and coworkers (2010a) were also in line with this study. They detected 1 to 3 x 10^{10} total cells per mL in a thermophilic biogas fermenter supplied with fodder beet silage and juice.

Further increase in the operation temperature led to a reduction in cell numbers by nearly one log in this study. Still, average values of 5.2 x 10^{9} total cells per mL and 3.5 x 10^{10} bacterial *rrs* gene copies per mL were obtained at LBR temperatures of 70 and 75 °C. Although reduced, these values showed no strong differences to the total cell and *rrs* gene copy numbers obtained by the studies of Nettmann and coworkers (2010), analyzing full-scale biogas systems, and Blume and coworkers (2010), analyzing a mesophilic lab-scale system. Hence, an evidence for the decrease in the reactor performance due to reduced cell numbers is rather unlikely.

The number of archaeal cells represented only 0.3 to 0.6% of the total cell count. In the full-scale biogas systems analyzed by Nettmann and coworkers (2010), the number of archaeal cells represented even 3 to 7% of the total cells. However, although the number of archaeal cells was low, some studies indicated that Archaea are highly active in different biogas systems leading to high methane rates. For instance, Zakrzewski and coworkers (2012) have suggested that Archaea are highly transcriptionally active analyzing the metatranscriptome of a mesophilic biogas-producing community. Furthermore, a metaproteome study on a thermophilic biogas reactor revealed a considerable number of enzymes relevant for methanogenesis also implying a high transcriptional activity of methanogenic archaea (Hanreich et al., 2012).

The quantification of specific taxonomic groups relevant for the anaerobic digestion and the downstream methanogenesis is of major importance for gaining further insights into

the biogas-producing community and for monitoring changes within the microbial community. Particularly, bacteria involved in the time-limiting step of carbohydrate degradation, were of major interest. Therefore, a TaqMan primer-set for qPCR analysis was developed for the monitoring of a potentially process-relevant bacterium, which was dominantly detected by TRFLP analysis at LBR temperatures of 55 and 60 °C. This specific primer set 304 targets a small group of unclassified Lachnospiracea, representing bacteria whose rrs sequence resulted in a TRF 304 after TRFLP analysis.

At thermophilic temperatures, the number of *rrs* gene copies of these bacteria accounted to 2 to 3% of the total bacterial *rrs* gene copies, which implies an accumulation of these bacteria (unclassified Lachnospiraceae) at least at thermophilic temperatures in the system studied here. Furthermore, these bacteria could also be detected in another thermophilic biogas reactor system (UASSR) as shown in this study, indicating a distribution and a putative process-relevance also in other thermophilic biogas systems.

The development of primer sets, such as the primer set 304, is of importance for the monitoring of biogas processes. Other studies have also developed primer sets for the detection of process-relevant bacteria. For instance, McDonald and coworkers (2012) have shown that qPCR analyses of different *Clostridium* clusters (III, IV, XIV) revealed an emergence of these taxonomic groups in different leachate samples derived from a landfill site. In most cases, the *rrs* gene copies of the *Clostridium* clusters showed a relative abundance of 1 to 3% of the bacterial *rrs* gene copies. In two cases, the relative abundance of the *Clostridium* III and XIV cluster increased up to approximately 7% and 17%, respectively. Furthermore, Bauer and coworkers (2012) developed specific qPCR primer sets for different bacterial groups, such as for a cluster of the Ruminococcaceae, Prevotellaceae and Syntrophomonadaceae, which are also involved in the biogas formation process. They have demonstrated a temperature-dependent proliferation of these groups. For instance, members of the Syntrophomonadaceae evolved at thermophilic temperatures, whereas members of the Prevotellaceae at mesophilic temperatures.

In addition, the archaeal community responsible for methanogenesis has also been in the focus of interest. Yu and coworkers (2005) developed TaqMan qPCR primers for the quantification of methanogenic archaea, which served as a basis for the monitoring of the archaeal community in biogas plants by different authors (Yu et al., 2006; Blume et al., 2010; Nettmann et al., 2010).

The development and application of such primer sets for the detection of specific bacteria or archaea is of major importance for the monitoring of biogas systems and may lead to a valuable tool for the detection of process instabilities in future.

5 Outlook

The results gained in this study provide a deeper understanding of biogas-producing communities in phase-separated biogas systems operated at high temperatures (55 - 75 °C). The impact of temperature increase on the microbial biogas community and the overall reactor performance was shown as well as the dynamic changes in the bacterial community as a consequence of the anaerobic digestion of the substrate supplied.

A certain number of unclassifiable and hence currently unknown species were also found in the biogas system. In future, culture-independent methods must be amended by culture-dependent methods, such as isolation and characterization of microbial strains. This will lead to an improved interpretability of results obtained by culture-independent methods.

Nevertheless, this study identified bacteria and glycoside hydrolases, which are potentially relevant for the degradation of carbohydrates. Specific markers for these targets can be used for the monitoring of those potentially process-relevant, but uncultured microorganisms. This is of major importance due to the fact that the majority of microorganisms in biogas systems are still uncultivated. In a first approach, the specific detection of one potentially process-relevant bacterium, belonging to the unclassified Lachnospiraceae, was shown for the biogas system under study and also for another thermophilic biogas system. In future, such marker-based approaches may facilitate not only the monitoring of biogas communities, but also the detection of emerging disturbances in biogas systems.

In addition, the results also indicated that an unintended proliferation of pathogens infecting plants, animals or humans is very low, which may help to improve the public opinion about the risk of biogas plants.

Furthermore, the results of this study provide insights into the operation and optimization of such phase-separated systems. The best reactor performance of the system was achieved between 55 and 60 °C. Although dynamic changes in the bacterial community occurred between these temperatures, the community was mostly dominated by the same members of the Clostridia class. Therefore, the bacterial community of this biogas reactor seemed to be resilient to temperature fluctuations in this temperature range (55 - 60 °C), which is important for reactor operation. In addition, an option for an optimization of such biogas systems is bioaugmentation with compost or microbial strains. The results indicated that a bioaugmentation could be advantageous, although this effect was not persistent in this study. Future studies need to evaluate the positive effect and profitability of continuous bioaugmentation.

Hence, the results gained in this study provide not only a promising basis for the monitoring of biogas communities, but also for a prospective improvement of thermophilic biogas systems with phase-separation.

6 REFERENCES

454 Life Science (2012) Performance of the GS FLX+ System. URL: http://454.com/products/gs-flx-system/index.asp. Last access December 13, 2012.

Abdo Z, Schüette UME, Bent SJ, Williams CJ, Forney LJ & Joyce P (2006) Statistical methods for characterizing diversity of microbial communities by analysis of terminal restriction fragment length polymorphisms of 16S rRNA genes. *Environ Microbiol* **8**, 929-938.

Ahmad M, Taylor CR, Pink D, Burton K, Eastwood D, Bending GD & Bugg TD (2010) Development of novel assays for lignin degradation: comparative analysis of bacterial and fungal lignin degraders. *Mol Bio Syst* **6**, 815-821.

Ahring BK (1995) Methanogenesis in thermophilic biogas reactors. *Anton Leeuw* **67**, 91-102.

Ahring BK, Ibrahim AA & Mladenovska Z (2001) Effect of temperature increase from 55 to 68 °C on performance and microbial population dynamics of an anaerobic reactor treating cattle manure. *Water Res* **35**, 2446-2452.

Ahring BK (2003) Perspectives for anaerobic digestion. In *Biomethanation I* ed. Scheper, T, pp. 1-30. Berlin Heidelberg, Germany: Springer.

Altschul SF, Gish W, Miller W, Myers EW & Lipman DJ (1990) Basic local alignment search tool. *J Mol Biol* **215**, 403-410.

Amann RI, Binder BJ, Olson RJ, Chisholm SW, Devereux R & Stahl DA (1990) Combination of 16S ribosomal-RNA-targeted oligonucleotide probes with flow-cytometry for analyzing mixed microbial-populations. *Appl Environ Microbiol* **56**, 1919-1925.

Amann RI, Ludwig W & Schleifer KH (1995) Phylogenetic dentification and *in-situ* detection of individual microbial cells without cultivation. *Microbiol Rev* **59**, 143-169.

Anthonisen AC, Loehr RC, Prakasam TBS & Srinath EG (1976) Inhibition of nitrification by ammonia and nitrous acid. *J Water Pollut Control Fed* **48**, 835-852.

Applied Biosystems by Life Technologies (2011) 5500 SOLiD™ System. URL: http://www3.appliedbiosystems.com/cms/groups/global_marketing_group/documents/generaldocuments/cms_088662.pdf. Last access November 23, 2012.

Ashelford KE, Chuzhanova NA, Fry JC, Jonas AJ & Weightman AJ (2006) New screening software shows that most recent large 16S rRNA gene clone libraries contain chimeras. *Appl Environ Microbiol* **72**, 5734-5741.

Bagi Z, Acs N, Balint B, Horvath L, Dobo K, Perei KR, Rakhely G & Kovacs KL (2007) Biotechnological intensification of biogas production. *Appl Microbiol Biotechnol* **76**, 473-482.

Bai Y, Shi Q, Wen D, Li Z, Jefferson WA, Feng C & Tang X (2012) Bacterial communities in the sediments of Dianchi Lake, a partitioned eutrophic waterbody in China. *Plos One* **7**, e37796.

Balk M, Weijma J & Stams AJM (2002) *Thermotoga lettingae* sp. nov., a novel thermophilic, methanol-degrading bacterium isolated from a thermophilic anaerobic reactor. *Int J Syst Evol Micr* **52**, 1361-1368.

Barnby FM, Morpeth FF & Pyle DL (1990) Endopolygalacturonase production from *Kluyveromyces marxianus*. 1. resolution, purification, and partial characterization of the enzyme. *Enzyme Microb Technol* **12**, 891-897.

Bauer C, Korthals M, Gronauer A & Lebuhn M (2008) Methanogens in biogas production from renewable resources - a novel molecular population analysis approach. *Water Sci Technol* **58**, 1433-1439.

Bauer C, Marin-Perez C, Munk B & Lebuhn M (2012) Bakterielle Populationen in der Hydrolysephase der Vergärung einer Stroh- und Heumischung - Bacterial populations in the hydrolysis phase of an anaerobically digested straw/hay mixture. In *Bornimer Agrartechnische Berichte* 79, pp. 87-98. Potsdam, Germany: Leibniz-Institut für Agrartechnik Potsdam-Bornim e.V.

Bayer EA, Setter E & Lamed R (1985) Organization and distribution of the cellulosome in *Clostridium thermocellum*. *J Bacteriol* **163**, 552-559.

Bayer EA & Lamed R (1986) Ultrastructure of the cell-surface cellulosome of *Clostridium thermocellum* and its interaction with cellulose. *J Bacteriol* **167**, 828-836.

Bayer EA, Morag E & Lamed R (1994) The cellulosome - a treasure-trove for biotechnology. *Trends Biotechnol* **12**, 379-386.

Bayer EA, Belaich J-P, Shoham Y & Lamed R (2004) The cellulosomes: multienzyme machines for degradation of plant cell wall polysaccharides. *Annu Rev Microbiol* **58**, 521-554.

Belloc F, Dumain P, Boisseau MR, Jalloustre C, Reiffers J, Bernard P & Lacombe F (1994) A flow cytometric method using Hoechst-33342 and propidium iodide for simultaneous cell-cycle analysis and apoptosis determination in unfixed cells. *Cytometry* **17**, 59-65.

Bench SR, Hanson TE, Williamson KE, Ghosh D, Radosovich M, Wang K & Wommack K (2007) Metagenomic characterization of Chesapeake bay virioplankton. *Appl Environ Microbiol* **73**, 7629-7641.

Bergmann I, Nettmann E, Mundt K & Klocke M (2010) Determination of methanogenic Archaea abundance in a mesophilic biogas plant based on 16S rRNA gene sequence analysis. *Can J Microbiol* **56**, 440-444.

Bergmann I (2012) Characterization of methanogenic Archaea communities in biogas reactors by quantitative PCR. Dissertation. Berlin, Germany: Technische Universität Berlin.

BfR – Bundesinstitut für Risikobewertung (2011) EHEC O104:H4-Ausbruchsgeschehen in Deutschland aufgeklärt: Auslöser waren Sprossen von aus Ägypten importierten Bockshornkleesamen. URL: http://www.bfr.bund.de/de/presseinformation/2011/21/ehec_o104_h4_ausbruchsgeschehen_in_deutschland_aufgeklaert__ausloeser_waren_sprossen_von_aus_aegypten_importierten_bockshornkleesamen-82843.html. Last access December 10, 2012.

Bhattarai S, Ross KA, Schmid M, Anselmetti FS & Buergmann H (2012) Local conditions structure unique archaeal communities in the anoxic sediments of meromictic Lake Kivu. *Microbiol Ecol* **64**, 291-310.

Biswas K & Turner SJ (2012) Microbial community composition and dynamics of moving bed biofilm reactor systems treating municipal sewage. *Appl Environ Microbiol* **78**, 855-864.

Blackwood CB & Buyer JS (2007) Evaluating the physical capture method of terminal restriction fragment length polymorphism for comparison of soil microbial communities. *Soil Biol Biochem* **39**, 590-599.

Blaut M (1994) Metabolism of methanogens. *Anton Leeuw Int J G* **66**, 187-208.

Blume F, Bergmann I, Nettmann E, Schelle H, Rehde G, Mundt K & Klocke M (2010) Methanogenic population dynamics during semi-continuous biogas fermentation and acidification by overloading. *J Appl Microbiol* **109**, 441-450.

BMU ed. - Bundesministerium für Umwelt, Naturschutz und Reaktorsicherheit (2012) Erneuerbare Energien in Zahlen - Nationale und internationale Entwicklung. pp. 1-136. Berlin, Germany: BMU.

Böckelmann U, Szewzyk U & Grohmann E (2003) A new enzymatic method for the detachment of particle associated soil bacteria. *J Microbiol Methods* **55**, 201-211.

Boone DR & Bryant MP (1980) Propionate-degrading bacterium, *Syntrophobacter wolinii* sp. nov. gen. nov., from methanogenic ecosystems. *Appl Environ Microbiol* **40**, 626-632.

Boone DR & Castenholz RW eds. (2001) Volume One: The *Archaea* and the deeply branching and phototrophic Bacteria. In *Bergey's Manual® of Systematic Bacteriology* ed. Garrity, GM, pp. 1-721, New York, USA: Springer.

Brosius J, Palmer ML, Kennedy PJ & Noller HF (1978) Complete nucleotide sequence of a 16S ribosomal RNA gene from *Escherichia coli*. *Proc Natl Acad Sci USA* **75**, 4801-4805.

Bugg TD, Ahmad M, Hardiman EM & Singh R (2011) The emerging role for bacteria in lignin degradation and bio-product formation. *Curr Opin Biotechnol* **22**, 394-400.

Bukovska P, Jelinkova M, Hrselova H, Sykorova Z & Gryndler M (2010) Terminal restriction fragment length measurement errors are affected mainly by fragment length, G+C nucleotide content and secondary structure melting point. *J Microbiol Methods* **82**, 223-228.

Burrell PC, O'Sullivan C, Song H, Clarke WP & Blackall LL (2004) Identification, detection, and spatial resolution of *Clostridium* populations responsible for cellulose degradation in a methanogenic landfill leachate bioreactor. *Appl Environ Microbiol* **70**, 2414-2419.

Caffaro-Filho RA, Fantinatti-Garboggini F & Durrant LR (2007) Quantitative analysis of terminal restriction fragment length polymorphism (T-RFLP) microbial community profiles: peak height data showed to be more reproducible than peak area. *Braz J Microbiol* **38**, 736-738.

Cai J, Wang Y, Liu D, Zeng Y, Xue Y, Ma Y & Feng Y (2007) *Fervidobacterium changbaicum* sp. nov., a novel thermophilic anaerobic bacterium isolated from a hot spring of the Changbai Mountains, China. *Int J Syst Evol Microbiol* **57**, 2333-2336.

Cantarel BL, Coutinho PM, Rancurel C, Bernard T, Lombard V & Henrissat B (2009) The Carbohydrate-Active EnZymes database (CAZy): an expert resource for glycogenomics. *Nucleic Acids Res* **37**, D233-D238.

Cao P, Zhang LM, Shen JP, Zheng YM, Di HJ & He JZ (2012) Distribution and diversity of archaeal communities in selected Chinese soils. *FEMS Microbiol Ecol* **80**, 146-158.

Carballa M, Smits M, Etchebehere C, Boon N & Verstraete W (2011) Correlations between molecular and operational parameters in continuous lab-scale anaerobic reactors. *Appl Microbiol Biotechnol* **89**, 303-314.

Cardinali-Rezende J, Debarry RB, Colturato LF, Carneiro EV, Chartone-Souza E & Nascimento AM (2009) Molecular identification and dynamics of microbial communities in reactor treating organic household waste. *Appl Microbiol Biotechnol* **84**, 777-789.

Cattell RB (1966) The scree test for the number of factors. *Multivariate Behavioral Research* **1**, 245-276.

Chackhiani M, Dabert P, Abzianidze T, Partskhaladze G, Tsiklauri L, Dudauri T & Godon JJ (2004) 16S rDNA characterization of bacterial and archaeal communities during start-up of anaerobic thermophilic digestion of cattle manure. *Bioresour Technol* **93**, 227-232.

Chan OC, Claus P, Casper P, Ulrich A, Lueders T & Conrad R (2005) Vertical distribution of structure and function of the methanogenic archaeal community in Lake Dagow sediment. *Environ Microbiol* **7**, 1139-1149.

Chao A (1987) Estimating the population size for capture-recapture data with unequal catchability. *Biometrics* **43**, 783-791.

Chao A, Chazdon RL, Colwell RK & Shen TJ (2005) A new statistical approach for assessing similarity of species composition with incidence and abundance data. *Ecol Lett* **8**, 148-159.

Chen X & Stewart PS (2000) Biofilm removal caused by chemical treatments. *Water Res* **34**, 4229-4233.

Chouari R, Le Paslier D, Daegelen P, Ginestet P, Weissenbach J & Sghir A (2005) Novel predominant archaeal and bacterial groups revealed by molecular analysis of an anaerobic sludge digester. *Environ Microbiol* **7**, 1104-1115.

Clarke KR (1993) Nonparametric multivariate analyses of changes in community structure. *Austral Ecol* **18**, 117-143.

Claus H (2004) Laccases: structure, reactions, distribution. *Micron* **35**, 93-96.

Cole JR, Wang Q, Cardenas E et al. (2009) The Ribosomal Database Project: improved alignments and new tools for rRNA analysis. *Nucleic Acids Res* **37**, D141-D145.

Collins T, Gerday C & Feller G (2005) Xylanases, xylanase families and extremophilic xylanases. *FEMS Microbiol Rev* **29**, 3-23.

Colwell RK (2009) EstimateS: Statistical estimation of species richness and shared species from samples. URL: http://purl.oclc.org/estimates. Last access November 15, 2012.

Culman SW, Bukowski R, Gauch HG, Cadillo-Quiroz H & Buckley DH (2009) Software open access T-REX: software for the processing and analysis of T-RFLP data. *BMC Bioinformatics* **10**, 171.

Dahlenborg M, Borch E & Radström P (2003) Prevalence of *Clostridium botulinum* types B, E and F in faecal samples from Swedish cattle. *Int J Food Microbiol* **82**, 105-110.

Daims H, Bruhl A, Amann R, Schleifer KH & Wagner M (1999) The domain-specific probe EUB338 is insufficient for the detection of all Bacteria: Development and evaluation of a more comprehensive probe set. *Syst Appl Microbiol* **22**, 434-444.

Dang H, Li J, Chen M, Li T, Zeng Z & Yin X (2009) Fine-scale vertical distribution of bacteria in the East Pacific deep-sea sediments determined via 16S rRNA gene T-RFLP and clone library analyses. *World J Microbiol Biotechnol* **25**, 179-188.

Danon M, Franke-Whittle IH, Insam H, Chen Y & Hadar Y (2008) Molecular analysis of bacterial community succession during prolonged compost curing. *FEMS Microbiol Ecol* **65**, 133-144.

Dashtban M, Schraft H, Syed TA & Qin W (2010) Fungal biodegradation and enzymatic modification of lignin. *Int J Biochem Mol Biol* **1**, 36-50.

Davey HM & Hexley P (2011) Red but not dead? Membranes of stressed *Saccharomyces cerevisiae* are permeable to propidium iodide. *Environ Microbiol* **13**, 163-171.

DBFZ ed. - Deutsches BiomasseForschungsZentrum (2011) Monitoring zur Wirkung des Erneuerbare-Energien-Gesetz (EEG) auf die Entwicklung der Stromerzeugung aus Biomasse (interim report). pp. 1-124. Leipzig, Germany: DBFZ.

De Vos P, Garrity GM, Jones D, Krieg NR, Ludwig W, Rainey FA, Schleifer K-H & Whitman WB eds. (2009) Volume three: The *Firmicutes*. In *BERGEY'S MANUAL® OF Systematic Bacteriology* ed. Whitman, WB, pp. 1-1450. New York, USA: Springer.

DeLong EF (1992) Archaea in coastal marine environments. *Proc Natl Acad Sci USA* **89**, 5685-5689.

Demirer GN & Chen S (2005) Two-phase anaerobic digestion of unscreened dairy manure. *Process Biochem* **40**: 3542-3549.

Denaro R, D'Auria G, Di Marco G, Genovese M, Troussellier M, Yakimov MM & Giuliano L (2005) Assessing terminal restriction fragment length polymorphism suitability for the description of bacterial community structure and dynamics in hydrocarbon-polluted marine environments. *Environ Microbiol* **7**, 78-87.

Deppenmeier U, Müller V & Gottschalk G (1996) Pathways of energy conservation in methanogenic archaea. *Arch Microbiol* **165**, 149-163.

DERA ed. - Deutsche Rohstoffagentur in der Bundesanstalt für Geowissenschaften und Rohstoffe (2011) DERA Rohstoffinformation - Reserven, Ressourcen und Verfügbarkeit von Energierohstoffen 2011, pp. 1-92. Hannover, Germany: DERA.

Despres VR, Nowoisky JF, Klose M, Conrad R, Andreae MO & Pöschl U (2007) Characterization of primary biogenic aerosol particles in urban, rural, and high-alpine air by DNA sequence and restriction fragment analysis of ribosomal RNA genes. *Biogeosciences* **4**, 1127-1141.

Dohrmann AB, Baumert S, Klingebiel L, Weiland P & Tebbe CC (2011) Bacterial community structure in experimental methanogenic bioreactors and search for pathogenic clostridia as community members. *Appl Microbiol Biotechnol* **89**, 1991-2004.

Downs CG, Brady CJ & Gooley A (1992) Exopolygalacturonase protein accumulates late in peach fruit ripening. *Physiol Plant* **85**, 133-140.

Drake HL & Daniel SL (2004) Physiology of the thermophilic acetogen *Moorella thermoacetica*. *Res Microbiol* **155**, 422-436.

Droege M & Hill B (2008) The Genome Sequencer FLX™ System - longer reads, more applications, straight forward bioinformatics and more complete data sets. *J Biotechnol* **136**, 3-10.

Dugba PN & Zhang RH (1999) Treatment of dairy wastewater with two-stage anaerobic sequencing batch reactor systems - thermophilic versus mesophilic operations. *Bioresour Technol* **68**, 225-233.

Dunbar J, Ticknor LO & Kuske CR (2001) Phylogenetic specificity and reproducibility and new method for analysis of terminal restriction fragment profiles of 16S rRNA genes from bacterial communities. *Appl Environ Microbiol* **67**, 190-197.

Egert M & Friedrich MW (2003) Formation of pseudo-terminal restriction fragments, a PCR-related bias affecting terminal restriction fragment length polymorphism analysis of microbial community structure. *Appl Environ Microbiol* **69**, 2555-2562.

Eikmeyer F, Rademacher A, Hanreich A et al. (2013) Detailed analysis of metagenome datasets obtained from biogas-producing microbial communities residing in biogas reactors does not indicate the presence of putative pathogenic microorganisms. *Biotechnology for Biofuels* **6**, 49.

Ellis JT, Tramp C, Sims RC & Miller CD (2012) Characterization of a methanogenic community within an algal fed anaerobic digester. *ISRN Microbiology* **2012**, 12pp.

Engebretson JJ & Moyer CL (2003) Fidelity of select restriction endonucleases in determining microbial diversity by terminal-restriction fragment length polymorphism. *Appl Environ Microbiol* **69**, 4823-4829.

Enwall K & Hallin S (2009) Comparison of T-RFLP and DGGE techniques to assess denitrifier community composition in soil. *Lett Appl Microbiol* **48**, 145-148.

Farrelly V, Rainey FA & Stackebrandt E (1995) Effect of genome size and *rrn* gene copy number on PCR amplification of 16S rRNA genes from a mixture of bacterial species. *Appl Environ Microbiol* **61**, 2798-2801.

Felix CR & Ljungdahl LC (1993) The cellulosome: the exocellular organelle of *Clostridium*. *Annu Rev Microbiol* **47**, 791-819.

Feng XM, Karlsson A, Svensson BH & Bertilsson S (2010) Impact of trace element addition on biogas production from food industrial waste - linking process to microbial communities. *FEMS Microbiol Ecol* **74**, 226-240.

Ferguson RL, Buckley EN & Palumbo AV (1984) Response of marine bacterioplankton to differential filtration and confinement. *Appl Environ Microbiol* **47**, 49-55.

Fernandez A, Huang SY, Seston S, Xing J, Hickey R, Criddle C & Tiedje J (1999) How stable is stable? Function versus community composition. *Appl Environ Microbiol* **65**, 3697-3704.

Finn RD, Tate J, Mistry J et al. (2008) The Pfam protein families database. *Nucleic Acids Res* **36**, D281-D288.

FNR ed. - Fachagentur Nachwachsende Rohstoffe e.V. (2010) Leitfaden Biogas - Von der Gewinnung zur Nutzung. pp. 1-274. Gülzow-Prüzen, Germany: FNR.

FNR ed. - Fachagentur Nachwachsende Rohstoffe e.V. (2012a) Biogas. pp. 1-44. Gülzow-Prüzen, Germany: FNR.

FNR ed. - Fachagentur Nachwachsende Rohstoffe e.V. (2012b) Biomethan. pp. 1-25. Gülzow-Prüzen, Germany: FNR.

FNR ed. - Fachagentur Nachwachsende Rohstoffe e.V. (2012c) Bioenergie - die vielfältige erneuerbare Energie. pp. 1-52. Gülzow-Prüzen, Germany: FNR.

FNR ed. - Fachagentur Nachwachsende Rohstoffe e.V. (2012d) Verbundvorhaben: Untersuchungen zum phytosanitären Risiko durch die anaerobe Vergärung von pflanzlichen Biomassen in Biogasanlagen; Teilvorhaben 1 (Projekt 22013207). URL: http://www.fnr-server.de/ftp/pdf/berichte/22013207.pdf. Last access January 10, 2013

Fröhling A (2010) A flow cytometric approach to monitor the effects of gentle preservation techniques in the postharvest chain. Dissertation. Berlin, Germany: Technische Universität Berlin.

Gaillard BD (1965) Comparison of the hemicelluloses from plants belonging to two different plant families. *Phytochemistry* **4**, 631-634.

Garrity GM, Lilburn TG, Cole JR, Harrison SH, Euzeby J & Tindall BJ (2007) The taxonomic outline of Bacteria and Archaea. TOBA Release 7.7, March 2007. Michigan State University Board of Trustees. (http://www.taxonomicoutline.org/)

Gartemann KH, Kirchner O, Engemann J, Gräfen I, Eichenlaub R & Burger A (2003) *Clavibacter michiganensis* subsp. *michiganensis*: first steps in the understanding of virulence of a gram-positive phytopathogenic bacterium. *J Biotechnol* **106**, 179-191.

Gilbert M, Brisson JR, Karwaski MF, Michniewicz J, Cunningham AM, Wu YY, Young NM & Wakarchuk WW (2000) Biosynthesis of ganglioside mimics in *Campylobacter jejuni* OH4384 - Identification of the glycosyltransferase genes, enzymatic synthesis of model compounds, and characterization of nanomole amounts by 600-MHz H-1 and C-13 NMR analysis. *J Biol Chem* **275**, 3896-3906.

Gilles A, Meglecz E, Pech N, Ferreira S, Malausa T & Martin JF (2011) Accuracy and quality assessment of 454 GS-FLX Titanium pyrosequencing. *BMC Genomics* **12**, 245.

Giovannoni JJ, Dellapenna D, Bennett AB & Fischer RL (1989) Expression of a chimeric polygalacturonase gene in transgenic rin (ripening inhibitor) tomato fruit results in polyuronide degradation but not fruit softening. *Plant Cell* **1**, 53-63.

Goberna M, Podmirseg SM, Waldhuber S, Knapp BA, Garcia C & Insam H (2011) Pathogenic bacteria and mineral N in soils following the land spreading of biogas digestates and fresh manure. *Appl Soil Ecol* **49**, 18-25.

Godon JJ, Zumstein E, Dabert P, Habouzit F & Moletta R (1997) Molecular microbial diversity of an anaerobic digestor as determined by small-subunit rDNA sequence analysis. *Appl Environ Microbiol* **63**, 2802-2813.

Good IJ (1953) The population frequencies of species and the estimation of population parameters. *Biometrika* **40**, 237-264.

Großkopf R, Janssen PH & Liesack W (1998) Diversity and structure of the methanogenic community in anoxic rice paddy soil microcosms as examined by cultivation and direct 16S rRNA gene sequence retrieval. *Appl Environ Microbiol* **64**, 960-969.

Hammer Ø, Harper DAT & Ryan PD (2001) Past: Paleontological statistics software package for education and data analysis. *Palaeontol Electronica* **4**, 9pp.

Hanreich A, Heyer R, Benndorf D, Rapp E, Pioch M, Reichl U & Klocke M (2012) Metaproteome analysis to determine the metabolically active part of a thermophilic microbial community producing biogas from agricultural biomass. *Can J Microbiol* **58**, 917-922.

Harmsen HJM, van Kuijk BLM, Plugge CM, Akkermans ADL, de Vos WM & Stams AJM (1998) *Syntrophobacter fumaroxidans* sp. nov., a syntrophic propionate-degrading sulfate-reducing bacterium. *Int J Syst Evol Microbiol* **48**, 1383-1387.

Hattori S, Kamagata Y, Hanada S & Shoun H (2000) *Thermacetogenium phaeum* gen. nov., sp. nov., a strictly anaerobic, thermophilic, syntrophic acetate-oxidizing bacterium. *Int J Syst Evol Microbiol* **50**, 1601-1609.

Henrissat B (1991) A classification of glycosyl hydrolases based on amino-acid sequence similarities. *Biochem J* **280**, 309-316.

Hill MO (1973) Diversity and Evenness - unifying notation and its consequences. *Ecology* **54**, 427-432.

Hu ZH, Wang G & Yu HQ (2004) Anaerobic degradation of cellulose by rumen microorganisms at various pH values. *Biochem Eng J* **21**, 59-62.

Huse SM, Huber JA, Morrison HG, Sogin ML & Welch DM (2007) Accuracy and quality of massively parallel DNA pyrosequencing. *Genome Biol* **8**, R143.

Illumina Inc, (2012) HiSeq® 1500/2500 sequencing systems. URL: http://www.illumina.com/Documents/products/datasheets/datasheet_hiseq2500.pdf. Last access November 23, 2012.

Imachi H, Sekiguchi Y, Kamagata Y, Hanada S, Ohashi A & Harada H (2002) *Pelotomaculum thermopropionicum* gen. nov., sp. nov., an anaerobic, thermophilic, syntrophic propionate-oxidizing bacterium. *Int J Syst Evol Microbiol* **52**, 1729-1735.

Ishii S, Kosaka T, Hori K, Hotta Y & Watanabe K (2005) Coaggregation facilitates interspecies hydrogen transfer between *Pelotomaculum thermopropionicum* and *Methanothermobacter thermautotrophicus*. *Appl Environ Microbiol* **71**, 7838-7845.

Iwasaki M, Yamashiro T, Beneragama N, Nishida T, Kida K, Ihara I, Takahashi J & Umetsu K (2011) The effect of temperature on survival of pathogenic bacteria in biogas plants. *Anim Sci J* **82**, 707-712.

Jabari L, Gannoun H, Cayol JL, Hamdi M, Fauque G, Ollivier B & Fardeau ML (2012) Characterization of *Defluviitalea saccharophila* gen. nov., sp. nov., a thermophilic bacterium isolated from an upflow anaerobic filter treating abattoir wastewaters, and proposal of Defluviitaleaceae fam. nov. *Int J Syst Evol Microbiol* **62**, 550-555.

Jaenicke S, Ander C, Bekel T et al. (2011) Comparative and joint analysis of two metagenomic datasets from a biogas fermenter obtained by 454-pyrosequencing. *PLoS ONE* **6**, e14519.

Jayani RS, Saxena S & Gupta R (2005) Microbial pectinolytic enzymes: A review. *Process Biochem* **40**, 2931-2944.

Jetten MSM, Stams AJM & Zehnder AJB (1992) Methanogenesis from acetate - A comparison of the acetate metabolism in *Methanothrix soehngenii* and *Methanosarcina* spp.. *FEMS Microbiol Rev* **88**, 181-198.

Johansen C, Falholt P & Gram L (1997) Enzymatic removal and disinfection of bacterial biofilms. *Appl Environ Microbiol* **63**, 3724-3728.

Kaemmerer D, Büttner P, Seigner L & Friedrich R (2008) Phytopathogene im Biogasprozess - Phytopathogens in biogas plants. In *Mitteilungen aus dem Julius Kühn-Institut* (JKI) 417, pp. 239-240. Quedlinburg, Germany: JKI.

Kampmann K, Ratering S, Kramer I, Schmidt M, Zerr W & Schnell S (2012) Unexpected stability of Bacteroidetes and Firmicutes communities in laboratory biogas reactors fed with different defined substrates. *Appl Environ Microbiol* **78**, 2106-2119.

Kaplan CW & Kitts CL (2003) Variation between observed and true terminal restriction fragment length is dependent on true TRF length and purine content. *J Microbiol Methods* **54**, 121-125.

Karakashev D, Batstone DJ & Angelidaki I (2005) Influence of environmental conditions on methanogenic compositions in anaerobic biogas reactors. *Appl Environ Microbiol* **71**, 331-338.

Karakashev D, Batstone DJ, Trably E & Angelidaki I (2006) Acetate oxidation is the dominant methanogenic pathway from acetate in the absence of Methanosaetaceae. *Appl Environ Microbiol* **72**, 5138-5141.

Karam NE & Belarbi A (1995) Detection of polygalacturonases and pectin esterases in lactic-acid bacteria. *World J Microbiol Biotechnol* **11**, 559-563.

Karita S, Nakayama K, Goto M, Sakka K, Kim WJ & Ogawa S (2003) A novel cellulolytic, anaerobic, and thermophilic bacterium, *Moorella* sp. strain F21. *Biosci Biotechnol Biochem* **67**, 183-185.

Kastner V, Somitsch W & Schnitzhofer W (2012) The anaerobic fermentation of food waste: a comparison of two bioreactor systems. *J Clean Prod* **34**, 82-90.

Khan MM, Pyle BH & Camper AK (2010) Specific and rapid enumeration of viable but nonculturable and viable-culturable gram-negative bacteria by using flow cytometry. *Appl Environ Microbiol* **76**, 5088-5096.

Kim OS, Imhoff JF, Witzel KP & Junier P (2011) Distribution of denitrifying bacterial communities in the stratified water column and sediment-water interface in two freshwater lakes and the Baltic Sea. *Aquat Ecol* **45**, 99-112.

Kitts CL (2001) Terminal restriction fragment patterns: a tool for comparing microbial communities and assessing community dynamics. *Curr Issues Intest Microbiol* **2**, 17-25.

Klocke M, Mähnert P, Mundt K, Souidi K & Linke B (2007) Microbial community analysis of a biogas-producing completely stirred tank reactor fed continuously with fodder beet silage as mono-substrate. *Syst Appl Microbiol* **30**, 139-151.

Klocke M, Nettmann E, Bergmann I, Mundt K, Souidi K, Mumme J & Linke B (2008) Characterization of the methanogenic Archaea within two-phase biogas reactor systems operated with plant biomass. *Syst Appl Microbiol* **31**, 190-205.

Kongjan P, Thong S & Angelidaki I (2011) Performance and microbial community analysis of two-stage process with extreme thermophilic hydrogen and thermophilic methane production from hydrolysate in UASB reactors. *Bioresour Technol* **102**, 4028-4035.

Koster IW & Lettinga G (1984) The influence of ammonium-nitrogen on the specific activity of pelletized methanogenic sludge. *Agricultural Wastes* **9**, 205-216.

Kouguchi H, Watanabe T, Sagane Y, Sunagawa H & Ohyama T (2002) In vitro reconstitution of the *Clostridium botulinum* type D progenitor toxin. *J Biol Chem* **277**, 2650-2656.

Krakat N, Westphal A, Schmidt S & Scherer P (2010a) Anaerobic digestion of renewable biomass: thermophilic temperature governs methanogen population dynamics. *Appl Environ Microbiol* **76**, 1842-1850.

Krakat N, Westphal A, Satke K, Schmidt S & Scherer P (2010b) The microcosm of a biogas fermenter: Comparison of moderate hyperthermophilic (60 °C) with thermophilic (55 °C) conditions. *Eng Life Sci* **10**, 520-527.

Krause L, Diaz NN, Edwards RA et al. (2008a) Taxonomic composition and gene content of a methane-producing microbial community isolated from a biogas reactor. *J Biotechnol* **136**, 91-101.

Krause L, Diaz NN, Goesmann A, Kelley S, Nattkemper TW, Rohwer F, Edwards RA & Stoye J (2008b) Phylogenetic classification of short environmental DNA fragments. *Nucleic Acids Res* **36**, 2230-2239.

Krieg NR, Staley JT, Brown DR, Hedlund BP, Paster BJ, Ward NL, Ludwig W & Whitman WB eds. (2010) Volume Four: The Bacteroidetes, Spirochaetes, Tenericutes (Mollicutes), Acidobacteria, Fibrobacteres, Fusobacteria, Dictyoglomi, Gemmatimonadetes, Lentisphaerae, Verrucomicrobia, Chlamydiae, and Planctomycetes. In *BERGEY'S MANUAL® OF Systematic Bacteriology* ed. Whitman, WB, pp. 1-948. New York, USA: Springer.

Kröber M, Bekel T, Diaz NN et al. (2009) Phylogenetic characterization of a biogas plant microbial community integrating clone library 16S-rDNA sequences and metagenome sequence data obtained by 454-pyrosequencing. *J Biotechnol* **142**, 38-49.

Krsek M & Wellington EMH (1999) Comparison of different methods for the isolation and purification of total community DNA from soil. *J Microbiol Methods* **39**, 1-16.

Krumrei C (2010) Mikrobiologie thermophiler Biogasfermentationen im zweistufigen Verfahren. Diploma thesis. Berlin, Germany: Beuth Hochschule für Technik Berlin.

Kruskal JB (1964) Multidimensional scaling by optimizing goodness of fit to a nonmetric hypothesis. *Psychometrika* **29**, 1-27.

Kruskal JB & Wish M (1978) Multidimensional scaling. Beverly Hills, USA: Sage Publications.

Lamed R, Naimark J, Morgenstern E & Bayer EA (1987) Specialized cell-surface structures in cellulolytic bacteria. *J Bacteriol* **169**, 3792-3800.

Lane DJ (1991) 16S/23S rRNA sequencing. In *Nucleic Acid Techniques in Bacterial Systematics* ed. Stackebrandt, E and Goodfellow, M, pp. 115-147. New York, USA: Wiley.

Lee MJ & Zinder SH (1988) Isolation and characterization of a thermophilic bacterium which oxidizes acetate in syntrophic association with a methanogen and which grows acetogenically on H_2-CO_2. *Appl Environ Microbiol* **54**, 124-129.

Lehtomäki A, Huttunen S, Lehtinen T & Rintala JA (2008) Anaerobic digestion of grass silage in batch leach bed processes for methane production. *Bioresour Technol* **99**, 3267-3278.

Leininger S, Urich T, Schloter M, Schwark L, Qi J, Nicol GW, Prosser JI, Schuster SC & Schleper C (2006) Archaea predominate among ammonia-oxidizing prokaryotes in soils. *Nature* **442**, 806-809.

Lerm S, Kleyboecker A, Miethling-Graff R, Alawi M, Kasina M, Liebrich M & Wuerdemann H (2012) Archaeal community composition affects the function of anaerobic co-digesters in response to organic overload. *Waste Manag* **32**, 389-399.

Leyer I & Wesche K (2008) Multidimensionale Skalierung. In *Multivariate Statistik in der Ökologie*, pp. 137-152. Berlin Heidelberg, Germany: Springer.

Lien T, Madsen M, Rainey FA & Birkeland NK (1998) *Petrotoga mobilis* sp. nov., from a North Sea oil-production well. *Int J Syst Bacteriol* **48**, 1007-1013.

Liu WT, Marsh TL, Cheng H & Forney LJ (1997) Characterization of microbial diversity by determining terminal restriction fragment length polymorphisms of genes encoding 16S rRNA. *Appl Environ Microbiol* **63**, 4516-4522.

Liu FH, Wang SB, Zhang JS, Zhang J, Yan X, Zhou HK, Zhao GP & Zhou ZH (2009) The structure of the bacterial and archaeal community in a biogas digester as revealed by denaturing gradient gel electrophoresis and 16S rDNA sequencing analysis. *J Appl Microbiol* **106**, 952-966.

Lloyd M & Ghelardi RJ (1964) A table for calculating the "equitability" component of species diversity. *J Anim Ecology* **33**, 217-225.

Loy A, Maixner F, Wagner M & Horn M (2007) ProbeBase - an online resource for rRNA-targeted oligonucleotide probes: new features 2007. *Nucleic Acids Res* **35**, D800-D804.

Lueders T & Friedrich M (2000) Archaeal population dynamics during sequential reduction processes in rice field soil. *Appl Environ Microbiol* **66**, 2732-2742.

Lueders T & Friedrich MW (2003) Evaluation of PCR amplification bias by terminal restriction fragment length polymorphism analysis of small-subunit rRNA and *mcrA* genes by using defined template mixtures of methanogenic pure cultures and soil DNA extracts. *Appl Environ Microbiol* **69**, 320-326.

Lukow T, Dunfield PF & Liesack W (2000) Use of the T-RFLP technique to assess spatial and temporal changes in the bacterial community structure within an agricultural soil planted with transgenic and non-transgenic potato plants. *FEMS Microbiol Ecol* **32**, 241-247.

Lynd LR, Weimer PJ, van Zyl WH & Pretorius IS (2002) Microbial cellulose utilization: Fundamentals and biotechnology. *Microbiol Mol Biol Rev* **66**, 506-577.

Magurran AE (1988) *Ecological diversity and its measurement*. Princeton, USA: Princeton University Press.

Margulies M, Egholm M, Altman WE et al. (2005) Genome sequencing in open microfabricated high density picoliter reactors. *Nature* **437**, 376-380.

Marsh TL (1999) Terminal restriction fragment length polymorphism (T-RFLP): an emerging method for characterizing diversity among homologous populations of amplification products. *Curr Opin Microbiol* **2**, 323-327.

Marsh TL (2005) Culture-independent microbial community analysis with terminal restriction fragment length polymorphism. *Environ Microbiol* **397**, 308-329.

Masai E, Katayama Y & Fukuda M (2007) Genetic and biochemical investigations on bacterial catabolic pathways for lignin-derived aromatic compounds. *Biosci Biotechnol Biochem* **71**, 1-15.

Maune MW & Tanner RS (2012) Description of *Anaerobaculum hydrogeniformans* sp. nov., an anaerobe that produces hydrogen from glucose, and emended description of the genus *Anaerobaculum*. *Int J Syst Evol Microbiol* **62**, 832-838.

McDonald JE, Houghton JNI, Rooks DJ, Allison HE & McCarthy AJ (2012) The microbial ecology of anaerobic cellulose degradation in municipal waste landfill sites: evidence of a role for Fibrobacters. *Environ Microbiol* **14**, 1077-1087.

McEniry J, O'Kiely P, Clipson NJW, Forristal PD & Doyle EM (2008) Bacterial community dynamics during the ensilage of wilted grass. *J Appl Microbiol* **105**, 359-371.

McInerney MJ, Bryant MP, Hespell RB & Costerton JW (1981) *Syntrophomonas wolfei* gen. nov., sp. nov., an anaerobic, syntrophic, fatty-acid oxidizing bacterium. *Appl Environ Microbiol* **41,** 1029-1039.

McKay AM (1990) Degradation of polygalacturonic acid by *Saccharomyces cerevisiae*. *Lett Appl Microbiol* **11**, 41-44.

Mende DR, Waller AS, Sunagawa S, Jaervelin AI, Chan MM, Arumugam M, Raes J & Bork P (2012) Assessment of metagenomic assembly using simulated next generation sequencing data. *Plos One* **7**, e31386.

Menes RJ & Muxi L (2002) *Anaerobaculum mobile* sp. nov., a novel anaerobic, moderately thermophilic, peptide fermenting bacterium that uses crotonate as an electron acceptor, and emended description of the genus *Anaerobaculum*. *Int J Syst Evol Microbiol* **52**, 157-164.

Merlino G, Rizzi A, Villa F, Sorlini C, Brambilla M, Navarotto P, Bertazzoni B, Zagni M, Araldi F & Daffonchio D (2012) Shifts of microbial community structure during anaerobic digestion of agro-industrial energetic crops and food industry byproducts. *J Chem Technol Biotechnol* **87**, 1302-1311.

Mladenovska Z & Ahring B (2000) Growth kinetics of thermophilic *Methanosarcina* spp. isolated from full-scale biogas plants treating animal manures. *FEMS Microbiol Ecol* **31**, 225-229.

Moeseneder MM, Arrieta JM, Muyzer G, Winter C & Herndl GJ (1999) Optimization of terminal-restriction fragment length polymorphism analysis for complex marine bacterioplankton communities and comparison with denaturing gradient gel electrophoresis. *Appl Environ Microbiol* **65**, 3518-3525.

Mott IEC, Stickler DJ, Coakley WT & Bott TR (1998) The removal of bacterial biofilm from water-filled tubes using axially propagated ultrasound. *J Appl Microbiol* **84**, 509-514.

Muha I, Grillo A, Heisig M, Schönberg M, Linke B & Wittum G (2011) Mathematical modeling of process liquid flow and acetoclastic methanogenesis under mesophilic conditions in a two-phase biogas reactor. *Bioresour Technol* **106**, 1-9.

Muyzer G, Teske A, Wirsen CO & Jannasch HW (1995) Phylogenetic relationships of *Thiomicrospira* species and their identification in deep-sea hydrothermal vent samples by denaturing gradient gel-electrophoresis of 16S rDNA fragments. *Arch Microbiol* **164**, 165-172.

Nettmann E, Bergmann I, Mundt K, Linke B & Klocke M (2008) Archaea diversity within a commercial biogas plant utilizing herbal biomass determined by 16S rDNA and mcrA analysis. *J Appl Microbiol* **105**, 1835-1850.

Nettmann E, Bergmann I, Pramschüfer S, Mundt K, Plogsties V, Herrmann C & Klocke M (2010) Polyphasic analyses of methanogenic archaeal communities in agricultural biogas plants. *Appl Environ Microbiol* **76**, 2540-2548.

Neumann L & Scherer P (2011) Impact of bioaugmentation by compost on the performance and ecology of an anaerobic digester fed with energy crops. *Bioresour Technol* **102**, 2931-2935.

Nielsen HB, Mladenovska Z & Ahring BK (2007) Bioaugmentation of a two-stage thermophilic (68 °C/55 °C) anaerobic digestion concept for improvement of the methane yield from cattle manure. *Biotechnol Bioeng* **97**, 1638-1643.

Nizami A, Thamsiriroj T, Singh A & Murphy J (2010) Role of leaching and hydrolysis in a two-phase grass digestion system. *Energy Fuels* **24**, 4549-4559.

Nizami AS & Murphy JD (2011) Optimizing the operation of a two-phase anaerobic digestion system digesting grass silage. *Environ Sci Technol* **45**, 7561-7569.

Nizami AS, Singh A & Murphy JD (2011) Design, commissioning, and start-up of a sequentially fed leach bed reactor complete with an upflow anaerobic sludge blanket digesting grass silage. *Energy Fuels* **25**, 823-834.

Nolte C (2011) Entwicklung der mikrobiellen Lebensgemeinschaften in thermophilen Biogasfermentationen. Bachelor thesis. Berlin, Germany: Humboldt-Universität zu Berlin.

O'Neill MA, Albersheim P & Darvill A (1990) The pectic polysaccharides of primary cell walls. In *Methods in Plant Biochemistry* ed. Dey, PM, pp. 415–441. London, UK: Academic Press.

Ogata H, Goto S, Sato K, Fujibuchi W, Bono H & Kanehisa M (1999) KEGG: Kyoto Encyclopedia of Genes and Genomes. *Nucleic Acids Res* **27**, 29-34.

Opatkiewicz AD, Butterfield DA & Baross JA (2009) Individual hydrothermal vents at Axial Seamount harbor distinct subseafloor microbial communities. *FEMS Microbiol Ecol* **70**, 413-424.

Osborn AM, Moore ERB & Timmis KN (2000) An evaluation of terminal-restriction fragment length polymorphism (T-RFLP) analysis for the study of microbial community structure and dynamics. *Environ Microbiol* **2**, 39-50.

Osborne CA, Rees GN, Bernstein Y & Janssen PH (2006) New threshold and confidence estimates for terminal restriction fragment length polymorphism analysis of complex bacterial communities. *Appl Environ Microbiol* **72**, 1270-1278.

Pacific Biosciences (2012) SMRT sequencing advantage. URL: http://www.pacificbiosciences.com/products/smrt-technology/smrt-sequencing-advantage/. Last access November 23, 2012.

Pagani I, Liolios K, Jansson J, Chen IMA, Smirnova T, Nosrat B, Markowitz VM & Kyrpides NC (2012) The Genomes OnLine Database (GOLD) v.4: status of genomic and metagenomic projects and their associated metadata. *Nucleic Acids Res* **40**, D571-D579.

Patel BKC, Morgan HW & Daniel RM (1985) *Fervidobacterium nodosum* gen. nov. and spec. nov., a new chemoorganotrophic, caldoactive, anaerobic bacterium. *Arch Microbiol* **141**, 63-69.

Pereira MG, Latchford JW & Mudge SM (2006) The use of terminal restriction fragment length polymorphism (T-RFLP) for the characterisation of microbial communities in marine sediments. *Geomicrobiol J* **23**, 247-251.

Pereyra LP, Hiibel SR, Riquelme MVP, Reardon KF & Pruden A (2010) Detection and quantification of functional genes of cellulose-degrading, fermentative, and sulfate-reducing bacteria and methanogenic archaea. *Appl Environ Microbiol* **76**, 2192-2202.

Pernthaler A, Pernthaler J & Amann R (2002) Fluorescence *in situ* hybridization and catalyzed reporter deposition for the identification of marine bacteria. *Appl Environ Microbiol* **68**, 3094-3101.

Ponpium P, Ratanakhanokchai K & Kyu KL (2000) Isolation and properties of a cellulosome-type multienzyme complex of the thermophilic *Bacteroides* sp. strain P-1. *Enzyme Microb Technol* **26**, 459-465.

Punta M, Coggill PC, Eberhardt RY et al. (2012) The Pfam protein families database. *Nucleic Acids Res* **40**, D290-D301.

Pycke B, Etchebehere C, Van de Caveye P, Negroni A, Verstraete W & Boon N (2011) A time-course analysis of four full-scale anaerobic digesters in relation to the dynamics of change of their microbial communities. *Water Sci Technol* **63**, 769-775.

Rademacher A, Zakrzewski M, Schlüter A, Schönberg M, Szczepanowski R, Goesmann A, Pühler A & Klocke M (2012) Characterization of microbial biofilms in a thermophilic biogas system by high-throughput metagenome sequencing. *FEMS Microbiol Ecol* **79**, 785-799.

Raizada N (2004) Application of molecular-biological method for optimization of anaerobic reactors. In *Berichte aus Wassergüte- und Abfallwirtschaft.* Garching, Germany: Technische Universität München.

Reddy CA & D'Souza TM (1994) Physiology and molecular-biology of the lignin peroxidases of *Phanerochaete chrysosporium*. *FEMS Microbiol Rev* **13**, 137-152.

Rees GN, Patel BKC, Grassia GS & Sheehy AJ (1997) *Anaerobaculum themoterrenum* gen. nov. sp. nov., a novel, thermophilic bacterium which ferments citrate. *Int J Syst Bacteriol* **47**, 150-154.

Rheims H & Stackebrandt E (1999) Application of nested polymerase chain reaction for the detection of as yet uncultured organisms of the class Actinobacteria in environmental samples. *Environ Microbiol* **1**, 137-143.

Rochex A, Masse A, Escudie R, Godon JJ & Bernet N (2009) Influence of abrasion on biofilm detachment: evidence for stratification of the biofilm. *J Ind Microbiol Biot* **36**, 467-470.

Rozen S & Skaletsky HJ (2000) Primer3 on the WWW for general users and for biologist programmers. In *Bioinfomatics: Methods and Protocols* ed. Misener, S and Krawetz, SA, pp. 365-386. Totowa, USA: Humana Press.

Sait L, Galic M, Strugnell RA & Janssen PH (2003) Secretory antibodies do not affect the composition of the bacterial microbiota in the terminal ileum of 10-week-old mice. *Appl Environ Microbiol* **69**, 2100-2109.

Sakai S, Imachi H, Hanada S, Ohashi A, Harada H & Kamagata Y (2008) *Methanocella paludicola* gen. nov., sp. nov., a methane-producing archaeon, the first isolate of the lineage 'Rice Cluster I', and proposal of the new archaeal order Methanocellales ord. nov. *Int J Syst Evol Micr* **58**, 929-936.

Sanger F, Nicklen S & Coulson AR (1977) DNA sequencing with chain-terminating inhibitors. *Proc Natl Acad Sci USA* **74**, 5463-5467.

Schlüter A, Bekel T, Diaz NN et al. (2008) The metagenome of a biogas-producing microbial community of a production-scale biogas plant fermenter analysed by the 454-pyrosequencing technology. *J Biotechnol* **136**, 77-90.

Schnürer A, Schink B & Svensson BH (1996) *Clostridium ultunense* sp. nov., a mesophilic bacterium oxidizing acetate in syntrophic association with a hydrogenotrophic methanogenic bacterium. *Int J Syst Bacteriol* **46**, 1145-1152.

Scholten JCM & Conrad R (2000) Energetics of syntrophic propionate oxidation in defined batch and chemostat cocultures. *Appl Environ Microbiol* **66**, 2934-2942.

Schönberg M & Linke B (2012) The influence of the temperature regime on the formation of methane in a two-phase anaerobic digestion process. *Eng Life Sci* **12**, 279-286.

Schülein M (2000) Protein engineering of cellulases. *Biochim Biophys Acta* **1543**, 239-252.

Schütte UME, Abdo Z, Bent SJ, Shyu C, Williams CJ, Pierson JD & Forney LJ (2008) Advances in the use of terminal restriction fragment length polymorphism (T-RFLP) analysis of 16S rRNA genes to characterize microbial communities. *Appl Microbiol Biotechnol* **80**, 365-380.

Schwarz WH (2001) The cellulosome and cellulose degradation by anaerobic bacteria. *Appl Microbiol Biotechnol* **56**, 634-649.

Sekiguchi Y, Kamagata Y, Nakamura K, Ohashi A & Harada H (2000) *Syntrophothermus lipocalidus* gen. nov., sp. nov., a novel thermophilic, syntrophic, fatty-acid-oxidizing anaerobe which utilizes isobutyrate. *Int J Syst Evol Microbiol* **50**, 771-779.

Shannon CE & Weaver W (1963) *The mathematical theory of communication*. Urbana, USA: University of Illinous press.

Sharkey FH, Banat IM & Marchant R (2004) Detection and quantification of gene expression in environmental bacteriology. *Appl Environ Microbiol* **70**, 3795-3806.

Shoham Y, Lamed R & Bayer EA (1999) The cellulosome concept as an efficient microbial strategy for the degradation of insoluble polysaccharides. *Trends Microbiol* **7**, 275-281.

Simpson EH (1949) Measurement of diversity. *Nature* **163**, 688-688.

Singh BK, Nazaries L, Munro S, Anderson IC & Campbell CD (2006) Use of multiplex terminal restriction fragment length polymorphism for rapid and simultaneous analysis of different components of the soil microbial community. *Appl Environ Microbiol* **72**, 7278-7285.

Sipos R, Szekely AJ, Palatinszky M, Revesz S, Marialigeti K & Nikolausz M (2007) Effect of primer mismatch, annealing temperature and PCR cycle number on 16S rRNA gene-targetting bacterial community analysis. *FEMS Microbiol Ecol* **60**, 341-350.

Siriwongrungson V, Zeng RJ & Angelidaki I (2007) Homoacetogenesis as the alternative pathway for H_2 sink during thermophilic anaerobic degradation of butyrate under suppressed methanogenesis. *Water Res* **41**, 4204-4210.

Sleat R, Mah RA & Robinson R (1984) Isolation and characterization of an anaerobic, cellulolytic bacterium, *Clostridium cellulovorans* sp. nov. *Appl Environ Microbiol* **48**, 88-93.

Smith CJ, Danilowicz BS, Clear AK, Costello FJ, Wilson B & Meijer WG (2005) T-Align, a web-based tool for comparison of multiple terminal restriction fragment length polymorphism profiles. *FEMS Microbiol Ecol* **54**, 375-380.

Soo RM, Wood SA, Grzymski JJ, McDonald IR & Cary SC (2009) Microbial biodiversity of thermophilic communities in hot mineral soils of Tramway Ridge, Mount Erebus, Antarctica. *Environ Microbiol* **11**, 715-728.

Speel EJM, Hopman AHN & Komminoth P (1999) Amplification methods to increase the sensitivity of *in situ* hybridization: Play CARD(S). *J Histochem Cytochem* **47**, 281-288.

Stahl DA & Amann R (1991) Development and application of nucleic acid probes. In *Nucleic acid techniques in bacterial systematics* ed. Stackebrandt, E, pp. 205-248. Chichester, England: John Wiley & Sons Ltd.

Staley JT & Konopka A (1985) Measurement of *in situ* activities of nonphotosynthetic microorganisms in aquatic and terrestrial habitats. *Ann Rev Microbiol* **39**, 321-346.

Statistisches Bundesamt (2012) Landwirtschaftlich genutzte Fläche nach Hauptnutzungsarten. https://www.destatis.de/DE/ZahlenFakten/Wirtschaftsbereiche/LandForstwirtschaft/Bodennutzung/Tabellen/HauptnutzungsartenLF.html. Last access December 03, 2012.

Steinberg LM & Regan JM (2009) McrA-targeted real-time quantitative PCR method to examine methanogen communities. *Appl Environ Microbiol* **75**, 4435-4442.

Stoecker K, Dorninger C, Daims H & Wagner M (2010) Double labeling of oligonucleotide probes for fluorescence i*n situ* hybridization (DOPE-FISH) improves signal intensity and increases rRNA accessibility. *Appl Environ Microbiol* **76**, 922-926.

Sun L, Ouyang X, Tang Y, Yang Y & Luo Y (2012) Effects of different methods of DNA extraction for activated sludge on the subsequent analysis of bacterial community profiles. *Water Environ Res* **84**, 108-114.

Takai K, Moser DP, Onstott TC, Spoelstra N, Pfiffner SM, Dohnalkova A & Fredrickson JK (2001) *Alkaliphilus transvaalensis* gen. nov., sp. nov., an extremely alkaliphilic bacterium isolated from a deep South African gold mine. *Int J Syst Evol Microbiol* **51**, 1245-1256.

Talbot G, Roy CS, Topp E, Kalmokoff ML, Brooks SPJ, Beaulieu C, Palin MF & Masse DI (2010) Spatial distribution of some microbial trophic groups in a plug-flow-type anaerobic bioreactor treating swine manure. *Water Sci Technol* **61**, 1147-1155.

Tale VP, Maki JS, Struble CA & Zitomer DH (2011) Methanogen community structure-activity relationship and bioaugmentation of overloaded anaerobic digesters. *Water Res* **45**, 5249-5256.

Tamura K, Peterson D, Peterson N, Stecher G, Nei M & Kumar S (2011) MEGA5: Molecular evolutionary genetics analysis using maximum likelihood, evolutionary distance, and maximum parsimony methods. *Mol Biol Evol* **28**, 2731-2739.

Tan KS, Wee BY & Song KP (2001) Evidence for holin function of tcdE gene in the pathogenicity of *Clostridium difficile*. *J Med Microbiol* **50**, 613-619.

Thauer RK, Hedderich R & Fischer R (1993) Reactions and enzymes involved in methanogenesis from CO_2 and H_2. In *Methanogenesis* ed. Ferry, JG, pp. 209-252. New York London: Chapman & Hall.

Tsuge H, Nagahama M, Nishimura H, Hisatsune J, Sakaguch Y, Itogawa Y, Katunuma N & Sakurai J (2003) Crystal structure and site-directed mutagenesis of enzymatic components from *Clostridium perfringens* iota-toxin. *J Mol Biol* **325**, 471-483.

Turnbaugh PJ, Ley RE, Mahowald MA, Magrini V, Mardis ER & Gordon JI (2006) An obesity-associated gut microbiome with increased capacity for energy harvest. *Nature* **444**, 1027-1031.

Ulrich A, Klimke G & Wirth S (2008) Diversity and activity of cellulose-decomposing bacteria, isolated from a sandy and a loamy soil after long-term manure application. *Microb Ecol* **55**, 512-522.

v. Wintzingerode F, Göbel UB & Stackebrandt E (1997) Determination of microbial diversity in environmental samples: pitfalls of PCR-based rRNA analysis. *FEMS Microbiol Rev* **21**, 213-229.

Van de Peer Y, Chapelle S & De Wachter R (1996) A quantitative map of nucleotide substitution rates in bacterial rRNA. *Nucleic Acids Res* **24**, 3381-3391.

Vanysacker L, Declerck SAJ, Hellemans B, De Meester L, Vankelecom I & Declerck P (2010) Bacterial community analysis of activated sludge: an evaluation of four commonly used DNA extraction methods. *Appl Microbiol Biotechnol* **88**, 299-307.

Vetriani C, Jannasch HW, MacGregor BJ, Stahl DA & Reysenbach AL (1999) Population structure and phylogenetic characterization of marine benthic Archaea in deep-sea sediments. *Appl Environ Microbiol* **65**, 4375-4384.

Vinneras B, Schönning C & Nordin A (2006) Identification of the microbiological community in biogas systems and evaluation of microbial risks from gas usage. *Sci Total Environ* **367**, 606-615.

Wagner M, Amann R, Lemmer H & Schleifer KH (1993) Probing activated sludge with oligonucleotides specific for Proteobacteria - Inadequacy of culture-dependent methods for describing microbial community structure. *Appl Environ Microbiol* **59**, 1520-1525.

Wallner G, Amann R & Beisker W (1993) Optimizing fluorescent *in situ* hybridization with ribosomal-RNA-targeted oligonucleotide probes for flow cytometric identification of microorganisms. *Cytometry* **14**, 136-143.

Wang Q, Garrity GM, Tiedje JM & Cole JR (2007) Naive Bayesian Classifier for rapid assignment of rRNA sequences into the new bacterial taxonomy. *Appl Environ Microbiol* **73**, 5261-5267.

Wang H, Vuorela M, Keränen AL, Lehtinen TM, Lensu A, Lehtomäki A & Rintala J (2010) Development of microbial populations in the anaerobic hydrolysis of grass silage for methane production. *FEMS Microbiol Ecol* **72**, 496-506.

Wang TY, Chen HL, Lu MYJ et al. (2011) Functional characterization of cellulases identified from the cow rumen fungus *Neocallimastix patriciarum* W5 by transcriptomic and secretomic analyses. *Biotechnol Biofuels* **4**, 24.

Warnecke F, Luginbuehl P, Ivanova N et al. (2007) Metagenomic and functional analysis of hindgut microbiota of a wood-feeding higher termite. *Nature* **450**, 560-565.

Weiland P (2010) Biogas production: current state and perspectives. *Appl Microbiol Biotechnol* **85**, 849-860.

Weisburg WG, Barns SM, Pelletier DA & Lane DJ (1991) 16S ribosomal DNA amplification for phylogenetic study. *J Bacteriol* **173**, 697-703.

Westerholm M, Roos S & Schnürer A (2010) *Syntrophaceticus schinkii* gen. nov., sp. nov., an anaerobic, syntrophic acetate-oxidizing bacterium isolated from a mesophilic anaerobic filter. *FEMS Microbiol Lett* **309**, 100-104.

Westerholm M, Roos S & Schnürer A (2011) *Tepidanaerobacter acetatoxydans* sp. nov., an anaerobic, syntrophic acetate-oxidizing bacterium isolated from two ammonium-enriched mesophilic methanogenic processes. *Syst Appl Microbiol* **34**, 260-266.

Wheeler DL, Barrett T, Benson DA et al. (2007) Database resources of the National Center for Biotechnology Information. *Nucleic Acids Res* **35**, D5-D12.

Whittaker MM, Kersten PJ, Cullen D & Whittaker JW (1999) Identification of catalytic residues in glyoxal oxidase by targeted mutagenesis. *J Biol Chem* **274**, 36226-36232.

WHO - World health organization (2011) Ausbrüche von *E. coli* O104:H4-Infektionen: Lagebericht 30. URL: http://www.euro.who.int/de/where-we-work/member-states/germany/sections/news/2011/07/outbreaks-of-e.-coli-o104h4-infection-update-30. Last access December 10, 2012.

Wiegel J (1992) The anaerobic thermophilic Bacteria. In *Thermophilic Bacteria* ed. Kristjansson, JK, pp. 105-184. Boca Raton, USA: CRC Press.

Willms M, Hufnagel J & Wagner B (2008) Nutzen und Risiken des Energiepflanzenanbaus für den Boden. In *Kongressband 2008* Jena - *Workshop "Bioenergie" des 120. VDLUFA-Kongresses* pp. 90-99. Darmstadt, Germany: VDLUFA-Verlag.

Wirth R, Kovacs E, Maroti G, Bagi Z, Rakhely G & Kovacs KL (2012) Characterization of a biogas-producing microbial community by short-read next generation DNA sequencing. *Biotechnol Biofuels* **5**, 41.

Wittmann J, Eichenlaub R & Dreiseikelmann B (2010) The endolysins of bacteriophages CMP1 and CN77 are specific for the lysis of *Clavibacter michiganensis* strains. *Microbiology SGM* **156**, 2366-2373.

Wu WM, Thiele JH, Jain MK & Zeikus JG (1993) Metabolic properties and kinetics of methanogenic granules. *Appl Microbiol Biotechnol* **39**, 804-811.

Xu Q, Gao WC, Ding SY, Kenig R, Shoham Y, Bayer EA & Lamed R (2003) The cellulosome system of *Acetivibrio cellulolyticus* includes a novel type of adaptor protein and a cell surface anchoring protein. *J Bacteriol* **185**, 4548-4557.

Yu Y, Lee C, Kim J & Hwang S (2005) Group-specific primer and probe sets to detect methanogenic communities using quantitative real-time polymerase chain reaction. *Biotechnol Bioeng* **89**, 670-679.

Yu Y, Kim J & Hwang S (2006) Use of real-time PCR for group-specific quantification of aceticlastic methanogens in anaerobic processes: Population dynamics and community structures. *Biotechnol Bioeng* **93**, 424-433.

Zakrzewski M, Goesmann A, Jaenicke S, Jünemann S, Eikmeyer F, Szczepanowski R, Abu Al-Soud W, Sorensen S, Pühler A & Schlüter A (2012) Profiling of the metabolically active community from a production-scale biogas plant by means of high-throughput metatranscriptome sequencing. *J Biotechnol* **158**, 248-258.

Zakrzewski M, Bekel T, Ander C, Pühler A, Rupp O, Stoye J, Schlüter A & Goesmann A (2013) MetaSAMS - A novel software platform for taxonomic classification, functional annotation and comparative analysis of metagenome datasets. *J Biotechnol* **167**, 156-165.

Zhang QJ, Meitzler JC, Huang SX & Morishita T (2000) Sequence polymorphism, predicted secondary structures, and surface-exposed conformational epitopes of *Campylobacter* major outer membrane protein. *Infect Immun* **68**, 5679-5689.

Zhang T & Fang HHP (2006) Applications of real-time polymerase chain reaction for quantification of microorganisms in environmental samples. *Appl Microbiol Biotechnol* **70**, 281-289.

Zheng DD, Alm EW, Stahl DA & Raskin L (1996) Characterization of universal small-subunit rRNA hybridization probes for quantitative molecular microbial ecology studies. *Appl Environ Microbiol* **62**, 4504-4513.

Zhu CG, Zhang JY, Tang YP, Xu ZK & Song RT (2011) Diversity of methanogenic archaea in a biogas reactor fed with swine feces as the mono-substrate by mcrA analysis. *Microbiol Res* **166**, 27-35.

Ziganshin AM, Schmidt T, Scholwin F, Il'inskaya ON, Harms H & Kleinsteuber S (2011) Bacteria and Archaea involved in anaerobic digestion of distillers grains with solubles. *Appl Microbiol Biotechnol* **89**, 2039-2052.

Zinder SH & Koch M (1984) Non-aceticlastic methanogenesis from acetate: acetate oxidation by a thermophilic syntrophic coculture. *Arch Microbiol* **138**, 263-272.

Zinder SH (1990) Conversion of acetic-acid to methane by thermophiles. *FEMS Microbiol Rev* **75**, 125-137.

7 APPENDIX

7.1 NMDS for TRFLP community profiles

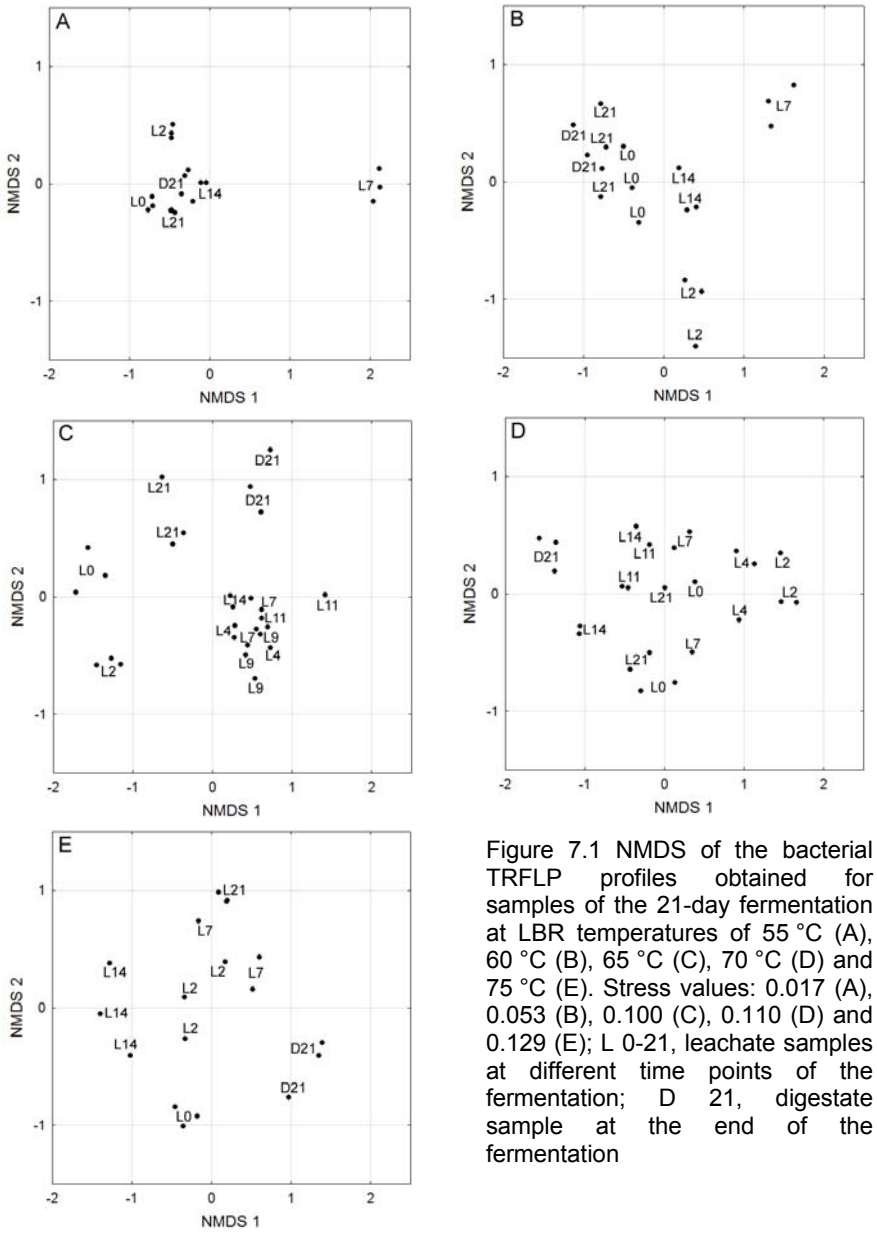

Figure 7.1 NMDS of the bacterial TRFLP profiles obtained for samples of the 21-day fermentation at LBR temperatures of 55 °C (A), 60 °C (B), 65 °C (C), 70 °C (D) and 75 °C (E). Stress values: 0.017 (A), 0.053 (B), 0.100 (C), 0.110 (D) and 0.129 (E); L 0-21, leachate samples at different time points of the fermentation; D 21, digestate sample at the end of the fermentation

7.2 Protein families relevant for the metagenomic analyses

Table 7.1 Accession numbers of protein families relevant for carbohydrate degradation (A) and methanogenesis (B) obtained from the Pfam database

(A) Carbohydrate degrading enzymes		(B) Methanogenic enzymes	
Pfam accession	**Protein family**	**Pfam accession**	**Protein family**
PF00150	Cellulase (glycosyl hydrolase family 5)	PF00871	Acetokinase family
PF00295	Glycosyl hydrolases family 28	PF02552	CO dehydrogenase beta subunit/acetyl-CoA synthase ε-subunit
PF00331	Glycosyl hydrolase family 10	PF03598	CO dehydrogenase/acetyl-CoA synthase complex β-subunit
PF00457	Glycosyl hydrolases family 11	PF03599	CO dehydrogenase/acetyl-CoA synthase δ-subunit
PF00544	Pectate lyase	PF02289	Cyclohydrolase (MCH)
PF00553	Cellulose binding domain	PF01913	Formylmethanofuran tetrahyromethanopterin formyltransferase, lobe
PF00703	Glycosyl hydrolases family 2, domain	PF02741	Formylmethanofuran tetrahyromethanopterin formyltransferase, proximal lobe
PF00759	Glycosyl hydrolase family 9	PF01493	GXGXG motif
PF00840	Glycosyl hydrolase family 7	PF03201	H_2-forming N5,N10-methylene-tetrahydromethanopterin dehydrogenase
PF00942	Cellulose binding domain	PF04609	Methyl-coenzyme M reductase operon protein C
PF01055	Glycosyl hydrolases family 31	PF02505	Methyl-coenzyme M reductase operon protein D
PF01095	Pectinesterase	PF02249	Methyl-coenzyme M reductase α-subunit, C-terminal domain
PF01270	Glycosyl hydrolases family 8	PF02745	Methyl-coenzyme M reductase α-subunit, N-terminal domain
PF01915	Glycosyl hydrolase family 3 C terminal domain	PF02241	Methyl-coenzyme M reductase β-subunit, C-terminal domain
PF02011	Glycosyl hydrolase family 48	PF02783	Methyl-coenzyme M reductase β-subunit, N-terminal domain
PF02056	Family 4 glycosyl hydrolase	PF02240	Methyl-coenzyme M reductase γ-subunit
PF02156	Glycosyl hydrolase family 26	PF01993	Methylene-5,6,7,8-tetrahydromethanopterin dehydrogenase
PF02255	PTS system, Lactose/ cellobiose specific IIA subunit	PF02663	Molybdenum formylmethanofuran dehydrogenase operon
PF02449	Beta-galactosidase	PF01515	Phosphate acetyl/butaryl transferase
PF02836	Glycosyl hydrolases family 2, TIM barrel domain	PF04208	Tetrahydromethanopterin S-methyltransferase, subunit A
PF02837	Glycosyl hydrolases family 2, sugar binding domain	PF05440	Tetrahydromethanopterin S-methyltransferase, subunit B
PF02929	Beta galactosidase small chain	PF04211	Tetrahydromethanopterin S-methyltransferase, subunit C
PF03422	Carbohydrate binding module	PF04207	Tetrahydromethanopterin S-methyltransferase, subunit D
PF04616	Glycosyl hydrolases family 43	PF04206	Tetrahydromethanopterin S-methyltransferase, subunit E
PF06165	Glycosyltransferase family 36	PF09472	Tetrahydromethanopterin S-methyltransferase, subunit F
PF08532	Beta-galactosidase trimerisation domain	PF04210	Tetrahydromethanopterin S-methyltransferase, subunit G
PF08533	Beta-galactosidase C-terminal domain	PF02007	Tetrahydromethanopterin S-methyltransferase, subunit H

Table 7.2 Accession numbers of protein families relevant for pathogenicity of selected pathogens obtained from the Pfam database

Pfam accession	Protein family
PF00161	Ribosome inactivating protein
PF01375	Heat-labile enterotoxin alpha chain
PF01376	Heat-labile enterotoxin beta chain
PF01742	Clostridial neurotoxin zinc protease
PF02048	Heat-stable enterotoxin
PF02258	Shiga-like toxin beta subunit family
PF03278	IpaB/EvcA family
PF03318	Clostridium epsilon toxin ETX/Bacillus mosquitocidal toxin MTX2
PF03495	Clostridial binary toxin B/anthrax toxin PA
PF03496	ADP-ribosyltransferase exoenzyme
PF03505	Clostridium enterotoxins
PF05058	ActA Protein
PF05105	Holin family
PF05538	Campylobacter major outer membrane protein
PF05588	Clostridium botulinum HA-17 protein
PF06002	Alpha-2,3-sialyltransferase (CST-I)
PF06109	Haemolysin E (HlyE)
PF06306	Beta-1,4-N-acetylgalactosaminyltransferase (CgtA)
PF07906	ShET2 enterotoxin, N-terminal region
PF07951	Clostridium neurotoxin, C-terminal receptor binding
PF07952	Clostridium neurotoxin, Translocation domain
PF07953	Clostridium neurotoxin, N-terminal receptor binding
PF08090	Heat stable E. coli enterotoxin 1
PF08191	Leucine-rich repeats (LLR) adjacent
PF08470	Nontoxic nonhaemagglutinin C-terminal
PF09052	Salmonella invasion protein A
PF09599	Salmonella-Shigella invasin protein C
PF12354	Bacterial adhesion/invasion protein N terminal
PF12918	TcdB toxin N-terminal helical domain
PF12919	TcdA/TcdB catalytic glycosyltransferase domain
PF12920	TcdA/TcdB pore forming domain